



Search for short- and long-lived axion-like particles in $H \rightarrow aa \rightarrow 4\gamma$ decays with the ATLAS experiment at the LHC

The ATLAS Collaboration

Presented is the search for anomalous Higgs boson decays into two axion-like particles (ALPs) using the full Run 2 data set of 140 fb^{-1} of proton-proton collisions at a centre-of-mass energy of 13 TeV recorded by the ATLAS experiment. The ALPs are assumed to decay into two photons, providing sensitivity to recently proposed models that could explain the $(g - 2)_\mu$ discrepancy. This analysis covers an ALP mass range from 100 MeV to 62 GeV and ALP-photon couplings in the range $10^{-5} \text{ TeV}^{-1} < C_{a\gamma\gamma}/\Lambda < 1 \text{ TeV}^{-1}$, and therefore includes signatures with significantly displaced vertices and highly collinear photons. No significant excess of events above the Standard Model background is observed. Upper limits at 95% confidence level are placed on the branching ratio of the Higgs boson to two ALPs in the four-photon final state, and are in the range of 10^{-5} to 3×10^{-2} , depending on the hypothesized ALP mass and ALP-photon coupling strength.

Contents

1	Introduction	2
2	The ATLAS Detector	3
3	Data Set and Simulated Events	4
4	Object Reconstruction and Event Selection	5
4.1	Object Reconstruction	5
4.2	Event Selection and Categorization	6
5	Background Estimation	7
5.1	Two-Photon Final States in the Search for Long-Lived Axion-Like Particles	7
5.2	Three- and Four-Photon Final States in the Search for Long-Lived Axion-Like Particles	9
5.3	Four-Photon Final States in the Search for Promptly Decaying Axion-Like Particles	10
5.4	Background Estimate Summary	11
6	Systematic Uncertainties	11
6.1	General Experimental Uncertainties	12
6.2	Uncertainties on the Background Estimation	13
6.3	Impact of Theory Uncertainties	14
7	Results	14
8	Conclusion	20

1 Introduction

Axion-like particles (ALPs), or more generally light (pseudo) scalars, are represented as gauge-singlets beyond the Standard Model (SM) that can couple to the 125 GeV Higgs boson [1, 2], and appear in many well-motivated extensions of the SM, e.g., the next-to-minimal supersymmetric standard model [3, 4]. These include models that address the baryon asymmetry of the universe [5, 6], offer a solution to the naturalness problem [7, 8], or provide insights into the nature of dark matter [9–14]. ALPs and light bosons produced in Higgs boson decays could also be mediators to dark sectors that do not otherwise couple to the SM [15].

A combination of ATLAS measurements of Higgs boson properties using 139 fb^{-1} of data constrains the branching ratios into invisible and undetected states to be $\mathcal{B}(H \rightarrow \text{invisible}) < 10.7\%$ and $\mathcal{B}(H \rightarrow \text{undetected}) < 12\%$ at 95% confidence level (CL) [16, 17]. Combined measurements of Higgs boson couplings performed by the CMS Collaboration using 138 fb^{-1} of data set upper limits of $\mathcal{B}(H \rightarrow \text{invisible}) < 16\%$ and $\mathcal{B}(H \rightarrow \text{undetected}) < 16\%$ at 95% CL [18]. These results allow potentially large branching fractions into beyond-the-standard-model (BSM) particles, $\mathcal{B}(H \rightarrow \text{BSM})$, such as ALPs.

In Ref. [19] it has been argued that if the ALP, denoted as a in the following, couples to at least some SM particles with couplings of order $(0.01-1)\text{TeV}^{-1}$, its mass must be above 1 MeV. Taking into account the possibility of a long-lived ALP, large regions of so far unconstrained parameter space can be explored by

searches for exotic, on-shell Higgs boson decays into two ALPs. In particular, this includes the parameter space in which ALPs can explain the observed discrepancy between the measurement [20–22] and the theoretical prediction [23, 24] of the anomalous magnetic moment of the muon [19]. It was suggested that subsequent ALP decays into photons provide unprecedented sensitivity to the ALP-photon couplings in the mass region above a few MeV, even if the relevant ALP-photon couplings are loop suppressed and the $a \rightarrow \gamma\gamma$ branching ratios are significantly less than 100% [19].

This paper presents a search for decays of the 125 GeV Higgs boson into two ALPs in proton–proton (pp) collisions at the LHC [25]. The search is sensitive to events where each a -boson decays into two photons. For the first time, a dedicated search for long-lived $a \rightarrow \gamma\gamma$ decays with a significantly displaced vertex within the tracking system of the ATLAS detector is performed, allowing a large region of the parameter space of the ALP-photon coupling $C_{a\gamma\gamma}$ to be probed. Previous searches for $H \rightarrow aa \rightarrow 4\gamma$ signatures were performed by the ATLAS [26] and CMS Collaborations [27, 28], but assumed promptly decaying ALPs and hence were valid only up to decay lengths of a few centimeters. The decay length scales with $\tau_a \propto \Lambda^2 / (m_a^3 |C_{a\gamma\gamma}|^2)$, where m_a is the ALP mass and Λ , the new physics scale, is assumed to be in the TeV range [19]. The limits obtained here for ALP masses $m_a > 15$ GeV are about one order of magnitude more stringent than previous ATLAS analyses using 8 TeV data, and reach sensitivities similar to or slightly better than previous analyses from CMS using 132 fb^{-1} of $\sqrt{s} = 13$ TeV data.

The paper is structured as follows. A brief discussion of the ATLAS detector and an overview of the Monte Carlo (MC) samples and data sets used are given in Sections 2 and 3. Object reconstruction and the event selection are described in Section 4, where special focus is given to the reconstruction of collimated photon signatures and to the categorization of the final state topologies that can be reconstructed in the detector. The background estimates are discussed in Section 5, followed by a description of the dominant systematic uncertainties in Section 6, in particular those that involve the reconstruction of photons with a displaced production vertex. The statistical interpretation and the final results are summarized in Section 7. The paper closes with a brief conclusion in Section 8.

2 The ATLAS Detector

The ATLAS detector [29] at the LHC covers nearly the entire solid angle around the collision point.¹ It consists of an inner tracking detector surrounded by a thin superconducting solenoid, electromagnetic and hadron calorimeters, and a muon spectrometer incorporating three large superconducting air-core toroidal magnets.

The inner-detector system (ID) is immersed in a 2 T axial magnetic field and provides charged-particle tracking in the range of $|\eta| < 2.5$. The high-granularity silicon pixel detector covers the vertex region and typically provides four measurements (hits) per track, the first hit normally being in the insertable B-layer (IBL) installed before Run 2 [30, 31]. It is followed by the silicon microstrip tracker (SCT), which usually provides eight measurements per track. These silicon detectors are complemented by the transition radiation tracker (TRT), which enables radially extended track reconstruction up to $|\eta| = 2.0$. The TRT

¹ ATLAS uses a right-handed coordinate system with its origin at the nominal interaction point (IP) in the centre of the detector and the z -axis along the beam pipe. The x -axis points from the IP to the centre of the LHC ring, and the y -axis points upwards. Cylindrical coordinates (r, ϕ) are used in the transverse plane, ϕ being the azimuthal angle around the z -axis. The pseudorapidity is defined in terms of the polar angle θ as $\eta = -\ln \tan(\theta/2)$. Angular distance is measured in units of $\Delta R \equiv \sqrt{(\Delta\eta)^2 + (\Delta\phi)^2}$.

also provides electron identification information based on the fraction of hits (typically 30 in total) above a higher energy-deposit threshold corresponding to transition radiation.

The calorimeter system covers the pseudorapidity range of $|\eta| < 4.9$. Within the region $|\eta| < 3.2$, electromagnetic calorimetry is provided by barrel and endcap high-granularity lead/liquid-argon (LAr) calorimeters, with an additional thin LAr presampler covering $|\eta| < 1.8$ to correct for energy loss in material upstream of the calorimeters. Hadron calorimetry is provided by the steel/scintillator-tile calorimeter, segmented into three barrel structures within $|\eta| < 1.7$, and two endcap copper/LAr hadron calorimeters up to $|\eta| < 3.2$. The solid angle coverage is completed with forward copper/LAr and tungsten/LAr calorimeter modules optimised for electromagnetic and hadronic energy measurements, respectively.

The muon spectrometer (MS) comprises separate trigger and high-precision tracking chambers that measure the deflection of muons in the magnetic field generated by the superconducting air-core toroidal magnets. The field integral of the toroids ranges between 2.0 and 6.0 Tm across most of the detector. Three layers of precision chambers, each consisting of layers of monitored drift tubes, cover the region $|\eta| < 2.7$, complemented by cathode-strip chambers in the forward region. The muon trigger system covers the range of $|\eta| < 2.4$ with resistive-plate chambers in the barrel, and thin-gap chambers in the endcap regions.

Events of interest for this analysis are selected using dedicated di-photon triggers. The first-level of the trigger system is implemented in custom hardware, followed by a high-level trigger [32] where further selections are made by algorithms implemented in software. The first-level trigger accepts events from the 40 MHz bunch crossings at a rate below 100 kHz, which the high-level trigger further reduces in order to record events to disk at about 1 kHz.

An extensive software suite [33] is used in MC simulation, in the reconstruction and analysis of real and simulated data, in detector operations, and in the trigger and data acquisition systems of the experiment.

3 Data Set and Simulated Events

This analysis uses pp collision data collected by the ATLAS experiment from 2015 to 2018 with a centre-of-mass energy of $\sqrt{s} = 13$ TeV. After data quality requirements [34] the full data set corresponds to an integrated luminosity of $140.1 \pm 1.2 \text{ fb}^{-1}$ [35]. The lowest-threshold unprescaled di-photon triggers are used to select events for further analysis, as discussed in Section 4.2.

Simulated events are used to validate the data-driven background estimation techniques described in Sections 5.1 – 5.2, and to model Higgs boson decays into photons for both signal and background processes. Background events from continuum 3γ , 4γ and $\gamma\gamma$ production, neglecting any interference effects with the $H \rightarrow \gamma\gamma$ decay, are generated using Sherpa 2.2.8 and Sherpa 2.2.4 [36–38], respectively, with the AZNLO set of tuned parameters [39] and the NNPDF30 [40] set of parton distribution functions (PDF). Production of the Higgs boson through gluon–gluon fusion (ggF) and vector-boson fusion (VBF) processes is modelled at next-to-leading order (NLO) using POWHEG-Box v2 [41–43] interfaced with PYTHIA 8.186 [44] using the AZNLO tune and NNPDF30 PDF. The change in selection efficiency between ggF and VBF and other Higgs boson production mechanisms is at the percent level, so its impact is negligible. Thus, all signal ($H \rightarrow aa \rightarrow \gamma\gamma\gamma\gamma$) samples use the ggF Higgs boson production mechanism and have their cross-sections scaled to the total Higgs boson production cross-section predicted by a next-to-next-to-next-to-leading-order QCD calculation with NLO electroweak corrections applied [45–48].

Signal samples are produced for ALP masses in the range of 0.1 GeV – 62 GeV, with a spacing of 0.1 GeV in the range of 0.1 GeV – 0.5 GeV, a spacing of 0.5 GeV in the range of 0.5 GeV – 5 GeV and a spacing of 1 GeV in the range of 5 GeV – 62 GeV, assuming $\Lambda = 1$ TeV. The full set of mass points is simulated for four different values of the coupling $C_{a\gamma\gamma}$: 1, 0.01, 5×10^{-4} and 10^{-5} . Samples of simulated signal events are generated using POWHEG-Box v2 at NLO. For hadronisation and parton showering, PYTHIA 8.212 is used, with the AZNLO tune and the CTEQ6L1 PDF set [49].

Different pile-up conditions due to additional pp interactions in the same and neighbouring bunch crossings are simulated by overlaying the hard-scattering event with inelastic pp events generated by PYTHIA 8.186 using the NNPDF2.3LO PDF set [50] and the A3 tune [51]. Differences between the simulated and observed distributions of the number of interactions per bunch crossing are corrected by reweighting the simulated events to match the data distribution.

All MC samples use a full simulation of the ATLAS detector [52] based on GEANT4 [53] to reproduce the detector response. Corrections are applied to the simulated events to match the photon selection efficiencies, energy scale and resolution to those determined in data.

4 Object Reconstruction and Event Selection

The experimental signature of $H \rightarrow aa \rightarrow 4\gamma$ depends significantly on the ALP mass and on its coupling to photons, $C_{a\gamma\gamma}$. ALP masses below 3.5 GeV dominantly yield collimated photon signatures, which are reconstructed as one energy cluster in the electromagnetic calorimeter. The decay photons of axion-like particles with higher masses can typically be resolved by the ATLAS calorimeter system and the ATLAS identification algorithms. The $C_{a\gamma\gamma}$ coupling determines the lifetime and hence the distance the ALPs travel after being produced, so the search for $H \rightarrow aa \rightarrow 4\gamma$ is divided into two sub-searches: a search for promptly decaying ALPs corresponding to couplings $C_{a\gamma\gamma} \geq 0.1$ and a search for long-lived ALPs that is optimised for smaller couplings. Coupling values smaller than $C_{a\gamma\gamma} = 10^{-5}$ cannot be probed since they yield ALP lifetimes that imply a decay outside of the detector volume for all ALP masses considered.

4.1 Object Reconstruction

Photons are reconstructed from topologically connected clusters [54] of energy deposits in the electromagnetic calorimeter in the region $|\eta| < 2.37$. The transition region between the barrel and endcap electromagnetic calorimeters, $1.37 < |\eta| < 1.52$, is excluded. Photon candidates matched to conversion vertices or tracks that are consistent with originating from photon conversions are classified as converted photons. Those without a matched conversion vertex or track are classified as unconverted photons.

Photon candidates are defined by the lateral shower profile of the energy deposits in the first and second electromagnetic calorimeter layers and by the fractional energy leakage into the hadron calorimeter. The analysis uses different photon identification criteria for different regions of the signal parameter space. Standard ‘Tight’ and ‘Loose’ photon identification criteria [55, 56], which are tuned for converted and unconverted photons separately, are applied in final states where individual photons can be separately reconstructed. Axion-like particles with small masses, e.g., $m_a < 3.5$ GeV, decay predominantly into a pair of highly collimated photons, which are reconstructed as single photon object. For these merged photon objects, the standard photon identification is not efficient. Hence, a neural network (NN)-based classification approach is developed. A first classifier is trained to separate real photon signatures, single or collimated,

from ‘fake photons’ that come from multijet background. A second classifier is then trained to separate single-photon signatures from collimated signatures. Both classifiers use eight shower-shape variables relevant for photon identification [56]. The training data sets are based on single- and collimated-photon signatures from simulation and fake-photon candidates from data; the fake-photon candidates are selected by inverting several isolation observables. If a photon passes a minimum threshold of the output neurons of both classifiers, it is labelled as a ‘merged’ photon.

The photon energy is reconstructed using the nominal ATLAS reconstruction and calibration procedures [57]. The energy of photon candidates that are identified as collimated photon signatures is corrected by adding the measured cluster energies in the calorimeter within a cone of $\Delta R = 0.2$ around the photon, if not yet associated with the photon.

To further improve the rejection of misidentified photons, a track-based variable p_T^{iso} is defined as the scalar sum of the transverse momenta of all tracks with transverse momentum (p_T) above 1 GeV that originate from the primary vertex and are within a cone of $\Delta R = 0.2$ around the photon candidate with transverse energy E_T^γ . Isolated photons must have $p_T^{\text{iso}}/E_T^\gamma < 0.05$. A calorimeter-based isolation requirement is not used due to its large signal rejection for collimated photon signatures.

4.2 Event Selection and Categorization

Events are selected using one of two di-photon triggers [58], each of which requires two reconstructed photon candidates. The first trigger requires a minimum transverse energy of 35 GeV for the leading photon and 25 GeV for the subleading photon where both photons must satisfy the Loose or Medium identification criteria, depending on the data-taking period. The alternative trigger requires that each photon satisfy the Tight identification criteria and have a transverse energy of at least 22 GeV. The terms ‘leading’ and ‘subleading’ refer to the photon candidate with the highest and second-highest transverse energy, respectively. Photon candidates in the event must have a minimum transverse energy corresponding to the trigger threshold for the leading and subleading photons and at least 15 GeV for any additional photon. For $H \rightarrow aa \rightarrow 4\gamma$ events with $C_{a\gamma\gamma} = 1$ and at least two selected photon candidates, the average trigger efficiency is larger than 60% for all ALP masses. This still holds for $C_{a\gamma\gamma} = 10^{-5}$ and $m_a > 50$ GeV, while for smaller masses the trigger efficiency decreases down to 30 %.

Signal events are fully reconstructed if all four photons are detected. However, the detector may miss photons or pairs of collinear photons may be reconstructed as individual objects, resulting in fewer reconstructed photons. At least two reconstructed photon candidates are required for the analysis. Further classification is based on the number and types of reconstructed photons.

The final states are classified into five categories according to their experimental signature, in the following order: 1) events with four reconstructed photons, where all photons satisfy the Loose identification and at least one satisfies the Tight identification, fall into the four-single (4S) category. 2) events with three reconstructed photons, where all photons satisfy the Tight identification, fall into the three-single (3S) category. 3) events with two merged photon candidates fall into the two-merged (2M) category. Additional loose photon candidates are likely to originate from background processes and are ignored, with negligible impact on the rate of falsely identified signal events. 4) events with two photon candidates, where one satisfies the merged classification and the other satisfies the Loose identification, fall into the one-merged-one-single (1M1S) category. This category accepts events where the merged classification of two photons is not efficient. 5) events with exactly two photons that satisfy the Tight identification but

without any further photon candidates that satisfy the Loose identification fall into the two-single category (2S), which is dominated by events from the $H \rightarrow \gamma\gamma$ process.

For long-lived ALPs, searches in the 3S and 4S categories provide the most sensitivity in the mass range $m_a > 3.5$ GeV. Long-lived ALPs with $m_a < 3.5$ GeV yield collimated photon signatures, and the 2M, 1M1S and 2S categories have the most sensitivity in this parameter space.

The 3S and 4S categories allow for the reconstruction of the ALP mass, m_a , since at least one photon pair stems from the decay of an ALP for the signal process. Separate neural networks were trained for the three- and four-photon categories to select the correct photon pairing(s). The inputs to the networks are the invariant masses of all photon pair combinations and differences in their transverse energies and directions. The training sample consists of both correct and wrong photon combinations. The combinations are based on MC signal samples for all ALP masses and couplings. In the 3S category, the invariant mass of the photon pair that is predicted to stem from the same mother particle is defined as the reconstructed ALP mass m_a^{reco} , while the average of both resulting invariant masses is defined as m_a^{reco} in the 4S category.

The signal region selection uses the invariant mass of all photon candidates, denoted by $m_{\text{inv}}^{\text{reco}}$, which is expected to peak around the Higgs boson mass for signal processes. The signal regions for all categories and searches are defined to contain at least 90% of the reconstructed signal contribution in simulated data. For the two-photon categories (2M, 1M1S and 2S), the signal region is defined by the invariant mass requirement $115 \text{ GeV} < m_{\text{inv}}^{\text{reco}} < 130 \text{ GeV}$ around the Higgs boson mass.

The 3S and 4S categories also require the reconstructed ALP mass m_a^{reco} to fall within a window around the generated ALP mass, whose size varies depending on the mass point being tested. In general, the requirements on $m_{\text{inv}}^{\text{reco}}$ are looser in the 3S category since one photon typically escapes detection, leading to a wider $m_{\text{inv}}^{\text{reco}}$ spectrum. The m_a^{reco} distribution also enables the definition of a control region in data by inverting the mass requirement on m_a^{reco} .

In the search for promptly decaying ALPs only the 4S category is used when estimating the limits on the signal process, as it has by far the largest sensitivity. In this case the category is defined by tightening the selection cuts so that at least three out of the four photons satisfy the Tight identification requirements and is labelled $4S_p$. Promptly decaying ALPs are only considered for $m_a > 5$ GeV, where a significant increase in sensitivity over the search for long-lived ALPs is observed. Table 1 summarizes the signal region definitions for all ALP mass hypotheses m_a .

5 Background Estimation

The signal is expected to peak in $m_{\text{inv}}^{\text{reco}}$, the invariant mass of the selected photons, near the Higgs boson mass, $m_H = 125$ GeV, in all categories and searches. The $m_{\text{inv}}^{\text{reco}}$ sidebands are used for the background estimate in the signal region and for the estimation of spurious signal effects.

5.1 Two-Photon Final States in the Search for Long-Lived Axion-Like Particles

The distribution of $m_{\text{inv}}^{\text{reco}}$ in all two-photon categories (2M, 1M1S, 2S) is fitted over a mass range from 100 to 150 GeV, excluding the signal region. A suitable fitting function should describe the data in the sidebands, provide an unbiased estimate of the background in the signal region, and produce small uncertainties on the yields of spurious signals. This is ensured by defining validation regions that use similar requirements to

Model Parameters	Signal Region Definition	
Long-lived ALP Search: $C_{a\gamma\gamma} < 0.1$		
2M, 1M1S and 2S Categories		
$0.1 \text{ GeV} < m_a < 3.5 \text{ GeV}$	$115 \text{ GeV} < m_{\text{inv}}^{\text{reco}} < 130 \text{ GeV}$	
	3S Category	4S Category
$3.5 \text{ GeV} < m_a < 10 \text{ GeV}$	$105 \text{ GeV} < m_{\text{inv}}^{\text{reco}} < 130 \text{ GeV}$ $0 \text{ GeV} < m_a^{\text{reco}} < 10 \text{ GeV}$	$120 \text{ GeV} < m_{\text{inv}}^{\text{reco}} < 130 \text{ GeV}$ $0 \text{ GeV} < m_a^{\text{reco}} < 12 \text{ GeV}$
$10 \text{ GeV} < m_a < 25 \text{ GeV}$	$100 \text{ GeV} < m_{\text{inv}}^{\text{reco}} < 125 \text{ GeV}$ $6 \text{ GeV} < m_a^{\text{reco}} < 26 \text{ GeV}$	$120 \text{ GeV} < m_{\text{inv}}^{\text{reco}} < 130 \text{ GeV}$ $8 \text{ GeV} < m_a^{\text{reco}} < 28 \text{ GeV}$
$25 \text{ GeV} < m_a < 40 \text{ GeV}$	$100 \text{ GeV} < m_{\text{inv}}^{\text{reco}} < 125 \text{ GeV}$ $20 \text{ GeV} < m_a^{\text{reco}} < 40 \text{ GeV}$	$120 \text{ GeV} < m_{\text{inv}}^{\text{reco}} < 130 \text{ GeV}$ $23 \text{ GeV} < m_a^{\text{reco}} < 43 \text{ GeV}$
$40 \text{ GeV} < m_a < 62 \text{ GeV}$	$90 \text{ GeV} < m_{\text{inv}}^{\text{reco}} < 115 \text{ GeV}$ $30 \text{ GeV} < m_a^{\text{reco}} < 65 \text{ GeV}$	$120 \text{ GeV} < m_{\text{inv}}^{\text{reco}} < 130 \text{ GeV}$ $38 \text{ GeV} < m_a^{\text{reco}} < 65 \text{ GeV}$
Prompt ALP Search: $0.1 < C_{a\gamma\gamma} < 1$		
	$4S_p$ Category	
$5 \text{ GeV} < m_a < 25 \text{ GeV}$	$120 \text{ GeV} < m_{\text{inv}}^{\text{reco}} < 130 \text{ GeV}$ $ m_a - m_a^{\text{reco}} < 1 \text{ GeV}$	
$25 \text{ GeV} \leq m_a < 40 \text{ GeV}$	$120 \text{ GeV} < m_{\text{inv}}^{\text{reco}} < 130 \text{ GeV}$ $ m_a - m_a^{\text{reco}} < 2 \text{ GeV}$	
$40 \text{ GeV} \leq m_a < 50 \text{ GeV}$	$120 \text{ GeV} < m_{\text{inv}}^{\text{reco}} < 130 \text{ GeV}$ $ m_a - m_a^{\text{reco}} < 3 \text{ GeV}$	
$50 \text{ GeV} \leq m_a < 55 \text{ GeV}$	$120 \text{ GeV} < m_{\text{inv}}^{\text{reco}} < 130 \text{ GeV}$ $ m_a - m_a^{\text{reco}} < 5 \text{ GeV}$	
$55 \text{ GeV} \leq m_a < 62 \text{ GeV}$	$120 \text{ GeV} < m_{\text{inv}}^{\text{reco}} < 130 \text{ GeV}$ $ m_a - m_a^{\text{reco}} < 8 \text{ GeV}$	

Table 1: Definition of the signal region for different event categories in the prompt and long-lived search.

those of the signal region but reject signal events. Simulated samples of two-photon continuum processes and a data-driven validation region are studied. The latter is defined using the nominal signal selection and classification, but inverting the isolation cuts on the photon candidates, thus yielding a multijet-enhanced data sample.² These validation regions are chosen to cover extreme cases for the two main parts of the background composition which are di-photon production and non-resonant multijet background. A Landau function gives unbiased background estimates in the signal region of the control sample and provides good χ^2 per number of degrees of freedom (χ^2/ndf) in all sideband regions for the 2S and 1M1S categories.

It is expected that the background shape in the 2M category differs from the 2S and 1M1S categories, due to the different background composition after the requirements on the NN-based classifiers. A second-order polynomial provides a good description of all validation regions of the 2M category. Variations of the background estimates using different fitting functions and different fitting ranges are used to define systematic uncertainties and are discussed in Section 6.

The $H \rightarrow \gamma\gamma$ process contributes not in the sideband but in the signal region, dominantly in the 2S and to a negligible extent in the 2M and 1M1S categories. Its contribution and shape are estimated by MC predictions.

Figure 1 shows the $m_{\text{inv}}^{\text{reco}}$ spectra including the sideband fit for the signal selection for the 2M and 1M1S

² It is ensured that there is no overlap with the training data of the NN-based photon identification classifiers.

categories, respectively. The expected signal shape for an ALP with $m_a = 0.5$ GeV and $C_{a\gamma\gamma} = 0.01$ is also shown for illustration.

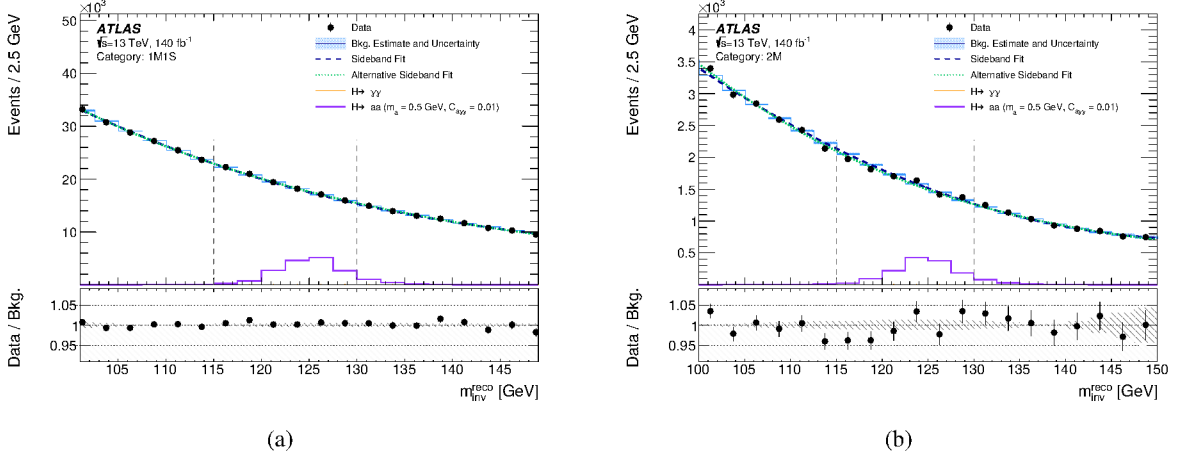


Figure 1: $m_{\text{inv}}^{\text{reco}}$ distribution for the nominal signal selection for the (a) 1M1S and (b) 2M category. The nominal sideband fitting function is shown as the blue dashed line. The estimated background and its systematic uncertainty is shown as a blue histogram for both cases. The green dotted line shows the alternative fitting function used to estimate the spurious signal uncertainty (discussed in Section 6). The expected signal shape for $C_{a\gamma\gamma} = 0.01$ is also shown with an arbitrary normalization. The signal region selection on $m_{\text{inv}}^{\text{reco}}$ is indicated using vertical dashed lines. The contribution from $H \rightarrow \gamma\gamma$ is negligible and not visible in the figures. The lower panels show the data divided by the estimated continuum background.

5.2 Three- and Four-Photon Final States in the Search for Long-Lived Axion-Like Particles

The background estimation in the long-lived ALPs searches also employs a sideband fit using the $m_{\text{inv}}^{\text{reco}}$ spectrum in the 3S and 4S categories.

Polynomials of third and second order serve as the nominal background fitting functions for the 3S and 4S categories, respectively, where the fits are carried out in the range of 80 GeV to 150 GeV and 105 GeV to 145 GeV, excluding the signal region. First, the suitability of the sideband functions for background estimation in both categories is tested on three- and four-photon continuum MC samples. Next, the sideband functions and corresponding background estimates are validated using an orthogonal set of data events in which the requirement on the reconstructed ALP mass is inverted.

This inverted sample can be used as a validation region, since the shape of background events should not change with a different choice of ALP mass apart from minor kinematic changes in the $m_{\text{inv}}^{\text{reco}}$ distribution. The multi-photon MC samples are used to correct for this kinematic effect.

The chosen fitting functions yield a χ^2/ndf close to unity in all validation regions and the estimated background using these validation regions is consistent with the observed numbers of background events from the signal region sidebands. Systematic uncertainties due to the choice of the background function and the fitting range are discussed in Section 6. Figure 2 depicts the $m_{\text{inv}}^{\text{reco}}$ spectrum for various ALP mass searches, and shows the sideband fitting functions, the estimated background in the signal region, and the expected signal shape for two $C_{a\gamma\gamma}$ coupling parameters.

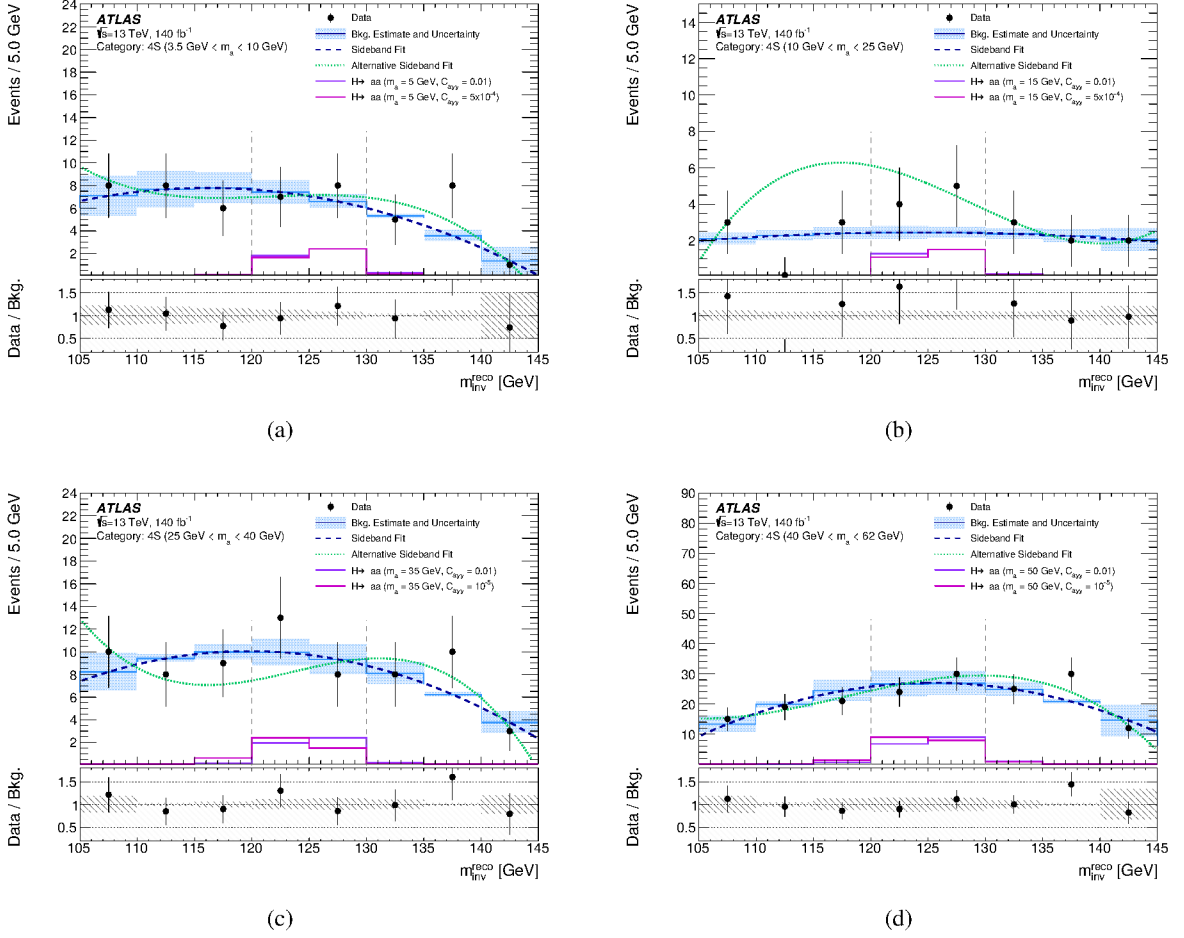


Figure 2: $m_{\text{inv}}^{\text{reco}}$ distribution for the nominal signal selection for the 4S category. The nominal sideband fitting function is shown as the blue dashed line. The estimated background and its systematic variation (obtained from a fit with reduced range) is shown as the blue histogram. The green dotted line shows the alternative fitting function which is used to estimate the spurious signal uncertainty (discussed in Sec. 6). The four subfigures show different ALP mass ranges: (a) $3.5 \text{ GeV} < m_a < 10 \text{ GeV}$, (b) $10 \text{ GeV} < m_a < 25 \text{ GeV}$, (c) $25 \text{ GeV} < m_a < 40 \text{ GeV}$, (d) $40 \text{ GeV} < m_a < 62 \text{ GeV}$. The signal region selection on m_a^{reco} is applied while the signal region selection on $m_{\text{inv}}^{\text{reco}}$ is indicated as dashed lines. The expected signal shape is shown with arbitrary normalization. The lower panels show the data divided by the estimated continuum background.

5.3 Four-Photon Final States in the Search for Promptly Decaying Axion-Like Particles

The number of selected events in the $4S_p$ category of the search for promptly decaying ALPs, also defined in the $m_{\text{inv}}^{\text{reco}}$ vs. m_a^{reco} plane, is significantly lower than that in the analysis optimised for long-lived ALPs due to the stricter rejection of fake-photon signatures using more stringent selection criteria such as Tight photon identification. To further suppress background contributions in the signal region, a tight selection around the m_a model parameter, as discussed in Section 4, is imposed. The size of the signal regions for each ALP mass are shown in Table 1. The background in the signal region of the search for promptly decaying ALPs is estimated by counting the events around the signal region in the $m_{\text{inv}}^{\text{reco}} - m_a^{\text{reco}}$ plane, extending the signal region by $\pm 5 \text{ GeV}$ in the $m_{\text{inv}}^{\text{reco}}$ dimension and by 1.5 times the signal region width

in the m_a^{reco} dimension. Due to the low statistics, the total number of background events in the shaded sideband area is scaled by the ratio of the areas of the signal region to the sideband region to estimate the number of background events in the signal region, as illustrated in Figure 3. This is equivalent to assuming a flat background distribution in the plane.

As an alternative background estimate, the size of the control region is taken to be 2.5 times the signal region instead of the 1.5 times used in the nominal background estimate. The difference between the nominal and the alternative background estimates is used as a systematic uncertainty. Figure 3 shows distributions in the $m_{\text{inv}}^{\text{reco}}-m_a^{\text{reco}}$ plane for events selected in the search for promptly decaying ALPs, with the sideband regions shown for the search parameters $m_a = 10$ GeV and $m_a = 40$ GeV. The validity of this procedure was tested using simulated multi-photon samples confirming that the associated statistical and systematic uncertainties cover potential shape differences.

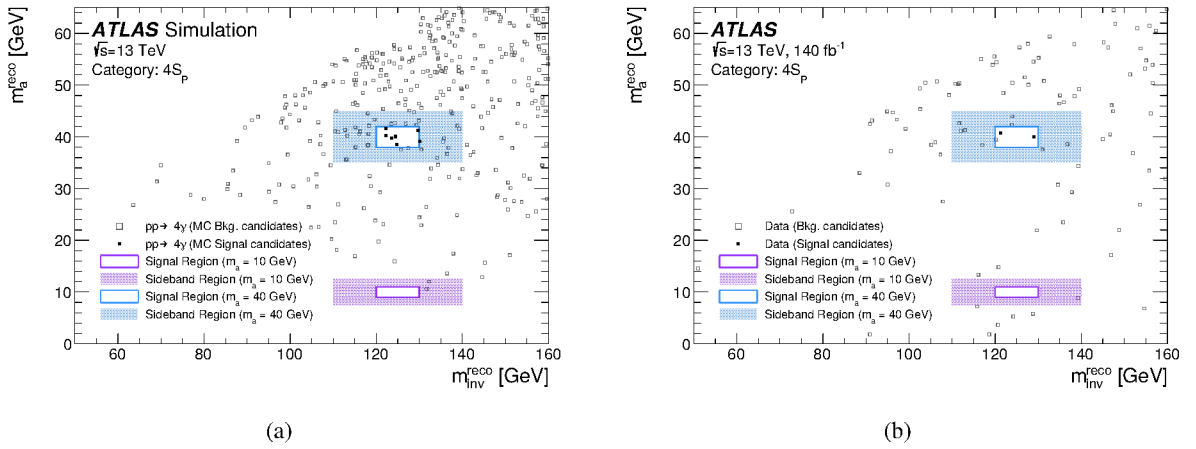


Figure 3: $m_{\text{inv}}^{\text{reco}}$ vs. m_a^{reco} for the $4S_p$ categories in the search for promptly decaying ALPs, for (a) simulated $pp \rightarrow 4\gamma$ sample and (b) for data. The signal (sideband) regions are indicated by solid lines (shaded areas) for the searches for ALPs with masses of 10 GeV and 40 GeV. Events within the signal region are shown with filled markers, those outside with open markers.

5.4 Background Estimate Summary

Table 2 summarizes the data and the expected background contribution in the signal region for the different categories. The acceptance times selection efficiency of a signal event in any of the categories is largely dependent on the ALP mass and coupling parameters under investigation. It ranges from 9% to 23% for low ALP masses ($m_a < 5$ GeV) and large couplings ($C_{a\gamma\gamma} = 1$) and is around 13% for large ALP masses ($m_a \approx 60$ GeV) at all studied couplings.

6 Systematic Uncertainties

The systematic uncertainties are assessed below, and their impact on the results is discussed in Section 7. First the general experimental uncertainties are discussed, where special attention is given to the uncertainties

Long-lived ALP Search			Prompt ALP Search		
Category $C_{a\gamma\gamma} < 0.1$	Events	Background Estimate	Category $0.1 < C_{a\gamma\gamma} < 1$	Events	Background Estimate
2M	9917	10000 ± 200	$4S_p (m_a = 5 \text{ GeV})$	2	0.35 ± 0.27
1M1S	113875	113100 ± 700	$4S_p (m_a = 10 \text{ GeV})$	0	0.24 ± 0.18
2S	632484	634000 ± 1500	$4S_p (m_a = 15 \text{ GeV})$	1	0.24 ± 0.28
3S ($3.5 \text{ GeV} < m_a < 10 \text{ GeV}$)	4782	4800 ± 100	$4S_p (m_a = 20 \text{ GeV})$	0	0.24 ± 0.28
3S ($10 \text{ GeV} < m_a < 25 \text{ GeV}$)	3166	3200 ± 100	$4S_p (m_a = 25 \text{ GeV})$	0	0.24 ± 0.28
3S ($25 \text{ GeV} < m_a < 40 \text{ GeV}$)	3843	3900 ± 150	$4S_p (m_a = 30 \text{ GeV})$	0	0.60 ± 0.27
3S ($40 \text{ GeV} < m_a < 62 \text{ GeV}$)	5389	5600 ± 90	$4S_p (m_a = 35 \text{ GeV})$	0	1.31 ± 0.76
4S ($3.5 \text{ GeV} < m_a \leq 10 \text{ GeV}$)	15	14 ± 3	$4S_p (m_a = 40 \text{ GeV})$	2	1.55 ± 0.94
4S ($10 \text{ GeV} < m_a \leq 25 \text{ GeV}$)	9	4 ± 2	$4S_p (m_a = 45 \text{ GeV})$	2	3.23 ± 0.95
4S ($25 \text{ GeV} < m_a \leq 40 \text{ GeV}$)	21	19 ± 3	$4S_p (m_a = 55 \text{ GeV})$	7	2.84 ± 1.51
4S ($40 \text{ GeV} < m_a < 62 \text{ GeV}$)	54	54 ± 6	$4S_p (m_a = 62 \text{ GeV})$	4	4.52 ± 1.50

Table 2: Overview of the number of observed events in the search for long-lived ALPs (left) and selected mass points from the search for prompt ALPs (right) in comparison to the expected number of background events. The uncertainty on the background estimate includes statistical and systematic uncertainties as described in Section 6.

arising from the displaced decay of long lived ALPs. Then the uncertainties impacting the background estimation are detailed followed by a discussion of the relevant theoretical uncertainties.

The experimental systematic uncertainty ranges, depending on the category and the hypothesized ALP mass and coupling, from 6.5% to 18% for most categories, with the exception of the 4S category where the uncertainty rises to 40% for masses $m_a < 15 \text{ GeV}$ and small couplings $C_{a\gamma\gamma}$ due to low statistics and large contributions from the photon identification uncertainties. The theoretical uncertainty is around 6% for all categories.

6.1 General Experimental Uncertainties

The uncertainty in the combined 2015–2018 integrated luminosity is 0.83% [35], obtained using the LUCID-2 detector [59] for the primary luminosity measurements, complemented by measurements using the inner detector and calorimeters.

To evaluate any impact on the expected signal yield due to imperfect modelling of pile-up, the average number of pile-up interactions is varied in the simulation. The corresponding uncertainty is below 1%.

The trigger efficiency used to select events is evaluated in simulation and data using a bootstrap method and radiative Z -boson decays [58]. The difference between data and simulation, which ranges from 2% to 3%, is taken as a systematic uncertainty.

The systematic uncertainties from the standard photon identification and isolation efficiencies are estimated following the prescriptions in Ref. [56]. They affect the di-photon selection efficiency and are evaluated by varying the correction factors for photon selection efficiencies in simulation by their corresponding uncertainties. The experimental uncertainties in the photon energy scale and resolution are obtained as described in Ref. [56]. These variations produce uncertainties below 3% on the expected number of events in the signal region in the search for promptly decaying ALPs.

The uncertainties of the NN-based classifiers are estimated by comparing their identification performance using $Z \rightarrow ee$ events in simulation and data, where the electron shower-shape variables are used as the network input variables. Very good agreement of the network output between data and simulation is observed. The residual differences are fully propagated as uncertainties on the expected signal yields and produce normalisation uncertainties of up to 15% in the 2M and 1M1S categories, respectively.

6.1.1 Uncertainties due to displaced ALP decays

The uncertainties related to photon identification and energy reconstruction for photons produced with displaced vertices – i.e., those arising from long-lived ALP decays – are estimated by studying the decays of long-lived hadrons, mainly kaons, which can be reconstructed as displaced tracks in the ATLAS tracking system. The daughter tracks from these decays, which originate from a displaced vertex, can be matched to reconstructed clusters in the electromagnetic calorimeter. A comparison of the shower shapes predicted by simulations to those from data for signatures with displaced vertices can then be used to estimate systematic uncertainties in photon reconstruction. The MC prediction of the shower shapes of hadronic particles also relies on the correct description of particle multiplicities and energies. To correct for any mismatch of particle composition in data and simulation, scale factors are derived from the differences between data and MC predictions for shower-shape variables of tracks close to the primary vertex ($z_0 < 20$ mm and $d_0 < 1$ mm, where z_0 and d_0 are the longitudinal distance from the IP and the impact parameter, respectively). These deviations are taken as a nominal bias and are used to correct tracks originating from a distance between $20 \text{ mm} < z_0 < 500 \text{ mm}$ and $1 \text{ mm} < d_0 < 80 \text{ mm}$ from the primary vertex (medium regime), and tracks with an origin further than $z_0 > 500 \text{ mm}$ and $d_0 > 80 \text{ mm}$ from the interaction point (far regime). These systematic uncertainties are used additionally for all photons stemming from a displaced decay. The systematic uncertainty from the modelling of the NN classifier that discriminates real photons from fakes due to displaced photon vertices is 3%. The corresponding uncertainties from the modelling of the photon identification and the second NN, which discriminates between merged and resolved photons, ranges from 4% to 23%, depending on the displacement.

Long-lived hadrons are also utilized to estimate systematic uncertainties in energy reconstruction. The observed differences in the momentum over energy ratio between the prompt, medium and far regimes are found to be negligible compared to the nominal energy reconstruction uncertainty.

Systematic uncertainties in identifying the correct ALP pairing are mainly caused by variations in the photon energy scale corrections within their uncertainties. The final impact on the number of reconstructed events in a particular ALP mass signal region is less than 5% and hence negligible.

6.2 Uncertainties on the Background Estimation

The continuum background processes are estimated from data and are subject to uncertainties related to the potential bias arising from the selected background model, as detailed in Section 5. The nominal background estimate in each bin is calculated using the nominal fitting functions, which have been fitted in the sideband regions. The shape uncertainty of the background is estimated by employing the same nominal fitting functions, but fitting them in a sideband region whose width is varied by 5 GeV, corresponding to a 25% to 100% change in the fit range, depending on the category, allowing for a large variability of the background shape. The spurious signal bias or background model bias is assessed as an additional uncertainty on the total number of signal events in each category. This bias is estimated by generating

pseudo-data using a modified background model and performing the full signal-plus-background fit (see Section 7) on these pseudo-data [60]. The alternative background model for the spurious signal bias estimate is based on a second-order polynomial for the 2M, 1M1S, 3S, and 4S categories, while the function $f_{\text{sys}} = N_0 \exp(p \cdot x) + N_1 + a \cdot x^2 + b \cdot x$ is used for the 2S category. The estimated signal-strength in these pseudo-data is considered as an additional systematic uncertainty in the final signal-strength estimation. The largest impact is found in the 4S category shifting the branching ratio limit by 10^{-6} .

6.3 Impact of Theory Uncertainties

To estimate the effects of scale uncertainties arising from missing higher-order corrections in the theoretical calculations, the factorisation and renormalisation scales are varied up and down by a factor of two from their nominal values. The cross-section is then recalculated for each case, and the largest deviation from the nominal cross-section is taken as the uncertainty. The uncertainties on the SM Higgs ggF production cross-section due to the choice of renormalisation scheme and top-quark mass, as well as their combination with those from factorisation and renormalisation scale variations, are based on Ref. [61]. The uncertainties in the cross-sections, which include the effects of uncertainties on the PDF and the strong coupling constant α_s , and the uncertainties in the $H \rightarrow \gamma\gamma$ branching fractions, are taken from Ref. [45] to be 5.7%. It is found that further uncertainties on the Higgs boson signal prediction are negligible.

The uncertainties on the Higgs boson production cross-section enter when calculating the limit on the branching ratio of the signal process on all Higgs boson decays. The values for the uncertainties are taken from Ref. [45].

7 Results

The statistical analysis is carried out using the PyHF framework [62]. In the long-lived ALP searches, the analysis results are obtained by performing a simultaneous maximum-likelihood fit to the $m_{\text{inv}}^{\text{reco}}$ distribution over the range 100 GeV to 150 GeV for the two most sensitive categories for each ALP mass and coupling parameter. The 2M and 1S1M categories are most sensitive for low ALP masses ($m_a < 5$ GeV), while for larger ALP masses, the 4S category dominates over the 3S category. Including more than two categories in the fit does not significantly improve the sensitivity for any model parameter. In the prompt ALP search, only the number of events in the signal region of the $4S_p$ category is used. The analysis sensitivity is limited by the available data statistics for the 4S and $4S_p$ categories, while the systematic uncertainties dominate in other categories. The likelihood function is defined as follows:

$$\mathcal{L} = \prod_c \left(\text{Pois}(n_c | N_c(\boldsymbol{\theta})) \cdot \prod_{i=1}^{n_{\text{bins}}^c} f_c(n_i, m_{\text{inv}}^{\text{reco},i}, \boldsymbol{\theta}) \right) \cdot G(\boldsymbol{\theta}). \quad (1)$$

Here, n_{bins}^c is the number of bins in the $m_{\text{inv}}^{\text{reco}}$ distribution, n_c is the observed number of events, and N_c is the expected number of events for each category c . For each bin i in the $m_{\text{inv}}^{\text{reco}}$ distribution of category c , f_c is the value of the probability density function (pdf) which is estimated from simulation, n_i is the number of observed events in bin i , $\boldsymbol{\theta}$ represents the nuisance parameters (NP) used to parametrize the effect of systematic uncertainties, and $G(\boldsymbol{\theta})$ represents constraint pdfs for the nuisance parameters. All constraints correspond to Gaussian pdfs. The expected number of events N_c is defined as the sum of the expected

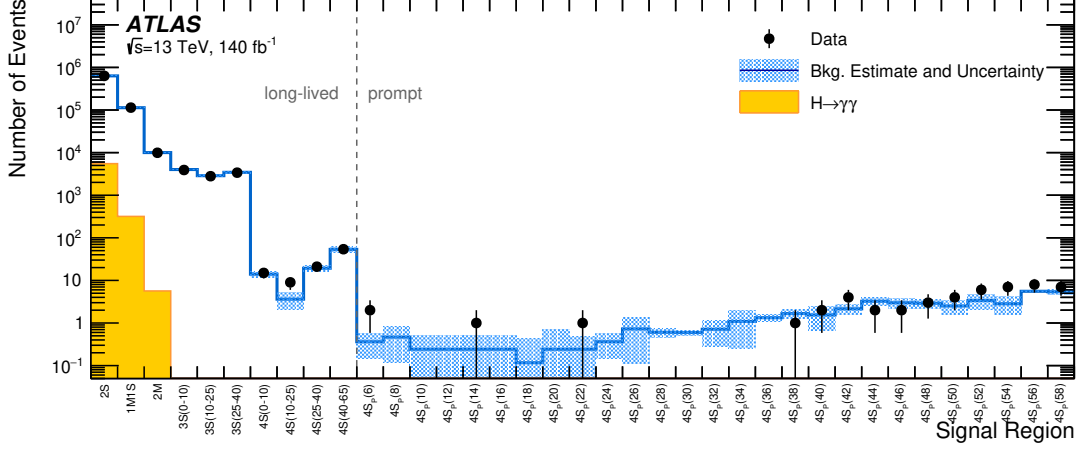


Figure 4: The number of data and estimated background events in the signal region of the most sensitive categories. The uncertainty in the background estimate is shown as shaded band. The left side shows the different categories of the long-lived ALP search, while the right side displays the $4S_p$ category of the prompt search for increasing mass hypotheses. The numbers in parentheses in the x-axis labels correspond to the probed ALP mass hypothesis in GeV. The SM $H \rightarrow \gamma\gamma$ background is only sizeable in the first three bins, corresponding to the two-photon categories.

yields from $H \rightarrow aa \rightarrow 4\gamma$ production processes ($N_{H \rightarrow aa}$), single Higgs-boson production ($N_{\text{bkg}}^{H \rightarrow \gamma\gamma}$), the non-resonant background ($N_{\text{bkg},c}^{\text{nonres}}$), and the spurious signal uncertainty ($N_{\text{SS},c}$). It is defined as:

$$N_c(\boldsymbol{\theta}) = \mu \cdot N_{H \rightarrow aa}(\boldsymbol{\theta}_{H \rightarrow aa}^{\text{yield}}) + N_{\text{bkg}}^{H \rightarrow \gamma\gamma}(\boldsymbol{\theta}_{H \rightarrow \gamma\gamma}^{\text{yield}}) + N_{\text{bkg},c}^{\text{nonres}}(\boldsymbol{\theta}_{\text{nonres}}^{\text{yield}}) + N_{\text{SS},c}. \quad (2)$$

Here, μ is the signal strength, and $\boldsymbol{\theta}^{\text{yield}}$ represents the NPs affecting the event yield, as described in Section 6. Correlation of the nuisance parameters across different signal and background components, and categories, is taken into account. The normalisation parameter for the $H \rightarrow \gamma\gamma$ production rate, $\boldsymbol{\theta}_{H \rightarrow \gamma\gamma}^{\text{yield}}$, is set to 1 and corresponds to the SM prediction for the $H \rightarrow \gamma\gamma$ cross-section. It is allowed to vary within its theoretical and experimental uncertainties.

The signal-plus-background hypothesis for the production of a Higgs boson that decays into ALPs is tested using the profile-likelihood-ratio test statistic derived from Eq. 1, and is parameterized with the signal-strength parameter μ . This parameter is defined as the ratio of the extracted signal events to the total number of signal events in the MC simulation.³

Figure 4 shows the distribution of the number of estimated and observed events in the signal region of the most sensitive category for various ALP masses and coupling parameters for the prompt and long-lived ALP searches. Good agreement is observed between the estimated backgrounds and the data. No significant pulls of the NP are observed after the fits. The NP $\boldsymbol{\theta}_{H \rightarrow \gamma\gamma}^{\text{yield}}$ is found to be consistent with 1, corresponding to the expected SM Higgs boson production cross-section on the 2S category.

Upper limits, derived using the CLs technique [63], are set on $\mathcal{B}(H \rightarrow aa \rightarrow 4\gamma)$. The branching ratio is obtained by dividing the fitted signal cross-section by the total Higgs-boson production cross-section of 55.6 pb [45]. The expected and observed limits as a function of m_a from the search optimized for long-lived

³ Only $H \rightarrow aa \rightarrow 4\gamma$ events are simulated in the signal samples, i.e., the branching ratio for this process is unity in the simulation.

ALPs, i.e., $C_{a\gamma\gamma} < 0.1$, are shown in Figure 5 along with the performance on prompt decays for $C_{a\gamma\gamma} = 1$. For low masses and low couplings, the lifetime of the ALP gets significantly larger and most of the ALPs decay outside the active detector area. Therefore there are no limits available for $C_{a\gamma\gamma} \geq 5 \times 10^{-4}$ and $m_a < 10$ GeV. Limits for prompt decays with $C_{a\gamma\gamma} = 1$ are also shown. A relatively uniform sensitivity is achieved for larger ALP masses, above 10 GeV for $C_{a\gamma\gamma} \geq 5 \times 10^{-4}$ and above 25 GeV for $C_{a\gamma\gamma} = 10^{-5}$. The sensitivity for low ALP masses decreases with smaller coupling values, as more ALP decays happen outside the sensitive detector volume. The largest differences between expected and observed limits are found in long-lived ALP searches for masses between 10 and 25 GeV at 1.5σ . It should be noted that the background estimation is the same for all couplings in this mass region. Hence correlated behaviour is expected for all relevant couplings. The limits for the couplings $C_{a\gamma\gamma} = 1$ and $C_{a\gamma\gamma} = 0.01$ as a function of m_a are shown in Figure 6, separated for low ALP masses ($m_a < 5$ GeV) and higher ALP masses. The upper limits at 95% CL on $\mathcal{B}(H \rightarrow aa \rightarrow 4\gamma)$ range from 10^{-4} to 3×10^{-2} for low ALP masses and from 2×10^{-5} to 2×10^{-4} for higher ALP masses. The observed limits are compatible with the expected limits. The loss in sensitivity around 3 GeV is due to the transition between the merged and resolved photon categories, where the former have significantly larger background contributions.

The limits on $\mathcal{B}(H \rightarrow aa \rightarrow 4\gamma)$ derived from the $4S_p$ category assuming promptly decaying ALPs are shown in Figure 7. The derived limit is mostly flat at $\mathcal{B} < 2 \times 10^{-5}$ in the mass range $10 \text{ GeV} < m_a < 62 \text{ GeV}$. For the long-lived searches it is necessary to loosen the selection criteria to allow for displaced ALP decays. Therefore the background contributions are significantly larger and consequently the searches are less sensitive than the prompt searches. The observed limits are consistent with the expected limits.

The limits on ALP masses with $m_a > 15$ GeV are about one order of magnitude more stringent than previous ATLAS analyses [26] using 8 TeV data, and reach similar to slightly better sensitivity than previous analyses from CMS [28] using 132 fb^{-1} of $\sqrt{s} = 13$ TeV data. These are the first limits on ALPs with masses below 10 GeV from the ATLAS experiment, and are up to 40% more stringent than previous results from CMS [27] using 136 fb^{-1} of $\sqrt{s} = 13$ TeV data. The limits on long-lived ALPs in anomalous Higgs boson decays are the first obtained by any experiment.

The limit on the branching ratio can be converted into a limit on the coupling of axion-like particles to photons, $C_{a\gamma\gamma}$. The branching ratio, which depends on $C_{a\gamma\gamma}$, can be calculated using the method described in Ref. [19]:

$$\mathcal{B}^{\text{theo}} = \Gamma_{Haa} f_{aa}^2(C_{a\gamma\gamma}) \frac{\mathcal{B}(a \rightarrow \gamma\gamma)}{\Gamma_H + \Gamma_{Haa}}, \quad (3)$$

where it is assumed that all ALPs decay into photons and hence $\mathcal{B}(a \rightarrow \gamma\gamma) = 1$. In the following m_a and m_H refer to the masses of the ALP and Higgs boson, respectively, v is the vacuum expectation value, and the effective coupling of the ALP to the Higgs boson is assumed to be $C_{aH}^{\text{eff}}/\Lambda^2 = 1 \text{ TeV}^{-2}$. Γ_H is the total decay width of the Higgs boson. The Higgs boson to ALP decay width Γ_{Haa} is calculated as

$$\Gamma_{Haa} = \frac{v^2 m_H^3}{32\pi} \frac{|C_{aH}^{\text{eff}}|^2}{\Lambda^4} \left(1 - \frac{2m_a^2}{m_H^2}\right)^2 \sqrt{1 - \frac{4m_a^2}{m_H^2}}. \quad (4)$$

Using the Higgs mass of $m_H = 125$ GeV and assuming $m_a = 10$ GeV and $C_{aH}^{\text{eff}}/\Lambda^2 = 1 \text{ TeV}^{-2}$ yields a branching ratio of the $H \rightarrow aa$ process of 30%. The factor $f_{aa}^2(C_{a\gamma\gamma})$ represents the fraction of ALPs detected inside the detector volume. It depends on the ALP decay length, and hence on $C_{a\gamma\gamma}$, since the decay width is given by

$$\Gamma_{a\gamma\gamma} = \frac{4\pi\alpha^2 m_a^3}{\Lambda^2} |C_{a\gamma\gamma}|^2. \quad (5)$$

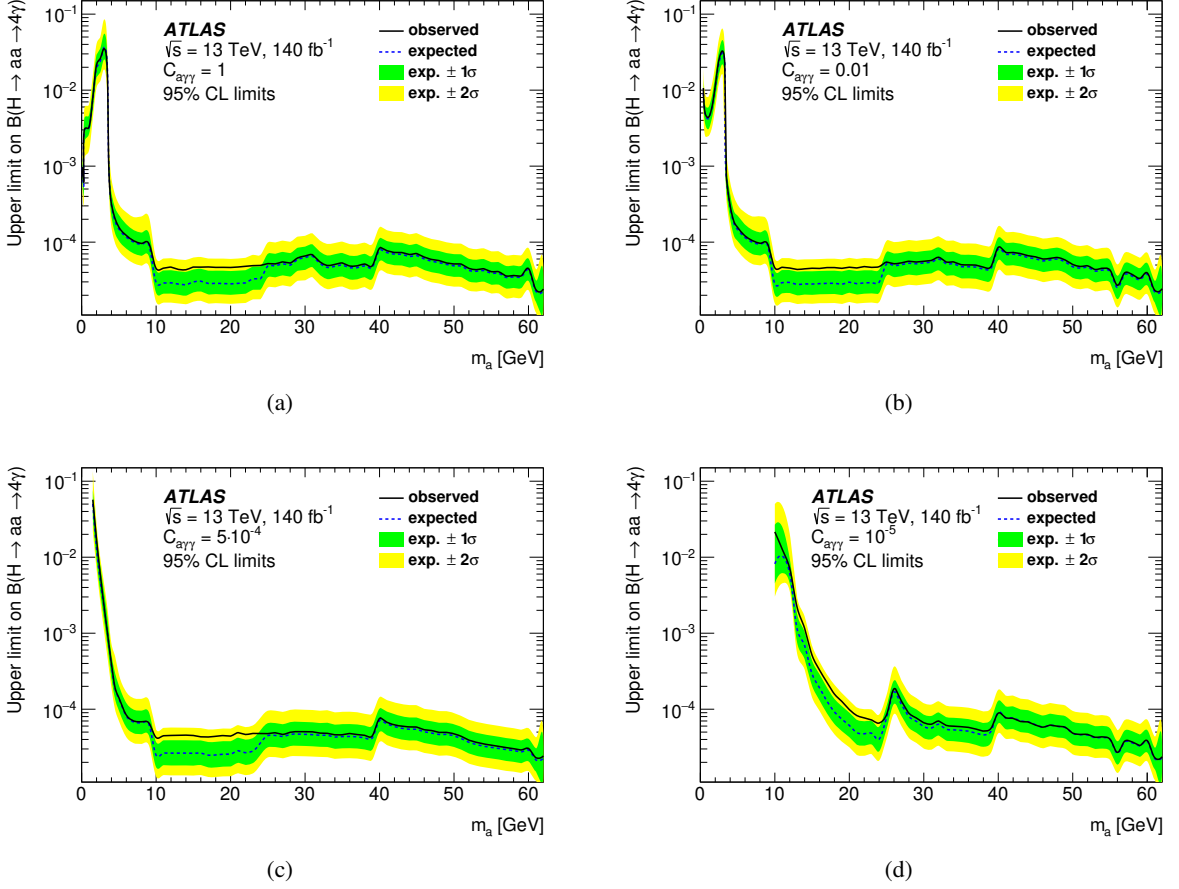


Figure 5: Upper limits on $\mathcal{B}(H \rightarrow aa \rightarrow 4\gamma)$ at 95% CL as a function of the axion mass and for different ALP-photon couplings, from (a) $C_{a\gamma\gamma} = 1$ to (d) $C_{a\gamma\gamma} = 10^{-5}$.

f_{aa} is determined from the signal simulation and interpolated between the simulated $C_{a\gamma\gamma}$ values. The coupling is adjusted until the expected branching ratio matches the observed limit on the branching ratio, yielding the corresponding limit on $C_{a\gamma\gamma}$.

The resulting limits are shown in the two-dimensional exclusion plot of $C_{a\gamma\gamma}$ vs. m_a presented in Figure 8. This search significantly reduces the allowed parameter space for ALP-based models that could explain the $(g-2)_\mu$ discrepancy in the $H \rightarrow aa \rightarrow 4\gamma$ decay mode, as suggested in Ref. [19].

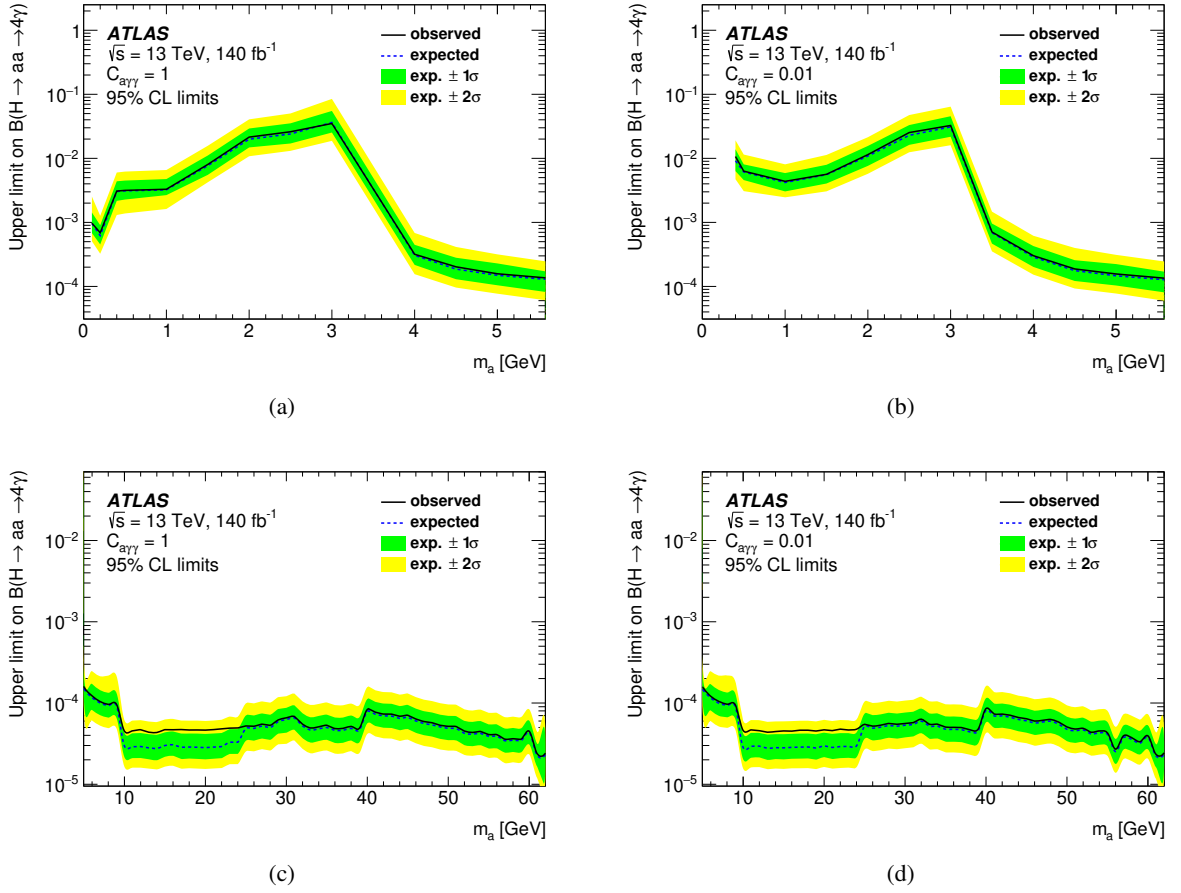


Figure 6: Zoomed in version of Fig. 5 showing upper limits on $\mathcal{B}(H \rightarrow aa \rightarrow 4\gamma)$ at 95% CL as a function of the signal mass hypothesis and for different ALP-photon couplings. (a) $m_a < 5.0$ GeV, $C_{a\gamma\gamma} = 1$; (b) $m_a < 5.0$ GeV, $C_{a\gamma\gamma} = 0.01$; (c) $m_a > 5.0$ GeV, $C_{a\gamma\gamma} = 1$; (d) $m_a > 5.0$ GeV, $C_{a\gamma\gamma} = 0.01$.

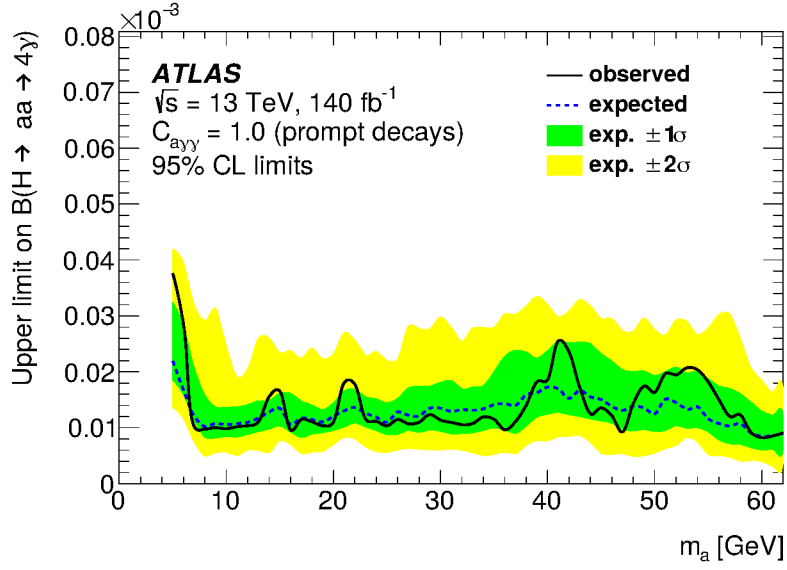


Figure 7: Upper limits on $\mathcal{B}(H \rightarrow aa \rightarrow 4\gamma)$ at 95% CL as a function of the signal mass hypothesis and for the assumption of promptly decaying ALPs.

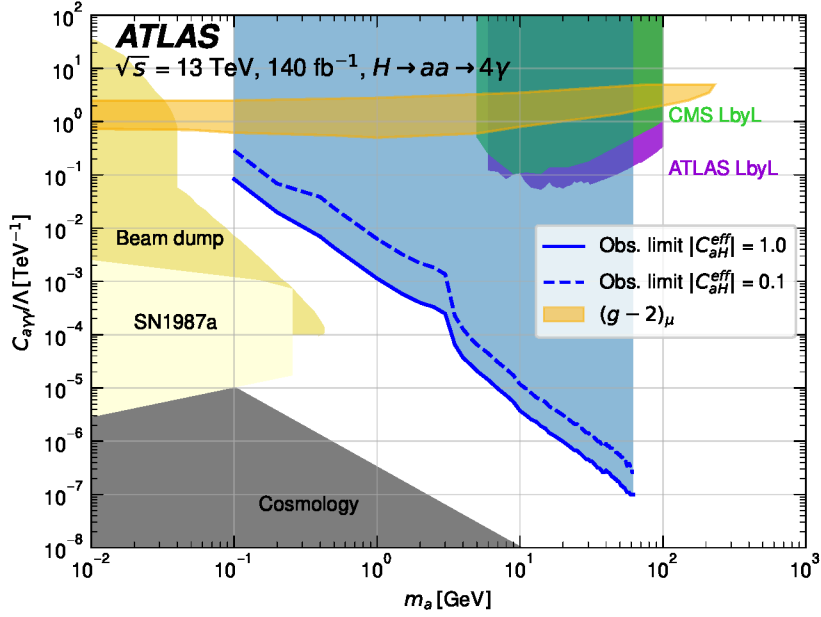


Figure 8: Limits on the ALP mass and coupling to photons at 95% CL, assuming $\mathcal{B}(a \rightarrow \gamma\gamma) = 1$, $\Lambda = 1$ TeV with $|C_{aH}^{\text{eff}}| = 1$ (solid line) and $|C_{aH}^{\text{eff}}| = 0.1$ (dashed line) as predicted in Ref. [19]. The shaded blue area represents the excluded region. The nearly horizontal orange shaded area indicates the region favoured by an ALP explanation for the $(g - 2)_\mu$ discrepancy [19]. Also shown are exclusion limits from the respective ATLAS [64] and CMS [65] Light-by-Light (LbyL) scattering analysis, and beam dump experiments, supernova SN1987a and cosmological observations adapted from Ref. [66].

8 Conclusion

This paper reports a search for a light pseudoscalar particle (a) produced in the decay $H \rightarrow aa$, where H is the 125 GeV Higgs boson. The a boson, which can have a short or long lifetime, decays into two photons, resulting in a final state with four photons with an invariant mass near 125 GeV. The analysis uses 140 fb^{-1} of pp collision data at a centre-of-mass energy of 13 TeV collected by the ATLAS detector between 2015 and 2018. The search aims to identify a narrow $a \rightarrow \gamma\gamma$ resonance with a mass in the range of 100 MeV to 62 GeV, where the resonance decay occurs within a distance of 1970 mm from the collision vertex. Dedicated search strategies for long-lived $a \rightarrow \gamma\gamma$ decays are developed for the first time. To enable the search for low resonance masses, neural network classifiers are trained to distinguish between single and collimated photon signatures.

No significant excess over the Standard Model backgrounds is observed in the data. The largest deviation from the expected limit, 1.5σ , is observed in the range of $10 \text{ GeV} < m_a < 25 \text{ GeV}$. Upper limits at 95% CL are set for $\mathcal{B}(H \rightarrow aa \rightarrow 4\gamma)$, which range from 2×10^{-5} to 3×10^{-2} depending on m_a for the prompt axion-like particle search. For the search for long-lived ALPs with significant displaced decay vertices, upper limits at 95% CL are set, ranging from 2×10^{-5} to 6×10^{-5} for $10 \text{ GeV} < m_a < 62 \text{ GeV}$ and from 10^{-4} to 3×10^{-2} for $0.1 \text{ GeV} < m_a < 10 \text{ GeV}$. These are the most stringent limits to date.

Acknowledgements

We thank CERN for the very successful operation of the LHC, as well as the support staff from our institutions without whom ATLAS could not be operated efficiently.

We acknowledge the support of ANPCyT, Argentina; YerPhI, Armenia; ARC, Australia; BMFWF and FWF, Austria; ANAS, Azerbaijan; CNPq and FAPESP, Brazil; NSERC, NRC and CFI, Canada; CERN; ANID, Chile; CAS, MOST and NSFC, China; Minciencias, Colombia; MEYS CR, Czech Republic; DNRF and DNSRC, Denmark; IN2P3-CNRS and CEA-DRF/IRFU, France; SRNSFG, Georgia; BMBF, HGF and MPG, Germany; GSRI, Greece; RGC and Hong Kong SAR, China; ISF and Benozziyo Center, Israel; INFN, Italy; MEXT and JSPS, Japan; CNRST, Morocco; NWO, Netherlands; RCN, Norway; MEiN, Poland; FCT, Portugal; MNE/IFA, Romania; MESTD, Serbia; MSSR, Slovakia; ARRS and MIZŠ, Slovenia; DSI/NRF, South Africa; MICINN, Spain; SRC and Wallenberg Foundation, Sweden; SERI, SNSF and Cantons of Bern and Geneva, Switzerland; MOST, Taiwan; TENMAK, Türkiye; STFC, United Kingdom; DOE and NSF, United States of America. In addition, individual groups and members have received support from BCKDF, CANARIE, Compute Canada and CRC, Canada; PRIMUS 21/SCI/017 and UNCE SCI/013, Czech Republic; COST, ERC, ERDF, Horizon 2020, ICSC-NextGenerationEU and Marie Skłodowska-Curie Actions, European Union; Investissements d’Avenir Labex, Investissements d’Avenir IDEX and ANR, France; DFG and AvH Foundation, Germany; Herakleitos, Thales and Aristeia programmes co-financed by EU-ESF and the Greek NSRF, Greece; BSF-NSF and MINERVA, Israel; Norwegian Financial Mechanism 2014-2021, Norway; NCN and NAWA, Poland; La Caixa Banking Foundation, CERCA Programme Generalitat de Catalunya and PROMETEO and GenT Programmes Generalitat Valenciana, Spain; Göran Gustafssons Stiftelse, Sweden; The Royal Society and Leverhulme Trust, United Kingdom.

The crucial computing support from all WLCG partners is acknowledged gratefully, in particular from CERN, the ATLAS Tier-1 facilities at TRIUMF (Canada), NDGF (Denmark, Norway, Sweden), CC-IN2P3 (France), KIT/GridKA (Germany), INFN-CNAF (Italy), NL-T1 (Netherlands), PIC (Spain), ASGC (Taiwan), RAL (UK) and BNL (USA), the Tier-2 facilities worldwide and large non-WLCG resource providers. Major contributors of computing resources are listed in Ref. [67].

References

- [1] ATLAS Collaboration, *Observation of a new particle in the search for the Standard Model Higgs boson with the ATLAS detector at the LHC*, *Phys. Lett. B* **716** (2012) 1, arXiv: [1207.7214 \[hep-ex\]](#).
- [2] CMS Collaboration, *Observation of a new boson at a mass of 125 GeV with the CMS experiment at the LHC*, *Phys. Lett. B* **716** (2012) 30, arXiv: [1207.7235 \[hep-ex\]](#).
- [3] B. A. Dobrescu and K. T. Matchev, *Light axion within the next-to-minimal supersymmetric standard model*, *JHEP* **09** (2000) 031, arXiv: [hep-ph/0008192](#).
- [4] U. Ellwanger, J. F. Gunion, C. Hugonie and S. Moretti, *Towards a No-Lose Theorem for NMSSM Higgs Discovery at the LHC*, (2003), arXiv: [hep-ph/0305109](#).

- [5] S. Profumo, M. J. Ramsey-Musolf and G. Shaughnessy, *Singlet Higgs phenomenology and the electroweak phase transition*, *JHEP* **08** (2007) 010, arXiv: [0705.2425 \[hep-ph\]](#).
- [6] N. Blinov, J. Kozaczuk, D. E. Morrissey and C. Tamarit, *Electroweak Baryogenesis from Exotic Electroweak Symmetry Breaking*, *Phys. Rev. D* **92** (2015) 035012, arXiv: [1504.05195 \[hep-ph\]](#).
- [7] N. Craig, A. Katz, M. Strassler and R. Sundrum, *Naturalness in the Dark at the LHC*, *JHEP* **07** (2015) 105, arXiv: [1501.05310 \[hep-ph\]](#).
- [8] D. Curtin and C. B. Verhaaren, *Discovering Uncolored Naturalness in Exotic Higgs Decays*, *JHEP* **12** (2015) 072, arXiv: [1506.06141 \[hep-ph\]](#).
- [9] V. Silveira and A. Zee, *SCALAR PHANTOMS*, *Phys. Lett. B* **161** (1985) 136.
- [10] M. Pospelov, A. Ritz and M. Voloshin, *Secluded WIMP Dark Matter*, *Phys. Lett. B* **662** (2008) 53, arXiv: [0711.4866 \[hep-ph\]](#).
- [11] P. Draper, T. Liu, C. E. M. Wagner, L.-T. Wang and H. Zhang, *Dark Light-Higgs Bosons*, *Phys. Rev. Lett.* **106** (2011) 121805, arXiv: [1009.3963 \[hep-ph\]](#).
- [12] S. Ipek, D. McKeen and A. E. Nelson, *Renormalizable model for the Galactic Center gamma-ray excess from dark matter annihilation*, *Phys. Rev. D* **90** (2014) 055021, arXiv: [1404.3716 \[hep-ph\]](#).
- [13] A. Martin, J. Shelton and J. Unwin, *Fitting the Galactic Center Gamma-Ray Excess with Cascade Annihilations*, *Phys. Rev. D* **90** (2014) 103513, arXiv: [1405.0272 \[hep-ph\]](#).
- [14] C. Boehm, M. J. Dolan, C. McCabe, M. Spannowsky and C. J. Wallace, *Extended gamma-ray emission from Coy Dark Matter*, *JCAP* **05** (2014) 009, arXiv: [1401.6458 \[hep-ph\]](#).
- [15] D. Curtin et al., *Exotic decays of the 125 GeV Higgs boson*, *Phys. Rev. D* **90** (2014) 075004, arXiv: [1312.4992 \[hep-ph\]](#).
- [16] ATLAS Collaboration, *Combination of searches for invisible decays of the Higgs boson using 139 fb⁻¹ of proton-proton collision data at $\sqrt{s} = 13$ TeV collected with the ATLAS experiment*, *Phys. Lett. B* **842** (2023) 137963, arXiv: [2301.10731 \[hep-ex\]](#).
- [17] ATLAS Collaboration, *A detailed map of Higgs boson interactions by the ATLAS experiment ten years after the discovery*, *Nature* **607** (2022) 52, arXiv: [2207.00092 \[hep-ex\]](#), Erratum: *Nature* **612** (2022) E24.
- [18] CMS Collaboration, *A portrait of the Higgs boson by the CMS experiment ten years after the discovery.*, *Nature* **607** (2022) 60, arXiv: [2207.00043 \[hep-ex\]](#).
- [19] M. Bauer, M. Neubert and A. Thamm, *Collider Probes of Axion-Like Particles*, *JHEP* **12** (2017) 044, arXiv: [1708.00443 \[hep-ph\]](#).
- [20] Muon g-2 Collaboration, *Measurement of the Positive Muon Anomalous Magnetic Moment to 0.46 ppm*, *Phys. Rev. Lett.* **126** (2021) 141801, arXiv: [2104.03281 \[hep-ex\]](#).

- [21] Muon g-2 Collaboration, *Final report of the E821 muon anomalous magnetic moment measurement at BNL*, *Phys. Rev. D* **73** (2006) 072003, arXiv: [hep-ex/0602035](#).
- [22] D. P. Aguillard et al., *Measurement of the Positive Muon Anomalous Magnetic Moment to 0.20 ppm*, (2023), arXiv: [2308.06230 \[hep-ex\]](#).
- [23] T. Aoyama et al., *The anomalous magnetic moment of the muon in the Standard Model*, *Phys. Rept.* **887** (2020) 1, arXiv: [2006.04822 \[hep-ph\]](#).
- [24] RBC and UKQCD Collaborations, *Calculation of the hadronic vacuum polarization contribution to the muon anomalous magnetic moment*, *Phys. Rev. Lett.* **121** (2018) 022003, arXiv: [1801.07224 \[hep-lat\]](#).
- [25] L. Evans and P. Bryant, *LHC Machine*, *JINST* **3** (2008) S08001.
- [26] ATLAS Collaboration, *Search for new phenomena in events with at least three photons collected in pp collisions at $\sqrt{s} = 8$ TeV with the ATLAS detector*, *Eur. Phys. J. C* **76** (2016) 210, arXiv: [1509.05051 \[hep-ex\]](#).
- [27] CMS Collaboration, *Search for exotic Higgs boson decays $H \rightarrow \mathcal{A}\mathcal{A} \rightarrow 4\gamma$ with events containing two merged diphotons in proton-proton collisions at $\sqrt{s} = 13$ TeV*, *Phys. Rev. Lett.* **131** (2023) 101801, arXiv: [2209.06197 \[hep-ex\]](#).
- [28] CMS Collaboration, *Search for the exotic decay of the Higgs boson into two light pseudoscalars with four photons in the final state in proton-proton collisions at $\sqrt{s} = 13$ TeV*, *JHEP* **07** (2023) 148, arXiv: [2208.01469 \[hep-ex\]](#).
- [29] ATLAS Collaboration, *The ATLAS Experiment at the CERN Large Hadron Collider*, *JINST* **3** (2008) S08003.
- [30] ATLAS Collaboration, *ATLAS Insertable B-Layer: Technical Design Report*, ATLAS-TDR-19; CERN-LHCC-2010-013, 2010, URL: <https://cds.cern.ch/record/1291633>, Addendum: ATLAS-TDR-19-ADD-1; CERN-LHCC-2012-009, 2012, URL: <https://cds.cern.ch/record/1451888>.
- [31] B. Abbott et al., *Production and integration of the ATLAS Insertable B-Layer*, *JINST* **13** (2018) T05008, arXiv: [1803.00844 \[physics.ins-det\]](#).
- [32] ATLAS Collaboration, *Performance of the ATLAS trigger system in 2015*, *Eur. Phys. J. C* **77** (2017) 317, arXiv: [1611.09661 \[hep-ex\]](#).
- [33] ATLAS Collaboration, *The ATLAS Collaboration Software and Firmware*, ATL-SOFT-PUB-2021-001, 2021, URL: <https://cds.cern.ch/record/2767187>.
- [34] ATLAS Collaboration, *ATLAS data quality operations and performance for 2015–2018 data-taking*, *JINST* **15** (2020) P04003, arXiv: [1911.04632 \[physics.ins-det\]](#).
- [35] ATLAS Collaboration, *Luminosity determination in pp collisions at $\sqrt{s} = 13$ TeV using the ATLAS detector at the LHC*, *Eur. Phys. J. C* **83** (2023) 982, arXiv: [2212.09379 \[hep-ex\]](#).
- [36] T. Gleisberg et al., *Event generation with SHERPA 1.1*, *JHEP* **02** (2009) 007, arXiv: [0811.4622 \[hep-ph\]](#).
- [37] E. Bothmann et al., *Event generation with Sherpa 2.2*, *SciPost Phys.* **7** (2019) 034, arXiv: [1905.09127 \[hep-ph\]](#).

- [38] S. Höche, F. Krauss, S. Schumann and F. Siegert, *QCD matrix elements and truncated showers*, **JHEP** **05** (2009) 053, arXiv: [0903.1219](#) [[hep-ph](#)].
- [39] ATLAS Collaboration, *Measurement of the Z/γ^* boson transverse momentum distribution in pp collisions at $\sqrt{s} = 7$ TeV with the ATLAS detector*, **JHEP** **09** (2014) 145, arXiv: [1406.3660](#) [[hep-ex](#)].
- [40] The NNPDF Collaboration, R. D. Ball et al., *Parton distributions for the LHC run II*, **JHEP** **04** (2015) 040, arXiv: [1410.8849](#) [[hep-ph](#)].
- [41] P. Nason, *A new method for combining NLO QCD with shower Monte Carlo algorithms*, **JHEP** **11** (2004) 040, arXiv: [hep-ph/0409146](#).
- [42] S. Frixione, P. Nason and C. Oleari, *Matching NLO QCD computations with parton shower simulations: the POWHEG method*, **JHEP** **11** (2007) 070, arXiv: [0709.2092](#) [[hep-ph](#)].
- [43] S. Alioli, P. Nason, C. Oleari and E. Re, *A general framework for implementing NLO calculations in shower Monte Carlo programs: the POWHEG BOX*, **JHEP** **06** (2010) 043, arXiv: [1002.2581](#) [[hep-ph](#)].
- [44] T. Sjöstrand et al., *An introduction to PYTHIA 8.2*, **Comput. Phys. Commun.** **191** (2015) 159, arXiv: [1410.3012](#) [[hep-ph](#)].
- [45] D. de Florian et al., *Handbook of LHC Higgs Cross Sections: 4. Deciphering the Nature of the Higgs Sector*, (2016), arXiv: [1610.07922](#) [[hep-ph](#)].
- [46] C. Anastasiou et al., *High precision determination of the gluon fusion Higgs boson cross-section at the LHC*, **JHEP** **05** (2016) 058, arXiv: [1602.00695](#) [[hep-ph](#)].
- [47] S. Actis, G. Passarino, C. Sturm and S. Uccirati, *NLO electroweak corrections to Higgs boson production at hadron colliders*, **Phys. Lett. B** **670** (2008) 12, arXiv: [0809.1301](#) [[hep-ph](#)].
- [48] C. Anastasiou, R. Boughezal and F. Petriello, *Mixed QCD-electroweak corrections to Higgs boson production in gluon fusion*, **JHEP** **04** (2009) 003, arXiv: [0811.3458](#) [[hep-ph](#)].
- [49] D. Stump et al., *Inclusive jet production, parton distributions, and the search for new physics*, **JHEP** **10** (2003) 046, arXiv: [hep-ph/0303013](#).
- [50] NNPDF Collaboration, R. D. Ball et al., *Parton distributions with LHC data*, **Nucl. Phys. B** **867** (2013) 244, arXiv: [1207.1303](#) [[hep-ph](#)].
- [51] ATLAS Collaboration, *The Pythia 8 A3 tune description of ATLAS minimum bias and inelastic measurements incorporating the Donnachie–Landshoff diffractive model*, ATL-PHYS-PUB-2016-017, 2016, URL: <https://cds.cern.ch/record/2206965>.
- [52] ATLAS Collaboration, *The ATLAS Simulation Infrastructure*, **Eur. Phys. J. C** **70** (2010) 823, arXiv: [1005.4568](#) [[physics.ins-det](#)].
- [53] S. Agostinelli et al., *GEANT4 – a simulation toolkit*, **Nucl. Instrum. Meth. A** **506** (2003) 250.
- [54] ATLAS Collaboration, *Electron and photon reconstruction and performance in ATLAS using a dynamical, topological cell clustering-based approach*, ATL-PHYS-PUB-2017-022, 2017, URL: <https://cds.cern.ch/record/2298955>.

- [55] ATLAS Collaboration, *Electron and photon efficiencies in LHC Run 2 with the ATLAS experiment*, (2023), arXiv: [2308.13362 \[hep-ex\]](#).
- [56] ATLAS Collaboration, *Electron and photon performance measurements with the ATLAS detector using the 2015–2017 LHC proton–proton collision data*, *JINST* **14** (2019) P12006, arXiv: [1908.00005 \[hep-ex\]](#).
- [57] ATLAS Collaboration, *Electron and photon energy calibration with the ATLAS detector using LHC Run 2 data*, (2023), arXiv: [2309.05471 \[hep-ex\]](#).
- [58] ATLAS Collaboration, *Performance of electron and photon triggers in ATLAS during LHC Run 2*, *Eur. Phys. J. C* **80** (2020) 47, arXiv: [1909.00761 \[hep-ex\]](#).
- [59] G. Avoni et al., *The new LUCID-2 detector for luminosity measurement and monitoring in ATLAS*, *JINST* **13** (2018) P07017.
- [60] ATLAS Collaboration, *Recommendations for the Modeling of Smooth Backgrounds*, ATL-PHYS-PUB-2020-028, 2020, URL: <https://cds.cern.ch/record/2743717>.
- [61] J. Baglio et al., *$gg \rightarrow HH$: Combined uncertainties*, *Phys. Rev. D* **103** (2021) 056002, arXiv: [2008.11626 \[hep-ph\]](#).
- [62] L. Heinrich, M. Feickert, G. Stark and K. Cranmer, *pyhf: pure-Python implementation of HistFactory statistical models*, *J. Open Source Softw.* **6** (2021) 2823.
- [63] A. L. Read, *Presentation of search results: the CL_S technique*, *J. Phys. G* **28** (2002) 2693.
- [64] ATLAS Collaboration, *Measurement of light-by-light scattering and search for axion-like particles with 2.2 nb^{-1} of Pb+Pb data with the ATLAS detector*, *JHEP* **03** (2021) 243, arXiv: [2008.05355 \[hep-ex\]](#), Erratum: *JHEP* **11** (2021) 050.
- [65] CMS Collaboration, *Evidence for light-by-light scattering and searches for axion-like particles in ultraperipheral PbPb collisions at $\sqrt{s_{NN}} = 5.02 \text{ TeV}$* , *Phys. Lett. B* **797** (2019) 134826, arXiv: [1810.04602 \[hep-ex\]](#).
- [66] J. Jaeckel and M. Spannowsky, *Probing MeV to 90 GeV axion-like particles with LEP and LHC*, *Phys. Lett. B* **753** (2016) 482, arXiv: [1509.00476 \[hep-ph\]](#).
- [67] ATLAS Collaboration, *ATLAS Computing Acknowledgements*, ATL-SOFT-PUB-2023-001, 2023, URL: <https://cds.cern.ch/record/2869272>.

The ATLAS Collaboration

G. Aad ¹⁰², B. Abbott ¹²⁰, K. Abeling ⁵⁵, N.J. Abicht ⁴⁹, S.H. Abidi ²⁹, A. Aboulhorma ^{35e}, H. Abramowicz ¹⁵¹, H. Abreu ¹⁵⁰, Y. Abulaiti ¹¹⁷, B.S. Acharya ^{69a,69b,m}, C. Adam Bourdarios ⁴, L. Adamczyk ^{86a}, S.V. Addepalli ²⁶, M.J. Addison ¹⁰¹, J. Adelman ¹¹⁵, A. Adiguzel ^{21c}, T. Adye ¹³⁴, A.A. Affolder ¹³⁶, Y. Afik ³⁶, M.N. Agaras ¹³, J. Agarwala ^{73a,73b}, A. Aggarwal ¹⁰⁰, C. Agheorghiesei ^{27c}, A. Ahmad ³⁶, F. Ahmadov ^{38,y}, W.S. Ahmed ¹⁰⁴, S. Ahuja ⁹⁵, X. Ai ^{62a}, G. Aielli ^{76a,76b}, A. Aikot ¹⁶³, M. Ait Tamlihat ^{35e}, B. Aitbenchikh ^{35a}, I. Aizenberg ¹⁶⁹, M. Akbiyik ¹⁰⁰, T.P.A. Åkesson ⁹⁸, A.V. Akimov ³⁷, D. Akiyama ¹⁶⁸, N.N. Akolkar ²⁴, K. Al Khoury ⁴¹, G.L. Alberghi ^{23b}, J. Albert ¹⁶⁵, P. Albicocco ⁵³, G.L. Albouy ⁶⁰, S. Alderweireldt ⁵², M. Aleksa ³⁶, I.N. Aleksandrov ³⁸, C. Alexa ^{27b}, T. Alexopoulos ¹⁰, F. Alfonsi ^{23b}, M. Algren ⁵⁶, M. Alhroob ¹²⁰, B. Ali ¹³², H.M.J. Ali ⁹¹, S. Ali ¹⁴⁸, S.W. Alibocus ⁹², M. Aliev ¹⁴⁵, G. Alimonti ^{71a}, W. Alkakhri ⁵⁵, C. Allaire ⁶⁶, B.M.M. Allbrooke ¹⁴⁶, J.F. Allen ⁵², C.A. Allendes Flores ^{137f}, P.P. Allport ²⁰, A. Aloisio ^{72a,72b}, F. Alonso ⁹⁰, C. Alpigiani ¹³⁸, M. Alvarez Estevez ⁹⁹, A. Alvarez Fernandez ¹⁰⁰, M. Alves Cardoso ⁵⁶, M.G. Alviggi ^{72a,72b}, M. Aly ¹⁰¹, Y. Amaral Coutinho ^{83b}, A. Ambler ¹⁰⁴, C. Amelung ³⁶, M. Amerl ¹⁰¹, C.G. Ames ¹⁰⁹, D. Amidei ¹⁰⁶, S.P. Amor Dos Santos ^{130a}, K.R. Amos ¹⁶³, V. Ananiev ¹²⁵, C. Anastopoulos ¹³⁹, T. Andeen ¹¹, J.K. Anders ³⁶, S.Y. Andreev ^{47a,47b}, A. Andreatta ^{71a,71b}, S. Angelidakis ⁹, A. Angerami ^{41,ab}, A.V. Anisenkov ³⁷, A. Annovi ^{74a}, C. Antel ⁵⁶, M.T. Anthony ¹³⁹, E. Antipov ¹⁴⁵, M. Antonelli ⁵³, F. Anulli ^{75a}, M. Aoki ⁸⁴, T. Aoki ¹⁵³, J.A. Aparisi Pozo ¹⁶³, M.A. Aparo ¹⁴⁶, L. Aperio Bella ⁴⁸, C. Appelt ¹⁸, A. Apyan ²⁶, N. Aranzabal ³⁶, S.J. Arbiol Val ⁸⁷, C. Arcangeletti ⁵³, A.T.H. Arce ⁵¹, E. Arena ⁹², J-F. Arguin ¹⁰⁸, S. Argyropoulos ⁵⁴, J.-H. Arling ⁴⁸, O. Arnaez ⁴, H. Arnold ¹¹⁴, G. Artoni ^{75a,75b}, H. Asada ¹¹¹, K. Asai ¹¹⁸, S. Asai ¹⁵³, N.A. Asbah ⁶¹, J. Assahsah ^{35d}, K. Assamagan ²⁹, R. Astalos ^{28a}, S. Atashi ¹⁶⁰, R.J. Atkin ^{33a}, M. Atkinson ¹⁶², H. Atmani ^{35f}, P.A. Atlasiddha ¹⁰⁶, K. Augsten ¹³², S. Auricchio ^{72a,72b}, A.D. Auriol ²⁰, V.A. Austrup ¹⁰¹, G. Avolio ³⁶, K. Axiotis ⁵⁶, G. Azuelos ^{108,af}, D. Babal ^{28b}, H. Bachacou ¹³⁵, K. Bachas ^{152,p}, A. Bachiu ³⁴, F. Backman ^{47a,47b}, A. Badea ⁶¹, T.M. Baer ¹⁰⁶, P. Bagnaia ^{75a,75b}, M. Bahmani ¹⁸, A.J. Bailey ¹⁶³, V.R. Bailey ¹⁶², J.T. Baines ¹³⁴, L. Baines ⁹⁴, O.K. Baker ¹⁷², E. Bakos ¹⁵, D. Bakshi Gupta ⁸, V. Balakrishnan ¹²⁰, R. Balasubramanian ¹¹⁴, E.M. Baldin ³⁷, P. Balek ^{86a}, E. Ballabene ^{23b,23a}, F. Balli ¹³⁵, L.M. Baltos ^{63a}, W.K. Balunas ³², J. Balz ¹⁰⁰, E. Banas ⁸⁷, M. Bandieramonte ¹²⁹, A. Bandyopadhyay ²⁴, S. Bansal ²⁴, L. Barak ¹⁵¹, M. Barakat ⁴⁸, E.L. Barberio ¹⁰⁵, D. Barberis ^{57b,57a}, M. Barbero ¹⁰², M.Z. Barel ¹¹⁴, K.N. Barends ^{33a}, T. Barillari ¹¹⁰, M-S. Barisits ³⁶, T. Barklow ¹⁴³, P. Baron ¹²², D.A. Baron Moreno ¹⁰¹, A. Baroncelli ^{62a}, G. Barone ²⁹, A.J. Barr ¹²⁶, J.D. Barr ⁹⁶, L. Barranco Navarro ^{47a,47b}, F. Barreiro ⁹⁹, J. Barreiro Guimarães da Costa ^{14a}, U. Barron ¹⁵¹, M.G. Barros Teixeira ^{130a}, S. Barsov ³⁷, F. Bartels ^{63a}, R. Bartoldus ¹⁴³, A.E. Barton ⁹¹, P. Bartos ^{28a}, A. Basan ¹⁰⁰, M. Baselga ⁴⁹, A. Bassalat ^{66,b}, M.J. Basso ^{156a}, C.R. Basson ¹⁰¹, R.L. Bates ⁵⁹, S. Batlamous ^{35e}, J.R. Batley ³², B. Batool ¹⁴¹, M. Battaglia ¹³⁶, D. Battulga ¹⁸, M. Bauge ^{75a,75b}, M. Bauer ³⁶, P. Bauer ²⁴, L.T. Bazzano Hurrell ³⁰, J.B. Beacham ⁵¹, T. Beau ¹²⁷, J.Y. Beaucamp ⁹⁰, P.H. Beauchemin ¹⁵⁸, F. Becherer ⁵⁴, P. Bechtel ²⁴, H.P. Beck ^{19,o}, K. Becker ¹⁶⁷, A.J. Beddall ⁸², V.A. Bednyakov ³⁸, C.P. Bee ¹⁴⁵, L.J. Beemster ¹⁵, T.A. Beermann ³⁶, M. Begalli ^{83d}, M. Begel ²⁹, A. Behera ¹⁴⁵, J.K. Behr ⁴⁸, J.F. Beirer ⁵⁵, F. Beisiegel ²⁴, M. Belfkir ¹⁵⁹, G. Bella ¹⁵¹, L. Bellagamba ^{23b}, A. Bellerive ³⁴, P. Bellos ²⁰, K. Beloborodov ³⁷, D. Benckekroun ^{35a}, F. Bendebba ^{35a}, Y. Benhammou ¹⁵¹, M. Benoit ²⁹, J.R. Bensinger ²⁶,

S. Bentvelsen ¹¹⁴, L. Beresford ⁴⁸, M. Beretta ⁵³, E. Bergeaas Kuutmann ¹⁶¹, N. Berger ⁴,
 B. Bergmann ¹³², J. Beringer ^{17a}, G. Bernardi ⁵, C. Bernius ¹⁴³, F.U. Bernlochner ²⁴,
 F. Bernon ^{36,102}, A. Berrocal Guardia ¹³, T. Berry ⁹⁵, P. Berta ¹³³, A. Berthold ⁵⁰,
 I.A. Bertram ⁹¹, S. Bethke ¹¹⁰, A. Betti ^{75a,75b}, A.J. Bevan ⁹⁴, N.K. Bhalla ⁵⁴, M. Bhamjee ^{33c},
 S. Bhatta ¹⁴⁵, D.S. Bhattacharya ¹⁶⁶, P. Bhattarai ¹⁴³, V.S. Bhopatkar ¹²¹, R. Bi ^{29,ai},
 R.M. Bianchi ¹²⁹, G. Bianco ^{23b,23a}, O. Biebel ¹⁰⁹, R. Bielski ¹²³, M. Biglietti ^{77a}, M. Bindi ⁵⁵,
 A. Bingul ^{21b}, C. Bini ^{75a,75b}, A. Biondini ⁹², C.J. Birch-sykes ¹⁰¹, G.A. Bird ^{20,134},
 M. Birman ¹⁶⁹, M. Biros ¹³³, S. Biryukov ¹⁴⁶, T. Bisanz ⁴⁹, E. Bisceglie ^{43b,43a}, J.P. Biswal ¹³⁴,
 D. Biswas ¹⁴¹, A. Bitadze ¹⁰¹, K. Bjørke ¹²⁵, I. Bloch ⁴⁸, C. Blocker ²⁶, A. Blue ⁵⁹,
 U. Blumenschein ⁹⁴, J. Blumenthal ¹⁰⁰, G.J. Bobbink ¹¹⁴, V.S. Bobrovnikov ³⁷, M. Boehler ⁵⁴,
 B. Boehm ¹⁶⁶, D. Bogavac ³⁶, A.G. Bogdanchikov ³⁷, C. Bohm ^{47a}, V. Boisvert ⁹⁵, P. Bokan ⁴⁸,
 T. Bold ^{86a}, M. Bomben ⁵, M. Bona ⁹⁴, M. Boonekamp ¹³⁵, C.D. Booth ⁹⁵, A.G. Borbély ⁵⁹,
 I.S. Bordulev ³⁷, H.M. Borecka-Bielska ¹⁰⁸, G. Borissov ⁹¹, D. Bortoletto ¹²⁶, D. Boscherini ^{23b},
 M. Bosman ¹³, J.D. Bossio Sola ³⁶, K. Bouaouda ^{35a}, N. Bouchhar ¹⁶³, J. Boudreau ¹²⁹,
 E.V. Bouhova-Thacker ⁹¹, D. Boumediene ⁴⁰, R. Bouquet ¹⁶⁵, A. Boveia ¹¹⁹, J. Boyd ³⁶,
 D. Boye ²⁹, I.R. Boyko ³⁸, J. Bracik ²⁰, N. Brahimi ^{62d}, G. Brandt ¹⁷¹, O. Brandt ³²,
 F. Braren ⁴⁸, B. Brau ¹⁰³, J.E. Brau ¹²³, R. Brenner ¹⁶⁹, L. Brenner ¹¹⁴, R. Brenner ¹⁶¹,
 S. Bressler ¹⁶⁹, D. Britton ⁵⁹, D. Britzger ¹¹⁰, I. Brock ²⁴, G. Brooijmans ⁴¹, W.K. Brooks ^{137f},
 E. Brost ²⁹, L.M. Brown ¹⁶⁵, L.E. Bruce ⁶¹, T.L. Bruckler ¹²⁶, P.A. Bruckman de Renstrom ⁸⁷,
 B. Brüers ⁴⁸, A. Bruni ^{23b}, G. Bruni ^{23b}, M. Bruschi ^{23b}, N. Bruscinò ^{75a,75b}, T. Buanes ¹⁶,
 Q. Buat ¹³⁸, D. Buchin ¹¹⁰, A.G. Buckley ⁵⁹, O. Bulekov ³⁷, B.A. Bullard ¹⁴³, S. Burdin ⁹²,
 C.D. Burgard ⁴⁹, A.M. Burger ⁴⁰, B. Burghgrave ⁸, O. Burlayenko ⁵⁴, J.T.P. Burr ³²,
 C.D. Burton ¹¹, J.C. Burzynski ¹⁴², E.L. Busch ⁴¹, V. Büscher ¹⁰⁰, P.J. Bussey ⁵⁹,
 J.M. Butler ²⁵, C.M. Buttar ⁵⁹, J.M. Butterworth ⁹⁶, W. Buttinger ¹³⁴, C.J. Buxo Vazquez ¹⁰⁷,
 A.R. Buzykaev ³⁷, S. Cabrera Urbán ¹⁶³, L. Cadamuro ⁶⁶, D. Caforio ⁵⁸, H. Cai ¹²⁹,
 Y. Cai ^{14a,14e}, Y. Cai ^{14c}, V.M.M. Cairo ³⁶, O. Cakir ^{3a}, N. Calace ³⁶, P. Calafiura ^{17a},
 G. Calderini ¹²⁷, P. Calfayan ⁶⁸, G. Callea ⁵⁹, L.P. Caloba ^{83b}, D. Calvet ⁴⁰, S. Calvet ⁴⁰,
 T.P. Calvet ¹⁰², M. Calvetti ^{74a,74b}, R. Camacho Toro ¹²⁷, S. Camarda ³⁶, D. Camarero Munoz ²⁶,
 P. Camarri ^{76a,76b}, M.T. Camerlingo ^{72a,72b}, D. Cameron ³⁶, C. Camincher ¹⁶⁵, M. Campanelli ⁹⁶,
 A. Camplani ⁴², V. Canale ^{72a,72b}, A. Canesse ¹⁰⁴, J. Cantero ¹⁶³, Y. Cao ¹⁶², F. Capocasa ²⁶,
 M. Capua ^{43b,43a}, A. Carbone ^{71a,71b}, R. Cardarelli ^{76a}, J.C.J. Cardenas ⁸, F. Cardillo ¹⁶³,
 G. Carducci ^{43b,43a}, T. Carli ³⁶, G. Carlino ^{72a}, J.I. Carlotto ¹³, B.T. Carlson ^{129,q},
 E.M. Carlson ^{165,156a}, L. Carminati ^{71a,71b}, A. Carnelli ¹³⁵, M. Carnesale ^{75a,75b}, S. Caron ¹¹³,
 E. Carquin ^{137f}, S. Carrá ^{71a,71b}, G. Carratta ^{23b,23a}, F. Carrio Argos ^{33g}, J.W.S. Carter ¹⁵⁵,
 T.M. Carter ⁵², M.P. Casado ^{13,i}, M. Caspar ⁴⁸, F.L. Castillo ⁴, L. Castillo Garcia ¹³,
 V. Castillo Gimenez ¹⁶³, N.F. Castro ^{130a,130e}, A. Catinaccio ³⁶, J.R. Catmore ¹²⁵, V. Cavaliere ²⁹,
 N. Cavalli ^{23b,23a}, V. Cavalanni ^{74a,74b}, Y.C. Cekmecelioglu ⁴⁸, E. Celebi ^{21a}, F. Celli ¹²⁶,
 M.S. Centonze ^{70a,70b}, V. Cepaitis ⁵⁶, K. Cerny ¹²², A.S. Cerqueira ^{83a}, A. Cerri ¹⁴⁶,
 L. Cerrito ^{76a,76b}, F. Cerutti ^{17a}, B. Cervato ¹⁴¹, A. Cervelli ^{23b}, G. Cesarini ⁵³, S.A. Cetin ⁸²,
 Z. Chadi ^{35a}, D. Chakraborty ¹¹⁵, J. Chan ¹⁷⁰, W.Y. Chan ¹⁵³, J.D. Chapman ³², E. Chapon ¹³⁵,
 B. Chargeishvili ^{149b}, D.G. Charlton ²⁰, T.P. Charman ⁹⁴, M. Chatterjee ¹⁹, C. Chauhan ¹³³,
 S. Chekanov ⁶, S.V. Chekulaev ^{156a}, G.A. Chelkov ^{38,a}, A. Chen ¹⁰⁶, B. Chen ¹⁵¹, B. Chen ¹⁶⁵,
 H. Chen ^{14c}, H. Chen ²⁹, J. Chen ^{62c}, J. Chen ¹⁴², M. Chen ¹²⁶, S. Chen ¹⁵³, S.J. Chen ^{14c},
 X. Chen ^{62c,135}, X. Chen ^{14b,ae}, Y. Chen ^{62a}, C.L. Cheng ¹⁷⁰, H.C. Cheng ^{64a}, S. Cheong ¹⁴³,
 A. Cheplakov ³⁸, E. Cheremushkina ⁴⁸, E. Cherepanova ¹¹⁴, R. Cherkaoui El Moursli ^{35e},
 E. Cheu ⁷, K. Cheung ⁶⁵, L. Chevalier ¹³⁵, V. Chiarella ⁵³, G. Chiarelli ^{74a}, N. Chiedde ¹⁰²,
 G. Chiodini ^{70a}, A.S. Chisholm ²⁰, A. Chitan ^{27b}, M. Chitishvili ¹⁶³, M.V. Chizhov ³⁸,

K. Choi ¹¹, A.R. Chomont ^{75a,75b}, Y. Chou ¹⁰³, E.Y.S. Chow ¹¹³, T. Chowdhury ^{33g}, K.L. Chu ¹⁶⁹,
 M.C. Chu ^{64a}, X. Chu ^{14a,14e}, J. Chudoba ¹³¹, J.J. Chwastowski ⁸⁷, D. Cieri ¹¹⁰, K.M. Ciesla ^{86a},
 V. Cindro ⁹³, A. Ciocio ^{17a}, F. Cirotto ^{72a,72b}, Z.H. Citron ^{169,k}, M. Citterio ^{71a},
 D.A. Ciubotaru ^{27b}, B.M. Ciungu ¹⁵⁵, A. Clark ⁵⁶, P.J. Clark ⁵², C. Clarry ¹⁵⁵,
 J.M. Clavijo Columbie ⁴⁸, S.E. Clawson ⁴⁸, C. Clement ^{47a,47b}, J. Clercx ⁴⁸, L. Clissa ^{23b,23a},
 Y. Coadou ¹⁰², M. Cobal ^{69a,69c}, A. Coccaro ^{57b}, R.F. Coelho Barrue ^{130a},
 R. Coelho Lopes De Sa ¹⁰³, S. Coelli ^{71a}, H. Cohen ¹⁵¹, A.E.C. Coimbra ^{71a,71b}, B. Cole ⁴¹,
 J. Collot ⁶⁰, P. Conde Muiño ^{130a,130g}, M.P. Connell ^{33c}, S.H. Connell ^{33c}, I.A. Connelly ⁵⁹,
 E.I. Conroy ¹²⁶, F. Conventi ^{72a,ag}, H.G. Cooke ²⁰, A.M. Cooper-Sarkar ¹²⁶,
 A. Cordeiro Oudot Choi ¹²⁷, L.D. Corpe ⁴⁰, M. Corradi ^{75a,75b}, F. Corriveau ^{104,w},
 A. Cortes-Gonzalez ¹⁸, M.J. Costa ¹⁶³, F. Costanza ⁴, D. Costanzo ¹³⁹, B.M. Cote ¹¹⁹,
 G. Cowan ⁹⁵, K. Cranmer ¹⁷⁰, D. Cremonini ^{23b,23a}, S. Crépe-Renaudin ⁶⁰, F. Crescioli ¹²⁷,
 M. Cristinziani ¹⁴¹, M. Cristoforetti ^{78a,78b}, V. Croft ¹¹⁴, J.E. Crosby ¹²¹, G. Crosetti ^{43b,43a},
 A. Cueto ⁹⁹, T. Cuhadar Donszelmann ¹⁶⁰, H. Cui ^{14a,14e}, Z. Cui ⁷, W.R. Cunningham ⁵⁹,
 F. Curcio ^{43b,43a}, P. Czodrowski ³⁶, M.M. Czurylo ^{63b}, M.J. Da Cunha Sargedas De Sousa ^{57b,57a},
 J.V. Da Fonseca Pinto ^{83b}, C. Da Via ¹⁰¹, W. Dabrowski ^{86a}, T. Dado ⁴⁹, S. Dahbi ^{33g},
 T. Dai ¹⁰⁶, D. Dal Santo ¹⁹, C. Dallapiccola ¹⁰³, M. Dam ⁴², G. D'amen ²⁹, V. D'Amico ¹⁰⁹,
 J. Damp ¹⁰⁰, J.R. Dandoy ¹²⁸, M.F. Daneri ³⁰, M. Danninger ¹⁴², V. Dao ³⁶, G. Darbo ^{57b},
 S. Darmora ⁶, S.J. Das ^{29,ai}, S. D'Auria ^{71a,71b}, C. David ^{156b}, T. Davidek ¹³³,
 B. Davis-Purcell ³⁴, I. Dawson ⁹⁴, H.A. Day-hall ¹³², K. De ⁸, R. De Asmundis ^{72a},
 N. De Biase ⁴⁸, S. De Castro ^{23b,23a}, N. De Groot ¹¹³, P. de Jong ¹¹⁴, H. De la Torre ¹¹⁵,
 A. De Maria ^{14c}, A. De Salvo ^{75a}, U. De Sanctis ^{76a,76b}, A. De Santo ¹⁴⁶,
 J.B. De Vivie De Regie ⁶⁰, D.V. Dedovich ³⁸, J. Degens ¹¹⁴, A.M. Deiana ⁴⁴, F. Del Corso ^{23b,23a},
 J. Del Peso ⁹⁹, F. Del Rio ^{63a}, F. Deliot ¹³⁵, C.M. Delitzsch ⁴⁹, M. Della Pietra ^{72a,72b},
 D. Della Volpe ⁵⁶, A. Dell'Acqua ³⁶, L. Dell'Asta ^{71a,71b}, M. Delmastro ⁴, P.A. Delsart ⁶⁰,
 S. Demers ¹⁷², M. Demichev ³⁸, S.P. Denisov ³⁷, L. D'Eramo ⁴⁰, D. Derendarz ⁸⁷, F. Derue ¹²⁷,
 P. Dervan ⁹², K. Desch ²⁴, C. Deutsch ²⁴, F.A. Di Bello ^{57b,57a}, A. Di Ciaccio ^{76a,76b},
 L. Di Ciaccio ⁴, A. Di Domenico ^{75a,75b}, C. Di Donato ^{72a,72b}, A. Di Girolamo ³⁶,
 G. Di Gregorio ³⁶, A. Di Luca ^{78a,78b}, B. Di Micco ^{77a,77b}, R. Di Nardo ^{77a,77b}, C. Diaconu ¹⁰²,
 M. Diamantopoulou ³⁴, F.A. Dias ¹¹⁴, T. Dias Do Vale ¹⁴², M.A. Diaz ^{137a,137b},
 F.G. Diaz Capriles ²⁴, M. Didenko ¹⁶³, E.B. Diehl ¹⁰⁶, L. Diehl ⁵⁴, S. Díez Cornell ⁴⁸,
 C. Diez Pardos ¹⁴¹, C. Dimitriadi ^{161,24,161}, A. Dimitrievska ^{17a}, J. Dingfelder ²⁴, I-M. Dinu ^{27b},
 S.J. Dittmeier ^{63b}, F. Dittus ³⁶, F. Djama ¹⁰², T. Djobava ^{149b}, J.I. Djuvsland ¹⁶,
 C. Doglioni ^{101,98}, A. Dohnalova ^{28a}, J. Dolejsi ¹³³, Z. Dolezal ¹³³, K.M. Dona ³⁹,
 M. Donadelli ^{83c}, B. Dong ¹⁰⁷, J. Donini ⁴⁰, A. D'Onofrio ^{77a,77b}, M. D'Onofrio ⁹²,
 J. Dopke ¹³⁴, A. Doria ^{72a}, N. Dos Santos Fernandes ^{130a}, P. Dougan ¹⁰¹, M.T. Dova ⁹⁰,
 A.T. Doyle ⁵⁹, M.A. Dragnet ¹²⁶, E. Dreyer ¹⁶⁹, I. Drivas-koulouris ¹⁰, M. Drnevich ¹¹⁷,
 A.S. Drobac ¹⁵⁸, M. Drozdova ⁵⁶, D. Du ^{62a}, T.A. du Pree ¹¹⁴, F. Dubinin ³⁷, M. Dubovsky ^{28a},
 E. Duchovni ¹⁶⁹, G. Duckeck ¹⁰⁹, O.A. Ducu ^{27b}, D. Duda ⁵², A. Dudarev ³⁶, E.R. Duden ²⁶,
 M. D'uffizi ¹⁰¹, L. Duflot ⁶⁶, M. Dührssen ³⁶, C. Dülsen ¹⁷¹, A.E. Dumitriu ^{27b}, M. Dunford ^{63a},
 S. Dungs ⁴⁹, K. Dunne ^{47a,47b}, A. Duperrin ¹⁰², H. Duran Yildiz ^{3a}, M. Düren ⁵⁸,
 A. Durglishvili ^{149b}, B.L. Dwyer ¹¹⁵, G.I. Dyckes ^{17a}, M. Dyndal ^{86a}, B.S. Dziedzic ⁸⁷,
 Z.O. Earnshaw ¹⁴⁶, G.H. Eberwein ¹²⁶, B. Eckerova ^{28a}, S. Eggebrecht ⁵⁵,
 E. Egidio Purcino De Souza ¹²⁷, L.F. Ehrke ⁵⁶, G. Eigen ¹⁶, K. Einsweiler ^{17a}, T. Ekelof ¹⁶¹,
 P.A. Ekman ⁹⁸, S. El Farkh ^{35b}, Y. El Ghazali ^{35b}, H. El Jarrari ^{35e,148}, A. El Moussaouy ¹⁰⁸,
 V. Ellajosyula ¹⁶¹, M. Ellert ¹⁶¹, F. Ellinghaus ¹⁷¹, N. Ellis ³⁶, J. Elmsheuser ²⁹, M. Elsing ³⁶,
 D. Emelianov ¹³⁴, Y. Enari ¹⁵³, I. Ene ^{17a}, S. Epari ¹³, J. Erdmann ⁴⁹, P.A. Erland ⁸⁷,

M. Errenst ¹⁷¹, M. Escalier ⁶⁶, C. Escobar ¹⁶³, E. Etzion ¹⁵¹, G. Evans ^{130a}, H. Evans ⁶⁸,
L.S. Evans ⁹⁵, M.O. Evans ¹⁴⁶, A. Ezhilov ³⁷, S. Ezzarqtouni ^{35a}, F. Fabbri ⁵⁹, L. Fabbri ^{23b,23a},
G. Facini ⁹⁶, V. Fadeyev ¹³⁶, R.M. Fakhrutdinov ³⁷, S. Falciano ^{75a}, L.F. Falda Ulhoa Coelho ³⁶,
P.J. Falke ²⁴, J. Faltova ¹³³, C. Fan ¹⁶², Y. Fan ^{14a}, Y. Fang ^{14a,14e}, M. Fanti ^{71a,71b},
M. Faraj ^{69a,69b}, Z. Farazpay ⁹⁷, A. Farbin ⁸, A. Farilla ^{77a}, T. Farooque ¹⁰⁷, S.M. Farrington ⁵²,
F. Fassi ^{35e}, D. Fassouliotis ⁹, M. Faucci Giannelli ^{76a,76b}, W.J. Fawcett ³², L. Fayard ⁶⁶,
P. Federic ¹³³, P. Federicova ¹³¹, O.L. Fedin ^{37,a}, G. Fedotov ³⁷, M. Feickert ¹⁷⁰,
L. Feligioni ¹⁰², D.E. Fellers ¹²³, C. Feng ^{62b}, M. Feng ^{14b}, Z. Feng ¹¹⁴, M.J. Fenton ¹⁶⁰,
A.B. Fenyuk ³⁷, L. Ferencz ⁴⁸, R.A.M. Ferguson ⁹¹, S.I. Fernandez Luengo ^{137f},
P. Fernandez Martinez ¹³, M.J.V. Fernoux ¹⁰², J. Ferrando ⁴⁸, A. Ferrari ¹⁶¹, P. Ferrari ^{114,113},
R. Ferrari ^{73a}, D. Ferrere ⁵⁶, C. Ferretti ¹⁰⁶, F. Fiedler ¹⁰⁰, P. Fiedler ¹³², A. Filipčič ⁹³,
E.K. Filmer ¹, F. Filthaut ¹¹³, M.C.N. Fiolhais ^{130a,130c,c}, L. Fiorini ¹⁶³, W.C. Fisher ¹⁰⁷,
T. Fitschen ¹⁰¹, P.M. Fitzhugh ¹³⁵, I. Fleck ¹⁴¹, P. Fleischmann ¹⁰⁶, T. Flick ¹⁷¹, M. Flores ^{33d,ac},
L.R. Flores Castillo ^{64a}, L. Flores Sanz De Acedo ³⁶, F.M. Follega ^{78a,78b}, N. Fomin ¹⁶,
J.H. Foo ¹⁵⁵, B.C. Forland ⁶⁸, A. Formica ¹³⁵, A.C. Forti ¹⁰¹, E. Fortin ³⁶, A.W. Fortman ⁶¹,
M.G. Foti ^{17a}, L. Fountas ^{9,j}, D. Fournier ⁶⁶, H. Fox ⁹¹, P. Francavilla ^{74a,74b}, S. Francescato ⁶¹,
S. Franchellucci ⁵⁶, M. Franchini ^{23b,23a}, S. Franchino ^{63a}, D. Francis ³⁶, L. Franco ¹¹³,
V. Franco Lima ³⁶, L. Franconi ⁴⁸, M. Franklin ⁶¹, G. Frattari ²⁶, A.C. Fregard ⁹⁴,
W.S. Freund ^{83b}, Y.Y. Frid ¹⁵¹, J. Friend ⁵⁹, N. Fritzsche ⁵⁰, A. Froch ⁵⁴, D. Froidevaux ³⁶,
J.A. Frost ¹²⁶, Y. Fu ^{62a}, S. Fuenzalida Garrido ^{137f}, M. Fujimoto ¹⁰², E. Fullana Torregrosa ^{163,*},
K.Y. Fung ^{64a}, E. Furtado De Simas Filho ^{83b}, M. Furukawa ¹⁵³, J. Fuster ¹⁶³, A. Gabrielli ^{23b,23a},
A. Gabrielli ¹⁵⁵, P. Gadow ³⁶, G. Gagliardi ^{57b,57a}, L.G. Gagnon ^{17a}, E.J. Gallas ¹²⁶,
B.J. Gallop ¹³⁴, K.K. Gan ¹¹⁹, S. Ganguly ¹⁵³, Y. Gao ⁵², F.M. Garay Walls ^{137a,137b},
B. Garcia ^{29,ai}, C. García ¹⁶³, A. Garcia Alonso ¹¹⁴, A.G. Garcia Caffaro ¹⁷²,
J.E. García Navarro ¹⁶³, M. Garcia-Sciveres ^{17a}, G.L. Gardner ¹²⁸, R.W. Gardner ³⁹,
N. Garelli ¹⁵⁸, D. Garg ⁸⁰, R.B. Garg ^{143,n}, J.M. Gargan ⁵², C.A. Garner ¹⁵⁵, C.M. Garvey ^{33a},
P. Gaspar ^{83b}, V.K. Gassmann ¹⁵⁸, G. Gaudio ^{73a}, V. Gautam ¹³, P. Gauzzi ^{75a,75b}, I.L. Gavrilenko ³⁷,
A. Gavriluk ³⁷, C. Gay ¹⁶⁴, G. Gaycken ⁴⁸, E.N. Gazis ¹⁰, A.A. Geanta ^{27b}, C.M. Gee ¹³⁶,
C. Gemme ^{57b}, M.H. Genest ⁶⁰, S. Gentile ^{75a,75b}, A.D. Gentry ¹¹², S. George ⁹⁵,
W.F. George ²⁰, T. Geralis ⁴⁶, P. Gessinger-Befurt ³⁶, M.E. Geyik ¹⁷¹, M. Ghani ¹⁶⁷,
M. Ghneimat ¹⁴¹, K. Ghorbanian ⁹⁴, A. Ghosal ¹⁴¹, A. Ghosh ¹⁶⁰, A. Ghosh ⁷, B. Giacobbe ^{23b},
S. Giagu ^{75a,75b}, T. Giani ¹¹⁴, P. Giannetti ^{74a}, A. Giannini ^{62a}, S.M. Gibson ⁹⁵, M. Gignac ¹³⁶,
D.T. Gil ^{86b}, A.K. Gilbert ^{86a}, B.J. Gilbert ⁴¹, D. Gillberg ³⁴, G. Gilles ¹¹⁴, N.E.K. Gillwald ⁴⁸,
L. Ginabat ¹²⁷, D.M. Gingrich ^{2,af}, M.P. Giordani ^{69a,69c}, P.F. Giraud ¹³⁵, G. Giugliarelli ^{69a,69c},
D. Giugni ^{71a}, F. Giuli ³⁶, I. Gkialas ^{9,j}, L.K. Gladilin ³⁷, C. Glasman ⁹⁹, G.R. Gledhill ¹²³,
G. Glemža ⁴⁸, M. Glisic ¹²³, I. Gnesi ^{43b,f}, Y. Go ^{29,ai}, M. Goblirsch-Kolb ³⁶, B. Gocke ⁴⁹,
D. Godin ¹⁰⁸, B. Gokturk ^{21a}, S. Goldfarb ¹⁰⁵, T. Golling ⁵⁶, M.G.D. Gololo ^{33g}, D. Golubkov ³⁷,
J.P. Gombas ¹⁰⁷, A. Gomes ^{130a,130b}, G. Gomes Da Silva ¹⁴¹, A.J. Gomez Delegido ¹⁶³,
R. Gonçalves ^{130a,130c}, G. Gonella ¹²³, L. Gonella ²⁰, A. Gongadze ^{149c}, F. Gonnella ²⁰,
J.L. Gonski ⁴¹, R.Y. González Andana ⁵², S. González de la Hoz ¹⁶³, S. Gonzalez Fernandez ¹³,
R. Gonzalez Lopez ⁹², C. Gonzalez Renteria ^{17a}, M.V. Gonzalez Rodrigues ⁴⁸,
R. Gonzalez Suarez ¹⁶¹, S. Gonzalez-Sevilla ⁵⁶, G.R. Gonzalvo Rodriguez ¹⁶³, L. Goossens ³⁶,
B. Gorini ³⁶, E. Gorini ^{70a,70b}, A. Gorišek ⁹³, T.C. Gosart ¹²⁸, A.T. Goshaw ⁵¹, M.I. Gostkin ³⁸,
S. Goswami ¹²¹, C.A. Gottardo ³⁶, S.A. Gotz ¹⁰⁹, M. Gouighri ^{35b}, V. Goumarre ⁴⁸,
A.G. Goussiou ¹³⁸, N. Govender ^{33c}, I. Grabowska-Bold ^{86a}, K. Graham ³⁴, E. Gramstad ¹²⁵,
S. Grancagnolo ^{70a,70b}, M. Grandi ¹⁴⁶, C.M. Grant ^{1,135}, P.M. Gravila ^{27f}, F.G. Gravili ^{70a,70b},
H.M. Gray ^{17a}, M. Greco ^{70a,70b}, C. Grefe ²⁴, I.M. Gregor ⁴⁸, P. Grenier ¹⁴³, S.G. Grewe ¹¹⁰,

C. Grieco ¹³, A.A. Grillo ¹³⁶, K. Grimm ³¹, S. Grinstein ^{13,s}, J.-F. Grivaz ⁶⁶, E. Gross ¹⁶⁹,
 J. Grosse-Knetter ⁵⁵, C. Grud ¹⁰⁶, J.C. Grundy ¹²⁶, L. Guan ¹⁰⁶, W. Guan ²⁹, C. Gubbels ¹⁶⁴,
 J.G.R. Guerrero Rojas ¹⁶³, G. Guerrieri ^{69a,69c}, F. Guescini ¹¹⁰, R. Gugel ¹⁰⁰, J.A.M. Guhit ¹⁰⁶,
 A. Guida ¹⁸, T. Guillemain ⁴, E. Guilloton ^{167,134}, S. Guindon ³⁶, F. Guo ^{14a,14e}, J. Guo ^{62c},
 L. Guo ⁴⁸, Y. Guo ¹⁰⁶, R. Gupta ⁴⁸, R. Gupta ¹²⁹, S. Gurbuz ²⁴, S.S. Gurdasani ⁵⁴,
 G. Gustavino ³⁶, M. Guth ⁵⁶, P. Gutierrez ¹²⁰, L.F. Gutierrez Zagazeta ¹²⁸, M. Gutsche ⁵⁰,
 C. Gutschow ⁹⁶, C. Gwenlan ¹²⁶, C.B. Gwilliam ⁹², E.S. Haaland ¹²⁵, A. Haas ¹¹⁷,
 M. Habedank ⁴⁸, C. Haber ^{17a}, H.K. Hadavand ⁸, A. Hadeef ¹⁰⁰, S. Hadzic ¹¹⁰, A.I. Hagan ⁹¹,
 J.J. Hahn ¹⁴¹, E.H. Haines ⁹⁶, M. Haleem ¹⁶⁶, J. Haley ¹²¹, J.J. Hall ¹³⁹, G.D. Hallowell ¹⁰²,
 L. Halser ¹⁹, K. Hamano ¹⁶⁵, M. Hamer ²⁴, G.N. Hamity ⁵², E.J. Hampshire ⁹⁵, J. Han ^{62b},
 K. Han ^{62a}, L. Han ^{14c}, L. Han ^{62a}, S. Han ^{17a}, Y.F. Han ¹⁵⁵, K. Hanagaki ⁸⁴, M. Hance ¹³⁶,
 D.A. Hangal ^{41,ab}, H. Hanif ¹⁴², M.D. Hank ¹²⁸, R. Hankache ¹⁰¹, J.B. Hansen ⁴²,
 J.D. Hansen ⁴², P.H. Hansen ⁴², K. Hara ¹⁵⁷, D. Harada ⁵⁶, T. Harenberg ¹⁷¹, S. Harkusha ³⁷,
 M.L. Harris ¹⁰³, Y.T. Harris ¹²⁶, J. Harrison ¹³, N.M. Harrison ¹¹⁹, P.F. Harrison ¹⁶⁷,
 N.M. Hartman ¹¹⁰, N.M. Hartmann ¹⁰⁹, Y. Hasegawa ¹⁴⁰, R. Hauser ¹⁰⁷, C.M. Hawkes ²⁰,
 R.J. Hawkings ³⁶, Y. Hayashi ¹⁵³, S. Hayashida ¹¹¹, D. Hayden ¹⁰⁷, C. Hayes ¹⁰⁶,
 R.L. Hayes ¹¹⁴, C.P. Hays ¹²⁶, J.M. Hays ⁹⁴, H.S. Hayward ⁹², F. He ^{62a}, M. He ^{14a,14e},
 Y. He ¹⁵⁴, Y. He ⁴⁸, N.B. Heatley ⁹⁴, V. Hedberg ⁹⁸, A.L. Heggelund ¹²⁵, N.D. Hehir ⁹⁴,
 C. Heidegger ⁵⁴, K.K. Heidegger ⁵⁴, W.D. Heidorn ⁸¹, J. Heilman ³⁴, S. Heim ⁴⁸, T. Heim ^{17a},
 J.G. Heinlein ¹²⁸, J.J. Heinrich ¹²³, L. Heinrich ^{110,ad}, J. Hejbal ¹³¹, L. Helary ⁴⁸, A. Held ¹⁷⁰,
 S. Hellesund ¹⁶, C.M. Helling ¹⁶⁴, S. Hellman ^{47a,47b}, R.C.W. Henderson ⁹¹, L. Henkelmann ³²,
 A.M. Henriques Correia ³⁶, H. Herde ⁹⁸, Y. Hernández Jiménez ¹⁴⁵, L.M. Herrmann ²⁴,
 T. Herrmann ⁵⁰, G. Herten ⁵⁴, R. Hertenberger ¹⁰⁹, L. Hervas ³⁶, M.E. Hespig ¹⁰⁰,
 N.P. Hessey ^{156a}, H. Hibi ⁸⁵, E. Hill ¹⁵⁵, S.J. Hillier ²⁰, J.R. Hinds ¹⁰⁷, F. Hinterkeuser ²⁴,
 M. Hirose ¹²⁴, S. Hirose ¹⁵⁷, D. Hirschbuehl ¹⁷¹, T.G. Hitchings ¹⁰¹, B. Hiti ⁹³, J. Hobbs ¹⁴⁵,
 R. Hobincu ^{27e}, N. Hod ¹⁶⁹, M.C. Hodgkinson ¹³⁹, B.H. Hodgkinson ³², A. Hoecker ³⁶,
 D.D. Hofer ¹⁰⁶, J. Hofer ⁴⁸, T. Holm ²⁴, M. Holzbock ¹¹⁰, L.B.A.H. Hommels ³²,
 B.P. Honan ¹⁰¹, J. Hong ^{62c}, T.M. Hong ¹²⁹, B.H. Hooberman ¹⁶², W.H. Hopkins ⁶, Y. Horii ¹¹¹,
 S. Hou ¹⁴⁸, A.S. Howard ⁹³, J. Howarth ⁵⁹, J. Hoya ⁶, M. Hrabovsky ¹²², A. Hrynevich ⁴⁸,
 T. Hryn'ova ⁴, P.J. Hsu ⁶⁵, S.-C. Hsu ¹³⁸, Q. Hu ^{62a}, Y.F. Hu ^{14a,14e}, S. Huang ^{64b},
 X. Huang ^{14c}, X. Huang ^{14a,14e}, Y. Huang ¹³⁹, Y. Huang ^{14a}, Z. Huang ¹⁰¹, Z. Hubacek ¹³²,
 M. Huebner ²⁴, F. Huegging ²⁴, T.B. Huffman ¹²⁶, C.A. Hugli ⁴⁸, M. Huhtinen ³⁶,
 S.K. Huiberts ¹⁶, R. Hulsken ¹⁰⁴, N. Huseynov ¹², J. Huston ¹⁰⁷, J. Huth ⁶¹, R. Hyneman ¹⁴³,
 G. Iacobucci ⁵⁶, G. Iakovidis ²⁹, I. Ibragimov ¹⁴¹, L. Iconomidou-Fayard ⁶⁶, P. Iengo ^{72a,72b},
 R. Iguchi ¹⁵³, T. Iizawa ¹²⁶, Y. Ikegami ⁸⁴, N. Ilic ¹⁵⁵, H. Imam ^{35a}, M. Ince Lezki ⁵⁶,
 T. Ingebretsen Carlson ^{47a,47b}, G. Introzzi ^{73a,73b}, M. Iodice ^{77a}, V. Ippolito ^{75a,75b}, R.K. Irwin ⁹²,
 M. Ishino ¹⁵³, W. Islam ¹⁷⁰, C. Issever ^{18,48}, S. Istin ^{21a,ak}, H. Ito ¹⁶⁸, J.M. Iturbe Ponce ^{64a},
 R. Iuppa ^{78a,78b}, A. Ivina ¹⁶⁹, J.M. Izen ⁴⁵, V. Izzo ^{72a}, P. Jacka ^{131,132}, P. Jackson ¹,
 R.M. Jacobs ⁴⁸, B.P. Jaeger ¹⁴², C.S. Jagfeld ¹⁰⁹, G. Jain ^{156a}, P. Jain ⁵⁴, K. Jakobs ⁵⁴,
 T. Jakoubek ¹⁶⁹, J. Jamieson ⁵⁹, K.W. Janas ^{86a}, M. Javurkova ¹⁰³, F. Jeanneau ¹³⁵,
 L. Jeanty ¹²³, J. Jejelava ^{149a,z}, P. Jenni ^{54,g}, C.E. Jessiman ³⁴, S. Jézéquel ⁴, C. Jia ^{62b}, J. Jia ¹⁴⁵,
 X. Jia ⁶¹, X. Jia ^{14a,14e}, Z. Jia ^{14c}, S. Jiggins ⁴⁸, J. Jimenez Pena ¹³, S. Jin ^{14c}, A. Jinaru ^{27b},
 O. Jinnouchi ¹⁵⁴, P. Johansson ¹³⁹, K.A. Johns ⁷, J.W. Johnson ¹³⁶, D.M. Jones ³², E. Jones ⁴⁸,
 P. Jones ³², R.W.L. Jones ⁹¹, T.J. Jones ⁹², H.L. Joos ^{55,36}, R. Joshi ¹¹⁹, J. Jovicevic ¹⁵,
 X. Ju ^{17a}, J.J. Junggeburth ¹⁰³, T. Junkermann ^{63a}, A. Juste Rozas ^{13,s}, M.K. Juzek ⁸⁷,
 S. Kabana ^{137e}, A. Kaczmarzka ⁸⁷, M. Kado ¹¹⁰, H. Kagan ¹¹⁹, M. Kagan ¹⁴³, A. Kahn ⁴¹,
 A. Kahn ¹²⁸, C. Kahra ¹⁰⁰, T. Kaji ¹⁵³, E. Kajomovitz ¹⁵⁰, N. Kakati ¹⁶⁹, I. Kalaitzidou ⁵⁴,

C.W. Kalderon [id²⁹](#), A. Kamenshchikov [id¹⁵⁵](#), N.J. Kang [id¹³⁶](#), D. Kar [id^{33g}](#), K. Karava [id¹²⁶](#),
 M.J. Kareem [id^{156b}](#), E. Karentzos [id⁵⁴](#), I. Karkanias [id¹⁵²](#), O. Karkout [id¹¹⁴](#), S.N. Karpov [id³⁸](#),
 Z.M. Karpova [id³⁸](#), V. Kartvelishvili [id⁹¹](#), A.N. Karyukhin [id³⁷](#), E. Kasimi [id¹⁵²](#), J. Katzy [id⁴⁸](#), S. Kaur [id³⁴](#),
 K. Kawade [id¹⁴⁰](#), M.P. Kawale [id¹²⁰](#), C. Kawamoto [id⁸⁸](#), T. Kawamoto [id¹³⁵](#), E.F. Kay [id³⁶](#), F.I. Kaya [id¹⁵⁸](#),
 S. Kazakos [id¹⁰⁷](#), V.F. Kazanin [id³⁷](#), Y. Ke [id¹⁴⁵](#), J.M. Keaveney [id^{33a}](#), R. Keeler [id¹⁶⁵](#), G.V. Kehris [id⁶¹](#),
 J.S. Keller [id³⁴](#), A.S. Kelly [id⁹⁶](#), J.J. Kempster [id¹⁴⁶](#), K.E. Kennedy [id⁴¹](#), P.D. Kennedy [id¹⁰⁰](#), O. Kepka [id¹³¹](#),
 B.P. Kerridge [id¹⁶⁷](#), S. Kersten [id¹⁷¹](#), B.P. Kerševan [id⁹³](#), S. Keshri [id⁶⁶](#), L. Keszeghova [id^{28a}](#),
 S. Kitabchi Haghighat [id¹⁵⁵](#), R.A. Khan [id¹²⁹](#), M. Khandoga [id¹²⁷](#), A. Khanov [id¹²¹](#), A.G. Kharlamov [id³⁷](#),
 T. Kharlamova [id³⁷](#), E.E. Khoda [id¹³⁸](#), M. Kholodenko [id³⁷](#), T.J. Khoo [id¹⁸](#), G. Khoriali [id¹⁶⁶](#),
 J. Khubua [id^{149b}](#), Y.A.R. Khwaira [id⁶⁶](#), A. Kilgallon [id¹²³](#), D.W. Kim [id^{47a,47b}](#), Y.K. Kim [id³⁹](#),
 N. Kimura [id⁹⁶](#), M.K. Kingston [id⁵⁵](#), A. Kirchhoff [id⁵⁵](#), C. Kirfel [id²⁴](#), F. Kirfel [id²⁴](#), J. Kirk [id¹³⁴](#),
 A.E. Kiryunin [id¹¹⁰](#), C. Kitsaki [id¹⁰](#), O. Kivernyk [id²⁴](#), M. Klassen [id^{63a}](#), C. Klein [id³⁴](#), L. Klein [id¹⁶⁶](#),
 M.H. Klein [id¹⁰⁶](#), M. Klein [id⁹²](#), S.B. Klein [id⁵⁶](#), U. Klein [id⁹²](#), P. Klimek [id³⁶](#), A. Klimentov [id²⁹](#),
 T. Klioutchnikova [id³⁶](#), P. Kluit [id¹¹⁴](#), S. Kluth [id¹¹⁰](#), E. Kneringer [id⁷⁹](#), T.M. Knight [id¹⁵⁵](#), A. Knue [id⁴⁹](#),
 R. Kobayashi [id⁸⁸](#), D. Kobylanski [id¹⁶⁹](#), S.F. Koch [id¹²⁶](#), M. Kocian [id¹⁴³](#), P. Kodyš [id¹³³](#),
 D.M. Koeck [id¹²³](#), P.T. Koenig [id²⁴](#), T. Koffas [id³⁴](#), O. Kolay [id⁵⁰](#), M. Kolb [id¹³⁵](#), I. Koletsou [id⁴](#),
 T. Komarek [id¹²²](#), K. Köneke [id⁵⁴](#), A.X.Y. Kong [id¹](#), T. Kono [id¹¹⁸](#), N. Konstantinidis [id⁹⁶](#),
 P. Kontaxakis [id⁵⁶](#), B. Konya [id⁹⁸](#), R. Kopeliansky [id⁶⁸](#), S. Koperny [id^{86a}](#), K. Korcyl [id⁸⁷](#), K. Kordas [id^{152,e}](#),
 G. Koren [id¹⁵¹](#), A. Korn [id⁹⁶](#), S. Korn [id⁵⁵](#), I. Korolkov [id¹³](#), N. Korotkova [id³⁷](#), B. Kortman [id¹¹⁴](#),
 O. Kortner [id¹¹⁰](#), S. Kortner [id¹¹⁰](#), W.H. Kostecka [id¹¹⁵](#), V.V. Kostyukhin [id¹⁴¹](#), A. Kotsokechagia [id¹³⁵](#),
 A. Kotwal [id⁵¹](#), A. Koulouris [id³⁶](#), A. Kourkoumeli-Charalampidi [id^{73a,73b}](#), C. Kourkoumelis [id⁹](#),
 E. Kourlitis [id^{110,ad}](#), O. Kovanda [id¹⁴⁶](#), R. Kowalewski [id¹⁶⁵](#), W. Kozanecki [id¹³⁵](#), A.S. Kozhin [id³⁷](#),
 V.A. Kramarenko [id³⁷](#), G. Kramberger [id⁹³](#), P. Kramer [id¹⁰⁰](#), M.W. Krasny [id¹²⁷](#), A. Krasznahorkay [id³⁶](#),
 J.W. Kraus [id¹⁷¹](#), J.A. Kremer [id⁴⁸](#), T. Kresse [id⁵⁰](#), J. Kretschmar [id⁹²](#), K. Kreul [id¹⁸](#), P. Krieger [id¹⁵⁵](#),
 S. Krishnamurthy [id¹⁰³](#), M. Krivos [id¹³³](#), K. Krizka [id²⁰](#), K. Kroeninger [id⁴⁹](#), H. Kroha [id¹¹⁰](#), J. Kroll [id¹³¹](#),
 J. Kroll [id¹²⁸](#), K.S. Krowpman [id¹⁰⁷](#), U. Kruchonak [id³⁸](#), H. Krüger [id²⁴](#), N. Krumnack [id⁸¹](#), M.C. Kruse [id⁵¹](#),
 J.A. Krzysiak [id⁸⁷](#), O. Kuchinskaia [id³⁷](#), S. Kuday [id^{3a}](#), S. Kuehn [id³⁶](#), R. Kuesters [id⁵⁴](#), T. Kuhl [id⁴⁸](#),
 V. Kukhtin [id³⁸](#), Y. Kulchitsky [id^{37,a}](#), S. Kuleshov [id^{137d,137b}](#), M. Kumar [id^{33g}](#), N. Kumari [id⁴⁸](#),
 A. Kupco [id¹³¹](#), T. Kupfer [id⁴⁹](#), A. Kupich [id³⁷](#), O. Kuprash [id⁵⁴](#), H. Kurashige [id⁸⁵](#), L.L. Kurchaninov [id^{156a}](#),
 O. Kurdysh [id⁶⁶](#), Y.A. Kurochkin [id³⁷](#), A. Kurova [id³⁷](#), M. Kuze [id¹⁵⁴](#), A.K. Kvam [id¹⁰³](#), J. Kvita [id¹²²](#),
 T. Kwan [id¹⁰⁴](#), N.G. Kyriacou [id¹⁰⁶](#), L.A.O. Laatu [id¹⁰²](#), C. Lacasta [id¹⁶³](#), F. Lacava [id^{75a,75b}](#),
 H. Lacker [id¹⁸](#), D. Lacour [id¹²⁷](#), N.N. Lad [id⁹⁶](#), E. Ladygin [id³⁸](#), B. Laforge [id¹²⁷](#), T. Lagouri [id^{137e}](#),
 F.Z. Lahbabi [id^{35a}](#), S. Lai [id⁵⁵](#), I.K. Lakomic [id^{86a}](#), N. Lalloue [id⁶⁰](#), J.E. Lambert [id¹⁶⁵](#), S. Lammers [id⁶⁸](#),
 W. Lampl [id⁷](#), C. Lampoudis [id^{152,e}](#), A.N. Lancaster [id¹¹⁵](#), E. Lançon [id²⁹](#), U. Landgraf [id⁵⁴](#),
 M.P.J. Landon [id⁹⁴](#), V.S. Lang [id⁵⁴](#), R.J. Langenberg [id¹⁰³](#), O.K.B. Langrekken [id¹²⁵](#), A.J. Lankford [id¹⁶⁰](#),
 F. Lanni [id³⁶](#), K. Lantzsch [id²⁴](#), A. Lanza [id^{73a}](#), A. Lapertosa [id^{57b,57a}](#), J.F. Laporte [id¹³⁵](#), T. Lari [id^{71a}](#),
 F. Lasagni Manghi [id^{23b}](#), M. Lassnig [id³⁶](#), V. Latonova [id¹³¹](#), A. Laudrain [id¹⁰⁰](#), A. Laurier [id¹⁵⁰](#),
 S.D. Lawlor [id¹³⁹](#), Z. Lawrence [id¹⁰¹](#), R. Lazaridou [id¹⁶⁷](#), M. Lazzaroni [id^{71a,71b}](#), B. Le [id¹⁰¹](#),
 E.M. Le Boulicaut [id⁵¹](#), B. Leban [id⁹³](#), A. Lebedev [id⁸¹](#), M. LeBlanc [id¹⁰¹](#), F. Ledroit-Guillon [id⁶⁰](#),
 A.C.A. Lee [id⁹⁶](#), S.C. Lee [id¹⁴⁸](#), S. Lee [id^{47a,47b}](#), T.F. Lee [id⁹²](#), L.L. Leeuw [id^{33c}](#), H.P. Lefebvre [id⁹⁵](#),
 M. Lefebvre [id¹⁶⁵](#), C. Leggett [id^{17a}](#), G. Lehmann Miotto [id³⁶](#), M. Leigh [id⁵⁶](#), W.A. Leight [id¹⁰³](#),
 W. Leinonen [id¹¹³](#), A. Leisos [id^{152,r}](#), M.A.L. Leite [id^{83c}](#), C.E. Leitgeb [id⁴⁸](#), R. Leitner [id¹³³](#),
 K.J.C. Leney [id⁴⁴](#), T. Lenz [id²⁴](#), S. Leone [id^{74a}](#), C. Leonidopoulos [id⁵²](#), A. Leopold [id¹⁴⁴](#), C. Leroy [id¹⁰⁸](#),
 R. Les [id¹⁰⁷](#), C.G. Lester [id³²](#), M. Levchenko [id³⁷](#), J. Levêque [id⁴](#), D. Levin [id¹⁰⁶](#), L.J. Levinson [id¹⁶⁹](#),
 M.P. Lewicki [id⁸⁷](#), D.J. Lewis [id⁴](#), A. Li [id⁵](#), B. Li [id^{62b}](#), C. Li [id^{62a}](#), C-Q. Li [id^{62c}](#), H. Li [id^{62a}](#), H. Li [id^{62b}](#),
 H. Li [id^{14c}](#), H. Li [id^{14b}](#), H. Li [id^{62b}](#), J. Li [id^{62c}](#), K. Li [id¹³⁸](#), L. Li [id^{62c}](#), M. Li [id^{14a,14e}](#), Q.Y. Li [id^{62a}](#),
 S. Li [id^{14a,14e}](#), S. Li [id^{62d,62c,d}](#), T. Li [id⁵](#), X. Li [id¹⁰⁴](#), Z. Li [id¹²⁶](#), Z. Li [id¹⁰⁴](#), Z. Li [id⁹²](#), Z. Li [id^{14a,14e}](#),

S. Liang^{14a,14e}, Z. Liang^{14a}, M. Liberatore¹³⁵, B. Liberti^{76a}, K. Lie^{64c}, J. Lieber Marin^{83b},
 H. Lien⁶⁸, K. Lin¹⁰⁷, R.E. Lindley⁷, J.H. Lindon², E. Lipeles¹²⁸, A. Lipniacka¹⁶,
 A. Lister¹⁶⁴, J.D. Little⁴, B. Liu^{14a}, B.X. Liu¹⁴², D. Liu^{62d,62c}, J.B. Liu^{62a}, J.K.K. Liu³²,
 K. Liu^{62d,62c}, M. Liu^{62a}, M.Y. Liu^{62a}, P. Liu^{14a}, Q. Liu^{62d,138,62c}, X. Liu^{62a}, Y. Liu^{14d,14e},
 Y.L. Liu^{62b}, Y.W. Liu^{62a}, J. Llorente Merino¹⁴², S.L. Lloyd⁹⁴, E.M. Lobodzinska⁴⁸,
 P. Loch⁷, T. Lohse¹⁸, K. Lohwasser¹³⁹, E. Loiacono⁴⁸, M. Lokajicek^{131,*}, J.D. Lomas²⁰,
 J.D. Long¹⁶², I. Longarini¹⁶⁰, L. Longo^{70a,70b}, R. Longo¹⁶², I. Lopez Paz⁶⁷,
 A. Lopez Solis⁴⁸, J. Lorenz¹⁰⁹, N. Lorenzo Martinez⁴, A.M. Lory¹⁰⁹,
 G. Löschcke Centeno¹⁴⁶, O. Loseva³⁷, X. Lou^{47a,47b}, X. Lou^{14a,14e}, A. Lounis⁶⁶, J. Love⁶,
 P.A. Love⁹¹, G. Lu^{14a,14e}, M. Lu⁸⁰, S. Lu¹²⁸, Y.J. Lu⁶⁵, H.J. Lubatti¹³⁸, C. Luci^{75a,75b},
 F.L. Lucio Alves^{14c}, A. Lucotte⁶⁰, F. Luehring⁶⁸, I. Luise¹⁴⁵, O. Lukianchuk⁶⁶,
 O. Lundberg¹⁴⁴, B. Lund-Jensen¹⁴⁴, N.A. Luongo¹²³, M.S. Lutz¹⁵¹, A.B. Lux²⁵, D. Lynn²⁹,
 H. Lyons⁹², R. Lysak¹³¹, E. Lytken⁹⁸, V. Lyubushkin³⁸, T. Lyubushkina³⁸, M.M. Lyukova¹⁴⁵,
 H. Ma²⁹, K. Ma^{62a}, L.L. Ma^{62b}, W. Ma^{62a}, Y. Ma¹²¹, D.M. Mac Donell¹⁶⁵,
 G. Maccarrone⁵³, J.C. MacDonald¹⁰⁰, P.C. Machado De Abreu Farias^{83b}, R. Madar⁴⁰,
 W.F. Mader⁵⁰, T. Madula⁹⁶, J. Maeda⁸⁵, T. Maeno²⁹, H. Maguire¹³⁹, V. Maiboroda¹³⁵,
 A. Maio^{130a,130b,130d}, K. Maj^{86a}, O. Majersky⁴⁸, S. Majewski¹²³, N. Makovec⁶⁶,
 V. Maksimovic¹⁵, B. Malaescu¹²⁷, Pa. Malecki⁸⁷, V.P. Maleev³⁷, F. Malek⁶⁰, M. Mali⁹³,
 D. Malito⁹⁵, U. Mallik⁸⁰, S. Maltezos¹⁰, S. Malyukov³⁸, J. Mamuzic¹³, G. Mancini⁵³,
 G. Manco^{73a,73b}, J.P. Mandalia⁹⁴, I. Mandić⁹³, L. Manhaes de Andrade Filho^{83a},
 I.M. Maniatis¹⁶⁹, J. Manjarres Ramos^{102,aa}, D.C. Mankad¹⁶⁹, A. Mann¹⁰⁹, B. Mansoulie¹³⁵,
 S. Manzoni³⁶, X. Mapekula^{33c}, A. Marantis^{152,r}, G. Marchiori⁵, M. Marcisovsky¹³¹,
 C. Marcon^{71a,71b}, M. Marinescu²⁰, M. Marjanovic¹²⁰, E.J. Marshall⁹¹, Z. Marshall^{17a},
 S. Marti-Garcia¹⁶³, T.A. Martin¹⁶⁷, V.J. Martin⁵², B. Martin dit Latour¹⁶, L. Martinelli^{75a,75b},
 M. Martinez^{13,s}, P. Martinez Agullo¹⁶³, V.I. Martinez Outschoorn¹⁰³, P. Martinez Suarez¹³,
 S. Martin-Haugh¹³⁴, V.S. Martoiu^{27b}, A.C. Martyniuk⁹⁶, A. Marzin³⁶, D. Mascione^{78a,78b},
 L. Masetti¹⁰⁰, T. Mashimo¹⁵³, J. Masik¹⁰¹, A.L. Maslennikov³⁷, L. Massa^{23b},
 P. Massarotti^{72a,72b}, P. Mastrandrea^{74a,74b}, A. Mastroberardino^{43b,43a}, T. Masubuchi¹⁵³,
 T. Mathisen¹⁶¹, J. Matousek¹³³, N. Matsuzawa¹⁵³, J. Maurer^{27b}, B. Maček⁹³,
 D.A. Maximov³⁷, R. Mazini¹⁴⁸, I. Maznas¹⁵², M. Mazza¹⁰⁷, S.M. Mazza¹³⁶,
 E. Mazzeo^{71a,71b}, C. Mc Ginn²⁹, J.P. Mc Gowan¹⁰⁴, S.P. Mc Kee¹⁰⁶, E.F. McDonald¹⁰⁵,
 A.E. McDougall¹¹⁴, J.A. Mcfayden¹⁴⁶, R.P. McGovern¹²⁸, G. Mchedlidze^{149b},
 R.P. Mckenzie^{33g}, T.C. Mclachlan⁴⁸, D.J. Mclaughlin⁹⁶, S.J. McMahon¹³⁴,
 C.M. Mcpartland⁹², R.A. McPherson^{165,w}, S. Mehlhase¹⁰⁹, A. Mehta⁹², D. Melini¹⁵⁰,
 B.R. Mellado Garcia^{33g}, A.H. Melo⁵⁵, F. Meloni⁴⁸, A.M. Mendes Jacques Da Costa¹⁰¹,
 H.Y. Meng¹⁵⁵, L. Meng⁹¹, S. Menke¹¹⁰, M. Mentink³⁶, E. Meoni^{43b,43a}, G. Mercado¹¹⁵,
 C. Merlassino¹²⁶, L. Merola^{72a,72b}, C. Meroni^{71a,71b}, G. Merz¹⁰⁶, O. Meshkov³⁷, J. Metcalfe⁶,
 A.S. Mete⁶, C. Meyer⁶⁸, J-P. Meyer¹³⁵, R.P. Middleton¹³⁴, L. Mijović⁵², G. Mikenberg¹⁶⁹,
 M. Mikestikova¹³¹, M. Mikuž⁹³, H. Mildner¹⁰⁰, A. Milic³⁶, C.D. Milke⁴⁴, D.W. Miller³⁹,
 L.S. Miller³⁴, A. Milov¹⁶⁹, D.A. Milstead^{47a,47b}, T. Min^{14c}, A.A. Minaenko³⁷,
 I.A. Minashvili^{149b}, L. Mince⁵⁹, A.I. Mincer¹¹⁷, B. Mindur^{86a}, M. Mineev³⁸, Y. Mino⁸⁸,
 L.M. Mir¹³, M. Miralles Lopez¹⁶³, M. Mironova^{17a}, A. Mishima¹⁵³, M.C. Missio¹¹³,
 A. Mitra¹⁶⁷, V.A. Mitsou¹⁶³, Y. Mitsumori¹¹¹, O. Miu¹⁵⁵, P.S. Miyagawa⁹⁴,
 T. Mkrtchyan^{63a}, M. Mlinarevic⁹⁶, T. Mlinarevic⁹⁶, M. Mlynarikova³⁶, S. Mobius¹⁹,
 P. Moder⁴⁸, P. Mogg¹⁰⁹, A.F. Mohammed^{14a,14e}, S. Mohapatra⁴¹, G. Mokgatitswane^{33g},
 L. Moleri¹⁶⁹, B. Mondal¹⁴¹, S. Mondal¹³², K. Mönig⁴⁸, E. Monnier¹⁰²,
 L. Monsonis Romero¹⁶³, J. Montejo Berlingen¹³, M. Montella¹¹⁹, F. Montekali^{77a,77b},

F. Monticelli ⁹⁰, S. Monzani ^{69a,69c}, N. Morange ⁶⁶, A.L. Moreira De Carvalho ^{130a}, M. Moreno Llácer ¹⁶³, C. Moreno Martinez ⁵⁶, P. Moretini ^{57b}, S. Morgenstern ³⁶, M. Morii ⁶¹, M. Morinaga ¹⁵³, A.K. Morley ³⁶, F. Morodei ^{75a,75b}, L. Morvaj ³⁶, P. Moschovakos ³⁶, B. Moser ³⁶, M. Mosidze ^{149b}, T. Moskalets ⁵⁴, P. Moskvitina ¹¹³, J. Moss ^{31,1}, E.J.W. Moyses ¹⁰³, O. Mtintsilana ^{33g}, S. Muanza ¹⁰², J. Mueller ¹²⁹, D. Muenstermann ⁹¹, R. Müller ¹⁹, G.A. Mullier ¹⁶¹, A.J. Mullin ³², J.J. Mullin ¹²⁸, D.P. Mungo ¹⁵⁵, D. Munoz Perez ¹⁶³, F.J. Munoz Sanchez ¹⁰¹, M. Murin ¹⁰¹, W.J. Murray ^{167,134}, A. Murrone ^{71a,71b}, M. Muškinja ^{17a}, C. Mwewa ²⁹, A.G. Myagkov ^{37,a}, A.J. Myers ⁸, G. Myers ⁶⁸, M. Myska ¹³², B.P. Nachman ^{17a}, O. Nackenhorst ⁴⁹, A. Nag ⁵⁰, K. Nagai ¹²⁶, K. Nagano ⁸⁴, J.L. Nagle ^{29,ai}, E. Nagy ¹⁰², A.M. Nairz ³⁶, Y. Nakahama ⁸⁴, K. Nakamura ⁸⁴, K. Nakkalil ⁵, H. Nanjo ¹²⁴, R. Narayan ⁴⁴, E.A. Narayanan ¹¹², I. Naryshkin ³⁷, M. Naseri ³⁴, S. Nasri ¹⁵⁹, C. Nass ²⁴, G. Navarro ^{22a}, J. Navarro-Gonzalez ¹⁶³, R. Nayak ¹⁵¹, A. Nayaz ¹⁸, P.Y. Nechaeva ³⁷, F. Nechansky ⁴⁸, L. Nedic ¹²⁶, T.J. Neep ²⁰, A. Negri ^{73a,73b}, M. Negrini ^{23b}, C. Nellist ¹¹⁴, C. Nelson ¹⁰⁴, K. Nelson ¹⁰⁶, S. Nemecek ¹³¹, M. Nessi ^{36,h}, M.S. Neubauer ¹⁶², F. Neuhaus ¹⁰⁰, J. Neundorff ⁴⁸, R. Newhouse ¹⁶⁴, P.R. Newman ²⁰, C.W. Ng ¹²⁹, Y.W.Y. Ng ⁴⁸, B. Ngair ^{35e}, H.D.N. Nguyen ¹⁰⁸, R.B. Nickerson ¹²⁶, R. Nicolaidou ¹³⁵, J. Nielsen ¹³⁶, M. Niemeyer ⁵⁵, J. Niermann ^{55,36}, N. Nikiforou ³⁶, V. Nikolaenko ^{37,a}, I. Nikolic-Audit ¹²⁷, K. Nikolopoulos ²⁰, P. Nilsson ²⁹, I. Ninca ⁴⁸, H.R. Nindhito ⁵⁶, G. Ninio ¹⁵¹, A. Nisati ^{75a}, N. Nishu ², R. Nisius ¹¹⁰, J-E. Nitschke ⁵⁰, E.K. Nkadimeng ^{33g}, T. Nobe ¹⁵³, D.L. Noel ³², T. Nommensen ¹⁴⁷, M.B. Norfolk ¹³⁹, R.R.B. Norisam ⁹⁶, B.J. Norman ³⁴, J. Novak ⁹³, T. Novak ⁴⁸, L. Novotny ¹³², R. Novotny ¹¹², L. Nozka ¹²², K. Ntekas ¹⁶⁰, N.M.J. Nunes De Moura Junior ^{83b}, E. Nurse ⁹⁶, J. Ocariz ¹²⁷, A. Ochi ⁸⁵, I. Ochoa ^{130a}, S. Oerdek ⁴⁸, J.T. Offermann ³⁹, A. Ogrodnik ¹³³, A. Oh ¹⁰¹, C.C. Ohm ¹⁴⁴, H. Oide ⁸⁴, R. Oishi ¹⁵³, M.L. Ojeda ⁴⁸, M.W. O'Keefe ⁹², Y. Okumura ¹⁵³, L.F. Oleiro Seabra ^{130a}, S.A. Olivares Pino ^{137d}, D. Oliveira Damazio ²⁹, D. Oliveira Goncalves ^{83a}, J.L. Oliver ¹⁶⁰, Ö.O. Öncel ⁵⁴, A.P. O'Neill ¹⁹, A. Onofre ^{130a,130e}, P.U.E. Onyisi ¹¹, M.J. Oreglia ³⁹, G.E. Orellana ⁹⁰, D. Orestano ^{77a,77b}, N. Orlando ¹³, R.S. Orr ¹⁵⁵, V. O'Shea ⁵⁹, L.M. Osojnak ¹²⁸, R. Ospanov ^{62a}, G. Otero y Garzon ³⁰, H. Otono ⁸⁹, P.S. Ott ^{63a}, G.J. Ottino ^{17a}, M. Ouchrif ^{35d}, J. Ouellette ²⁹, F. Ould-Saada ¹²⁵, M. Owen ⁵⁹, R.E. Owen ¹³⁴, K.Y. Oyulmaz ^{21a}, V.E. Ozcan ^{21a}, F. Ozturk ⁸⁷, N. Ozturk ⁸, S. Ozturk ⁸², H.A. Pacey ¹²⁶, A. Pacheco Pages ¹³, C. Padilla Aranda ¹³, G. Padovano ^{75a,75b}, S. Pagan Griso ^{17a}, G. Palacino ⁶⁸, A. Palazzo ^{70a,70b}, S. Palestini ³⁶, J. Pan ¹⁷², T. Pan ^{64a}, D.K. Panchal ¹¹, C.E. Pandini ¹¹⁴, J.G. Panduro Vazquez ⁹⁵, H.D. Pandya ¹, H. Pang ^{14b}, P. Pani ⁴⁸, G. Panizzo ^{69a,69c}, L. Paolozzi ⁵⁶, C. Papadatos ¹⁰⁸, S. Parajuli ⁴⁴, A. Paramonov ⁶, C. Paraskevopoulos ¹⁰, D. Paredes Hernandez ^{64b}, K.R. Park ⁴¹, T.H. Park ¹⁵⁵, M.A. Parker ³², F. Parodi ^{57b,57a}, E.W. Parrish ¹¹⁵, V.A. Parrish ⁵², J.A. Parsons ⁴¹, U. Parzefall ⁵⁴, B. Pascual Dias ¹⁰⁸, L. Pascual Dominguez ¹⁵¹, E. Pasqualucci ^{75a}, S. Passaggio ^{57b}, F. Pastore ⁹⁵, P. Pasuwan ^{47a,47b}, P. Patel ⁸⁷, U.M. Patel ⁵¹, J.R. Pater ¹⁰¹, T. Pauly ³⁶, J. Pearkes ¹⁴³, M. Pedersen ¹²⁵, R. Pedro ^{130a}, S.V. Peleganchuk ³⁷, O. Penc ³⁶, E.A. Pender ⁵², K.E. Penski ¹⁰⁹, M. Penzin ³⁷, B.S. Peralva ^{83d}, A.P. Pereira Peixoto ⁶⁰, L. Pereira Sanchez ^{47a,47b}, D.V. Perepelitsa ^{29,ai}, E. Perez Codina ^{156a}, M. Perganti ¹⁰, L. Perini ^{71a,71b,*}, H. Pernegger ³⁶, O. Perrin ⁴⁰, K. Peters ⁴⁸, R.F.Y. Peters ¹⁰¹, B.A. Petersen ³⁶, T.C. Petersen ⁴², E. Petit ¹⁰², V. Petousis ¹³², C. Petridou ^{152,e}, A. Petrukhin ¹⁴¹, M. Pettee ^{17a}, N.E. Pettersson ³⁶, A. Petukhov ³⁷, K. Petukhova ¹³³, R. Pezoa ^{137f}, L. Pezzotti ³⁶, G. Pezzullo ¹⁷², T.M. Pham ¹⁷⁰, T. Pham ¹⁰⁵, P.W. Phillips ¹³⁴, G. Piacquadio ¹⁴⁵, E. Pianori ^{17a}, F. Piazza ¹²³, R. Piegai ³⁰, D. Pietreanu ^{27b}, A.D. Pilkington ¹⁰¹, M. Pinamonti ^{69a,69c}, J.L. Pinfeld ², B.C. Pinheiro Pereira ^{130a}, A.E. Pinto Pinoargote ^{100,135}, L. Pintucci ^{69a,69c}, K.M. Piper ¹⁴⁶,

A. Pirttikoski ⁵⁶, D.A. Pizzi ³⁴, L. Pizzimento ^{64b}, A. Pizzini ¹¹⁴, M.-A. Pleier ²⁹, V. Plesanovs ⁵⁴,
 V. Pleskot ¹³³, E. Plotnikova ³⁸, G. Poddar ⁴, R. Poettgen ⁹⁸, L. Poggioli ¹²⁷, I. Pokharel ⁵⁵,
 S. Polacek ¹³³, G. Polesello ^{73a}, A. Poley ^{142,156a}, R. Polifka ¹³², A. Polini ^{23b}, C.S. Pollard ¹⁶⁷,
 Z.B. Pollock ¹¹⁹, V. Polychronakos ²⁹, E. Pompa Pacchi ^{75a,75b}, D. Ponomarenko ¹¹³,
 L. Pontecorvo ³⁶, S. Popa ^{27a}, G.A. Popeneciu ^{27d}, A. Poreba ³⁶, D.M. Portillo Quintero ^{156a},
 S. Pospisil ¹³², M.A. Postill ¹³⁹, P. Postolache ^{27c}, K. Potamianos ¹⁶⁷, P.A. Potepa ^{86a},
 I.N. Potrap ³⁸, C.J. Potter ³², H. Potti ¹, T. Poulsen ⁴⁸, J. Poveda ¹⁶³, M.E. Pozo Astigarraga ³⁶,
 A. Prades Ibanez ¹⁶³, J. Pretel ⁵⁴, D. Price ¹⁰¹, M. Primavera ^{70a}, M.A. Principe Martin ⁹⁹,
 R. Privara ¹²², T. Procter ⁵⁹, M.L. Proffitt ¹³⁸, N. Proklova ¹²⁸, K. Prokofiev ^{64c}, G. Proto ¹¹⁰,
 S. Protopopescu ²⁹, J. Proudfoot ⁶, M. Przybycien ^{86a}, W.W. Przygoda ^{86b}, J.E. Puddefoot ¹³⁹,
 D. Pudzha ³⁷, D. Pyatiiybyantseva ³⁷, J. Qian ¹⁰⁶, D. Qichen ¹⁰¹, Y. Qin ¹⁰¹, T. Qiu ⁵²,
 A. Quadt ⁵⁵, M. Queitsch-Maitland ¹⁰¹, G. Quetant ⁵⁶, R.P. Quinn ¹⁶⁴, G. Rabanal Bolanos ⁶¹,
 D. Rafanoharana ⁵⁴, F. Ragusa ^{71a,71b}, J.L. Rainbolt ³⁹, J.A. Raine ⁵⁶, S. Rajagopalan ²⁹,
 E. Ramakoti ³⁷, I.A. Ramirez-Berend ³⁴, K. Ran ^{48,14e}, N.P. Rapheeha ^{33g}, H. Rasheed ^{27b},
 V. Raskina ¹²⁷, D.F. Rassloff ^{63a}, S. Rave ¹⁰⁰, B. Ravina ⁵⁵, I. Ravinovich ¹⁶⁹, M. Raymond ³⁶,
 A.L. Read ¹²⁵, N.P. Readioff ¹³⁹, D.M. Rebutzi ^{73a,73b}, G. Redlinger ²⁹, A.S. Reed ¹¹⁰,
 K. Reeves ²⁶, J.A. Reidelsturz ¹⁷¹, D. Reikher ¹⁵¹, A. Rej ⁴⁹, C. Rembser ³⁶, A. Renardi ⁴⁸,
 M. Renda ^{27b}, M.B. Rendel ¹¹⁰, F. Renner ⁴⁸, A.G. Rennie ¹⁶⁰, A.L. Rescia ⁴⁸, S. Resconi ^{71a},
 M. Ressegotti ^{57b,57a}, S. Rettie ³⁶, J.G. Reyes Rivera ¹⁰⁷, E. Reynolds ^{17a}, O.L. Rezanova ³⁷,
 P. Reznicek ¹³³, N. Ribaric ⁹¹, E. Ricci ^{78a,78b}, R. Richter ¹¹⁰, S. Richter ^{47a,47b},
 E. Richter-Was ^{86b}, M. Ridel ¹²⁷, S. Ridouani ^{35d}, P. Rieck ¹¹⁷, P. Riedler ³⁶, E.M. Riefel ^{47a,47b},
 J.O. Rieger ¹¹⁴, M. Rijssenbeek ¹⁴⁵, A. Rimoldi ^{73a,73b}, M. Rimoldi ³⁶, L. Rinaldi ^{23b,23a},
 T.T. Rinn ²⁹, M.P. Rinnagel ¹⁰⁹, G. Ripellino ¹⁶¹, I. Riu ¹³, P. Rivadeneira ⁴⁸,
 J.C. Rivera Vergara ¹⁶⁵, F. Rizatdinova ¹²¹, E. Rizvi ⁹⁴, B.A. Roberts ¹⁶⁷, B.R. Roberts ^{17a},
 S.H. Robertson ^{104,w}, D. Robinson ³², C.M. Robles Gajardo ^{137f}, M. Robles Manzano ¹⁰⁰,
 A. Robson ⁵⁹, A. Rocchi ^{76a,76b}, C. Roda ^{74a,74b}, S. Rodriguez Bosca ^{63a}, Y. Rodriguez Garcia ^{22a},
 A. Rodriguez Rodriguez ⁵⁴, A.M. Rodríguez Vera ^{156b}, S. Roe ³⁶, J.T. Roemer ¹⁶⁰,
 A.R. Roepe-Gier ¹³⁶, J. Roggel ¹⁷¹, O. Røhne ¹²⁵, R.A. Rojas ¹⁰³, C.P.A. Roland ¹²⁷,
 J. Roloff ²⁹, A. Romaniouk ³⁷, E. Romano ^{73a,73b}, M. Romano ^{23b}, A.C. Romero Hernandez ¹⁶²,
 N. Rompotis ⁹², L. Roos ¹²⁷, S. Rosati ^{75a}, B.J. Rosser ³⁹, E. Rossi ¹²⁶, E. Rossi ^{72a,72b},
 L.P. Rossi ^{57b}, L. Rossini ⁵⁴, R. Rosten ¹¹⁹, M. Rotaru ^{27b}, B. Rottler ⁵⁴, C. Rougier ^{102,aa},
 D. Rousseau ⁶⁶, D. Rousso ³², A. Roy ¹⁶², S. Roy-Garand ¹⁵⁵, A. Rozanov ¹⁰²,
 Z.M.A. Rozario ⁵⁹, Y. Rozen ¹⁵⁰, X. Ruan ^{33g}, A. Rubio Jimenez ¹⁶³, A.J. Ruby ⁹²,
 V.H. Ruelas Rivera ¹⁸, T.A. Ruggeri ¹, A. Ruggiero ¹²⁶, A. Ruiz-Martinez ¹⁶³, A. Rummler ³⁶,
 Z. Rurikova ⁵⁴, N.A. Rusakovich ³⁸, H.L. Russell ¹⁶⁵, G. Russo ^{75a,75b}, J.P. Rutherford ⁷,
 S. Rutherford Colmenares ³², K. Rybacki ⁹¹, M. Rybar ¹³³, E.B. Rye ¹²⁵, A. Ryzhov ⁴⁴,
 J.A. Sabater Iglesias ⁵⁶, P. Sabatini ¹⁶³, L. Sabetta ^{75a,75b}, H.F-W. Sadrozinski ¹³⁶,
 F. Safai Tehrani ^{75a}, B. Safarzadeh Samani ¹³⁴, M. Safdari ¹⁴³, S. Saha ¹⁶⁵, M. Sahinsoy ¹¹⁰,
 M. Saimpert ¹³⁵, M. Saito ¹⁵³, T. Saito ¹⁵³, D. Salamani ³⁶, A. Salnikov ¹⁴³, J. Salt ¹⁶³,
 A. Salvador Salas ¹⁵¹, D. Salvatore ^{43b,43a}, F. Salvatore ¹⁴⁶, A. Salzburger ³⁶, D. Sammel ⁵⁴,
 D. Sampsonidis ^{152,e}, D. Sampsonidou ¹²³, J. Sánchez ¹⁶³, A. Sanchez Pineda ⁴,
 V. Sanchez Sebastian ¹⁶³, H. Sandaker ¹²⁵, C.O. Sander ⁴⁸, J.A. Sandesara ¹⁰³, M. Sandhoff ¹⁷¹,
 C. Sandoval ^{22b}, D.P.C. Sankey ¹³⁴, T. Sano ⁸⁸, A. Sansoni ⁵³, L. Santi ^{75a,75b}, C. Santoni ⁴⁰,
 H. Santos ^{130a,130b}, S.N. Santpur ^{17a}, A. Santra ¹⁶⁹, K.A. Saoucha ^{116b}, J.G. Saraiva ^{130a,130d},
 J. Sardain ⁷, O. Sasaki ⁸⁴, K. Sato ¹⁵⁷, C. Sauer ^{63b}, F. Sauerburger ⁵⁴, E. Sauvan ⁴,
 P. Savard ^{155,af}, R. Sawada ¹⁵³, C. Sawyer ¹³⁴, L. Sawyer ⁹⁷, I. Sayago Galvan ¹⁶³, C. Sbarra ^{23b},
 A. Sbrizzi ^{23b,23a}, T. Scanlon ⁹⁶, J. Schaarschmidt ¹³⁸, P. Schacht ¹¹⁰, U. Schäfer ¹⁰⁰,

A.C. Schaffer [id66,44](#), D. Schaile [id109](#), R.D. Schamberger [id145](#), C. Scharf [id18](#), M.M. Schefer [id19](#),
 V.A. Schegelsky [id37](#), D. Scheirich [id133](#), F. Schenck [id18](#), M. Schernau [id160](#), C. Scheulen [id55](#),
 C. Schiavi [id57b,57a](#), E.J. Schioppa [id70a,70b](#), M. Schioppa [id43b,43a](#), B. Schlag [id143,n](#), K.E. Schleicher [id54](#),
 S. Schlenker [id36](#), J. Schmeing [id171](#), M.A. Schmidt [id171](#), K. Schmieden [id100](#), C. Schmitt [id100](#),
 N. Schmitt [id100](#), S. Schmitt [id48](#), L. Schoeffel [id135](#), A. Schoening [id63b](#), P.G. Scholer [id54](#), E. Schopf [id126](#),
 M. Schott [id100](#), J. Schovancova [id36](#), S. Schramm [id56](#), F. Schroeder [id171](#), T. Schroer [id56](#),
 H-C. Schultz-Coulon [id63a](#), M. Schumacher [id54](#), B.A. Schumm [id136](#), Ph. Schune [id135](#), A.J. Schuy [id138](#),
 H.R. Schwartz [id136](#), A. Schwartzman [id143](#), T.A. Schwarz [id106](#), Ph. Schwemling [id135](#),
 R. Schwienhorst [id107](#), A. Sciandra [id136](#), G. Sciolla [id26](#), F. Scuri [id74a](#), C.D. Sebastiani [id92](#),
 K. Sedlaczek [id115](#), P. Seema [id18](#), S.C. Seidel [id112](#), A. Seiden [id136](#), B.D. Seidlitz [id41](#), C. Seitz [id48](#),
 J.M. Seixas [id83b](#), G. Sekhniaidze [id72a](#), S.J. Sekula [id44](#), L. Selem [id60](#), N. Semprini-Cesari [id23b,23a](#),
 D. Sengupta [id56](#), V. Senthikumar [id163](#), L. Serin [id66](#), L. Serkin [id69a,69b](#), M. Sessa [id76a,76b](#),
 H. Severini [id120](#), F. Sforza [id57b,57a](#), A. Sfyrta [id56](#), E. Shabalina [id55](#), R. Shaheen [id144](#),
 J.D. Shahinian [id128](#), D. Shaked Renous [id169](#), L.Y. Shan [id14a](#), M. Shapiro [id17a](#), A. Sharma [id36](#),
 A.S. Sharma [id164](#), P. Sharma [id80](#), S. Sharma [id48](#), P.B. Shatalov [id37](#), K. Shaw [id146](#), S.M. Shaw [id101](#),
 A. Shcherbakova [id37](#), Q. Shen [id62c,5](#), P. Sherwood [id96](#), L. Shi [id96](#), X. Shi [id14a](#), C.O. Shimmin [id172](#),
 J.D. Shinner [id95](#), I.P.J. Shipsey [id126](#), S. Shirabe [id56,h](#), M. Shiyakova [id38,u](#), J. Shlomi [id169](#),
 M.J. Shochet [id39](#), J. Shojaii [id105](#), D.R. Shope [id125](#), B. Shrestha [id120](#), S. Shrestha [id119,aj](#),
 E.M. Shrif [id33g](#), M.J. Shroff [id165](#), P. Sicho [id131](#), A.M. Sickles [id162](#), E. Sideras Haddad [id33g](#),
 A. Sidoti [id23b](#), F. Siegert [id50](#), Dj. Sijacki [id15](#), R. Sikora [id86a](#), F. Sili [id90](#), J.M. Silva [id20](#),
 M.V. Silva Oliveira [id29](#), S.B. Silverstein [id47a](#), S. Simion [id66](#), R. Simoniello [id36](#), E.L. Simpson [id59](#),
 H. Simpson [id146](#), L.R. Simpson [id106](#), N.D. Simpson [id98](#), S. Simsek [id82](#), S. Sindhu [id55](#), P. Sinervo [id155](#),
 S. Singh [id155](#), S. Sinha [id48](#), S. Sinha [id101](#), M. Sioli [id23b,23a](#), I. Siral [id36](#), E. Sitnikova [id48](#),
 S.Yu. Sivoklov [id37,*](#), J. Sjölin [id47a,47b](#), A. Skaf [id55](#), E. Skorda [id20](#), P. Skubic [id120](#), M. Slawinska [id87](#),
 V. Smakhtin [id169](#), B.H. Smart [id134](#), J. Smiesko [id36](#), S.Yu. Smirnov [id37](#), Y. Smirnov [id37](#),
 L.N. Smirnova [id37,a](#), O. Smirnova [id98](#), A.C. Smith [id41](#), E.A. Smith [id39](#), H.A. Smith [id126](#),
 J.L. Smith [id92](#), R. Smith [id143](#), M. Smizanska [id91](#), K. Smolek [id132](#), A.A. Snesarev [id37](#), S.R. Snider [id155](#),
 H.L. Snoek [id114](#), S. Snyder [id29](#), R. Sobie [id165,w](#), A. Soffer [id151](#), C.A. Solans Sanchez [id36](#),
 E.Yu. Soldatov [id37](#), U. Soldevila [id163](#), A.A. Solodkov [id37](#), S. Solomon [id26](#), A. Soloshenko [id38](#),
 K. Solovieva [id54](#), O.V. Solovyanov [id40](#), V. Solovyev [id37](#), P. Sommer [id36](#), A. Sonay [id13](#),
 W.Y. Song [id156b](#), J.M. Sonneveld [id114](#), A. Sopczak [id132](#), A.L. Soppio [id96](#), F. Sopkova [id28b](#),
 I.R. Sotarriva Alvarez [id154](#), V. Sothilingam [id63a](#), O.J. Soto Sandoval [id137c,137b](#), S. Sottocornola [id68](#),
 R. Soualah [id116b](#), Z. Soumami [id35e](#), D. South [id48](#), N. Soybelman [id169](#), S. Spagnolo [id70a,70b](#),
 M. Spalla [id110](#), D. Sperlich [id54](#), G. Spigo [id36](#), S. Spinali [id91](#), D.P. Spiteri [id59](#), M. Spousta [id133](#),
 E.J. Staats [id34](#), A. Stabile [id71a,71b](#), R. Stamen [id63a](#), A. Stampekis [id20](#), M. Standke [id24](#), E. Stanecka [id87](#),
 M.V. Stange [id50](#), B. Stanislaus [id17a](#), M.M. Stanitzki [id48](#), B. Stapf [id48](#), E.A. Starchenko [id37](#),
 G.H. Stark [id136](#), J. Stark [id102,aa](#), D.M. Starko [id156b](#), P. Staroba [id131](#), P. Starovoitov [id63a](#), S. Stärz [id104](#),
 R. Staszewski [id87](#), G. Stavropoulos [id46](#), J. Steentoft [id161](#), P. Steinberg [id29](#), B. Stelzer [id142,156a](#),
 H.J. Stelzer [id129](#), O. Stelzer-Chilton [id156a](#), H. Stenzel [id58](#), T.J. Stevenson [id146](#), G.A. Stewart [id36](#),
 J.R. Stewart [id121](#), M.C. Stockton [id36](#), G. Stoicea [id27b](#), M. Stolarski [id130a](#), S. Stonjek [id110](#),
 A. Straessner [id50](#), J. Strandberg [id144](#), S. Strandberg [id47a,47b](#), M. Stratmann [id171](#), M. Strauss [id120](#),
 T. Strebler [id102](#), P. Strizenc [id28b](#), R. Ströhmer [id166](#), D.M. Strom [id123](#), L.R. Strom [id48](#),
 R. Stroynowski [id44](#), A. Strubig [id47a,47b](#), S.A. Stucci [id29](#), B. Stugu [id16](#), J. Stupak [id120](#), N.A. Styles [id48](#),
 D. Su [id143](#), S. Su [id62a](#), W. Su [id62d](#), X. Su [id62a,66](#), K. Sugizaki [id153](#), V.V. Sulin [id37](#), M.J. Sullivan [id92](#),
 D.M.S. Sultan [id78a,78b](#), L. Sultanaliyeva [id37](#), S. Sultansoy [id3b](#), T. Sumida [id88](#), S. Sun [id106](#), S. Sun [id170](#),
 O. Sunneborn Gudnadottir [id161](#), N. Sur [id102](#), M.R. Sutton [id146](#), H. Suzuki [id157](#), M. Svatos [id131](#),
 M. Swiatlowski [id156a](#), T. Swirski [id166](#), I. Sykora [id28a](#), M. Sykora [id133](#), T. Sykora [id133](#), D. Ta [id100](#),

K. Tackmann [id](#)^{48,t}, A. Taffard [id](#)¹⁶⁰, R. Tafirout [id](#)^{156a}, J.S. Tafoya Vargas [id](#)⁶⁶, E.P. Takeva [id](#)⁵²,
 Y. Takubo [id](#)⁸⁴, M. Talby [id](#)¹⁰², A.A. Talyshev [id](#)³⁷, K.C. Tam [id](#)^{64b}, N.M. Tamir [id](#)¹⁵¹, A. Tanaka [id](#)¹⁵³,
 J. Tanaka [id](#)¹⁵³, R. Tanaka [id](#)⁶⁶, M. Tanasini [id](#)^{57b,57a}, Z. Tao [id](#)¹⁶⁴, S. Tapia Araya [id](#)^{137f},
 S. Tapprogge [id](#)¹⁰⁰, A. Tarek Abouelfadl Mohamed [id](#)¹⁰⁷, S. Tarem [id](#)¹⁵⁰, K. Tariq [id](#)^{14a}, G. Tarna [id](#)^{102,27b},
 G.F. Tartarelli [id](#)^{71a}, P. Tas [id](#)¹³³, M. Tasevsky [id](#)¹³¹, E. Tassi [id](#)^{43b,43a}, A.C. Tate [id](#)¹⁶², G. Tateno [id](#)¹⁵³,
 Y. Tayalati [id](#)^{35e,v}, G.N. Taylor [id](#)¹⁰⁵, W. Taylor [id](#)^{156b}, A.S. Tee [id](#)¹⁷⁰, R. Teixeira De Lima [id](#)¹⁴³,
 P. Teixeira-Dias [id](#)⁹⁵, J.J. Teoh [id](#)¹⁵⁵, K. Terashi [id](#)¹⁵³, J. Terron [id](#)⁹⁹, S. Terzo [id](#)¹³, M. Testa [id](#)⁵³,
 R.J. Teuscher [id](#)^{155,w}, A. Thaler [id](#)⁷⁹, O. Theiner [id](#)⁵⁶, N. Themistokleous [id](#)⁵², T. Theveneaux-Pelzer [id](#)¹⁰²,
 O. Thielmann [id](#)¹⁷¹, D.W. Thomas [id](#)⁹⁵, J.P. Thomas [id](#)²⁰, E.A. Thompson [id](#)^{17a}, P.D. Thompson [id](#)²⁰,
 E. Thomson [id](#)¹²⁸, Y. Tian [id](#)⁵⁵, V. Tikhomirov [id](#)^{37,a}, Yu.A. Tikhonov [id](#)³⁷, S. Timoshenko [id](#)³⁷,
 D. Timoshyn [id](#)¹³³, E.X.L. Ting [id](#)¹, P. Tipton [id](#)¹⁷², S.H. Tlou [id](#)^{33g}, A. Tnourji [id](#)⁴⁰, K. Todome [id](#)¹⁵⁴,
 S. Todorova-Nova [id](#)¹³³, S. Todt [id](#)⁵⁰, M. Togawa [id](#)⁸⁴, J. Tojo [id](#)⁸⁹, S. Tokár [id](#)^{28a}, K. Tokushuku [id](#)⁸⁴,
 O. Toldaiev [id](#)⁶⁸, R. Tombs [id](#)³², M. Tomoto [id](#)^{84,111}, L. Tompkins [id](#)^{143,n}, K.W. Topolnicki [id](#)^{86b},
 E. Torrence [id](#)¹²³, H. Torres [id](#)^{102,aa}, E. Torró Pastor [id](#)¹⁶³, M. Toscani [id](#)³⁰, C. Toscirri [id](#)³⁹, M. Tost [id](#)¹¹,
 D.R. Tovey [id](#)¹³⁹, A. Traeet [id](#)¹⁶, I.S. Trandafir [id](#)^{27b}, T. Trefzger [id](#)¹⁶⁶, A. Tricoli [id](#)²⁹, I.M. Trigger [id](#)^{156a},
 S. Trincaz-Duvoid [id](#)¹²⁷, D.A. Trischuk [id](#)²⁶, B. Trocmé [id](#)⁶⁰, C. Troncon [id](#)^{71a}, L. Truong [id](#)^{33c},
 M. Trzebinski [id](#)⁸⁷, A. Trzupiek [id](#)⁸⁷, F. Tsai [id](#)¹⁴⁵, M. Tsai [id](#)¹⁰⁶, A. Tsiamis [id](#)^{152,e}, P.V. Tsiareshka [id](#)³⁷,
 S. Tsigaridas [id](#)^{156a}, A. Tsirigotis [id](#)^{152,r}, V. Tsiskaridze [id](#)¹⁵⁵, E.G. Tskhadadze [id](#)^{149a},
 M. Tsopoulou [id](#)^{152,e}, Y. Tsujikawa [id](#)⁸⁸, I.I. Tsukerman [id](#)³⁷, V. Tsulaia [id](#)^{17a}, S. Tsuno [id](#)⁸⁴, O. Tsur [id](#)¹⁵⁰,
 K. Tsur [id](#)¹¹⁸, D. Tsybychev [id](#)¹⁴⁵, Y. Tu [id](#)^{64b}, A. Tudorache [id](#)^{27b}, V. Tudorache [id](#)^{27b}, A.N. Tuna [id](#)³⁶,
 S. Turchikhin [id](#)^{57b,57a}, I. Turk Cakir [id](#)^{3a}, R. Turra [id](#)^{71a}, T. Turtuvshin [id](#)^{38,x}, P.M. Tuts [id](#)⁴¹,
 S. Tzamarias [id](#)^{152,e}, P. Tzanis [id](#)¹⁰, E. Tzovara [id](#)¹⁰⁰, F. Ukegawa [id](#)¹⁵⁷, P.A. Ulloa Poblete [id](#)^{137c,137b},
 E.N. Umaka [id](#)²⁹, G. Unal [id](#)³⁶, M. Unal [id](#)¹¹, A. Undrus [id](#)²⁹, G. Unel [id](#)¹⁶⁰, J. Urban [id](#)^{28b},
 P. Urquijo [id](#)¹⁰⁵, P. Urrejola [id](#)^{137a}, G. Usai [id](#)⁸, R. Ushioda [id](#)¹⁵⁴, M. Usman [id](#)¹⁰⁸, Z. Uysal [id](#)^{21b},
 V. Vacek [id](#)¹³², B. Vachon [id](#)¹⁰⁴, K.O.H. Vadla [id](#)¹²⁵, T. Vafeiadis [id](#)³⁶, A. Vaitkus [id](#)⁹⁶, C. Valderanis [id](#)¹⁰⁹,
 E. Valdes Santurio [id](#)^{47a,47b}, M. Valente [id](#)^{156a}, S. Valentinetti [id](#)^{23b,23a}, A. Valero [id](#)¹⁶³,
 E. Valiente Moreno [id](#)¹⁶³, A. Vallier [id](#)^{102,aa}, J.A. Valls Ferrer [id](#)¹⁶³, D.R. Van Arneman [id](#)¹¹⁴,
 T.R. Van Daalen [id](#)¹³⁸, A. Van Der Graaf [id](#)⁴⁹, P. Van Gemmeren [id](#)⁶, M. Van Rijnbach [id](#)^{125,36},
 S. Van Stroud [id](#)⁹⁶, I. Van Vulpen [id](#)¹¹⁴, M. Vanadia [id](#)^{76a,76b}, W. Vandelli [id](#)³⁶, M. Vandenbroucke [id](#)¹³⁵,
 E.R. Vandewall [id](#)¹²¹, D. Vannicola [id](#)¹⁵¹, L. Vannoli [id](#)^{57b,57a}, R. Vari [id](#)^{75a}, E.W. Varnes [id](#)⁷,
 C. Varni [id](#)^{17b}, T. Varol [id](#)¹⁴⁸, D. Varouchas [id](#)⁶⁶, L. Varriale [id](#)¹⁶³, K.E. Varvell [id](#)¹⁴⁷, M.E. Vasile [id](#)^{27b},
 L. Vaslin [id](#)⁸⁴, G.A. Vasquez [id](#)¹⁶⁵, A. Vasyukov [id](#)³⁸, F. Vazeille [id](#)⁴⁰, T. Vazquez Schroeder [id](#)³⁶,
 J. Veatch [id](#)³¹, V. Vecchio [id](#)¹⁰¹, M.J. Veen [id](#)¹⁰³, I. Veliscek [id](#)¹²⁶, L.M. Veloce [id](#)¹⁵⁵, F. Veloso [id](#)^{130a,130c},
 S. Veneziano [id](#)^{75a}, A. Ventura [id](#)^{70a,70b}, S. Ventura Gonzalez [id](#)¹³⁵, A. Verbytskyi [id](#)¹¹⁰,
 M. Verducci [id](#)^{74a,74b}, C. Vergis [id](#)²⁴, M. Verissimo De Araujo [id](#)^{83b}, W. Verkerke [id](#)¹¹⁴,
 J.C. Vermeulen [id](#)¹¹⁴, C. Vernieri [id](#)¹⁴³, M. Vessella [id](#)¹⁰³, M.C. Vetterli [id](#)^{142,af}, A. Vgenopoulos [id](#)^{152,e},
 N. Viaux Maira [id](#)^{137f}, T. Vickey [id](#)¹³⁹, O.E. Vickey Boeriu [id](#)¹³⁹, G.H.A. Viehhauser [id](#)¹²⁶, L. Vignani [id](#)^{63b},
 M. Villa [id](#)^{23b,23a}, M. Villaplana Perez [id](#)¹⁶³, E.M. Villhauer [id](#)⁵², E. Vilucchi [id](#)⁵³, M.G. Vincter [id](#)³⁴,
 G.S. Virdee [id](#)²⁰, A. Vishwakarma [id](#)⁵², A. Visibile [id](#)¹¹⁴, C. Vittori [id](#)³⁶, I. Vivarelli [id](#)¹⁴⁶,
 E. Voevodina [id](#)¹¹⁰, F. Vogel [id](#)¹⁰⁹, J.C. Voigt [id](#)⁵⁰, P. Vokac [id](#)¹³², Yu. Volkotrub [id](#)^{86a}, J. Von Ahnen [id](#)⁴⁸,
 E. Von Toerne [id](#)²⁴, B. Vormwald [id](#)³⁶, V. Vorobel [id](#)¹³³, K. Vorobev [id](#)³⁷, M. Vos [id](#)¹⁶³, K. Voss [id](#)¹⁴¹,
 J.H. Vossebeld [id](#)⁹², M. Vozak [id](#)¹¹⁴, L. Vozdecky [id](#)⁹⁴, N. Vranjes [id](#)¹⁵, M. Vranjes Milosavljevic [id](#)¹⁵,
 M. Vreeswijk [id](#)¹¹⁴, R. Vuillermet [id](#)³⁶, O. Vujinovic [id](#)¹⁰⁰, I. Vukotic [id](#)³⁹, S. Wada [id](#)¹⁵⁷, C. Wagner [id](#)¹⁰³,
 J.M. Wagner [id](#)^{17a}, W. Wagner [id](#)¹⁷¹, S. Wahdan [id](#)¹⁷¹, H. Wahlberg [id](#)⁹⁰, M. Wakida [id](#)¹¹¹, J. Walder [id](#)¹³⁴,
 R. Walker [id](#)¹⁰⁹, W. Walkowiak [id](#)¹⁴¹, A. Wall [id](#)¹²⁸, T. Wamorkar [id](#)⁶, A.Z. Wang [id](#)¹³⁶, C. Wang [id](#)¹⁰⁰,
 C. Wang [id](#)^{62c}, H. Wang [id](#)^{17a}, J. Wang [id](#)^{64a}, R.-J. Wang [id](#)¹⁰⁰, R. Wang [id](#)⁶¹, R. Wang [id](#)⁶,
 S.M. Wang [id](#)¹⁴⁸, S. Wang [id](#)^{62b}, T. Wang [id](#)^{62a}, W.T. Wang [id](#)⁸⁰, W. Wang [id](#)^{14a}, X. Wang [id](#)^{14c},

X. Wang ¹⁶², X. Wang ^{62c}, Y. Wang ^{62d}, Y. Wang ^{14c}, Z. Wang ¹⁰⁶, Z. Wang ^{62d,51,62c},
Z. Wang ¹⁰⁶, A. Warburton ¹⁰⁴, R.J. Ward ²⁰, N. Warrack ⁵⁹, A.T. Watson ²⁰, H. Watson ⁵⁹,
M.F. Watson ²⁰, E. Watton ^{59,134}, G. Watts ¹³⁸, B.M. Waugh ⁹⁶, C. Weber ²⁹, H.A. Weber ¹⁸,
M.S. Weber ¹⁹, S.M. Weber ^{63a}, C. Wei ^{62a}, Y. Wei ¹²⁶, A.R. Weidberg ¹²⁶, E.J. Weik ¹¹⁷,
J. Weingarten ⁴⁹, M. Weirich ¹⁰⁰, C. Weiser ⁵⁴, C.J. Wells ⁴⁸, T. Wenaus ²⁹, B. Wendland ⁴⁹,
T. Wengler ³⁶, N.S. Wenke ¹¹⁰, N. Wermes ²⁴, M. Wessels ^{63a}, A.M. Wharton ⁹¹, A.S. White ⁶¹,
A. White ⁸, M.J. White ¹, D. Whiteson ¹⁶⁰, L. Wickremasinghe ¹²⁴, W. Wiedenmann ¹⁷⁰,
C. Wiel ⁵⁰, M. Wielers ¹³⁴, C. Wiglesworth ⁴², D.J. Wilbern ¹²⁰, H.G. Wilkens ³⁶,
D.M. Williams ⁴¹, H.H. Williams ¹²⁸, S. Williams ³², S. Willocq ¹⁰³, B.J. Wilson ¹⁰¹,
P.J. Windischhofer ³⁹, F.I. Winkel ³⁰, F. Winklmeier ¹²³, B.T. Winter ⁵⁴, J.K. Winter ¹⁰¹,
M. Wittgen ¹⁴³, M. Wobisch ⁹⁷, Z. Wolffs ¹¹⁴, J. Wollrath ¹⁶⁰, M.W. Wolter ⁸⁷, H. Wolters ^{130a,130c},
A.F. Wongel ⁴⁸, E.L. Woodward ⁴¹, S.D. Worm ⁴⁸, B.K. Wosiek ⁸⁷, K.W. Woźniak ⁸⁷,
S. Wozniowski ⁵⁵, K. Wraight ⁵⁹, C. Wu ²⁰, J. Wu ^{14a,14e}, M. Wu ^{64a}, M. Wu ¹¹³, S.L. Wu ¹⁷⁰,
X. Wu ⁵⁶, Y. Wu ^{62a}, Z. Wu ¹³⁵, J. Wuerzinger ^{110,ad}, T.R. Wyatt ¹⁰¹, B.M. Wynne ⁵²,
S. Xella ⁴², L. Xia ^{14c}, M. Xia ^{14b}, J. Xiang ^{64c}, M. Xie ^{62a}, X. Xie ^{62a}, S. Xin ^{14a,14e},
A. Xiong ¹²³, J. Xiong ^{17a}, D. Xu ^{14a}, H. Xu ^{62a}, L. Xu ^{62a}, R. Xu ¹²⁸, T. Xu ¹⁰⁶, Y. Xu ^{14b},
Z. Xu ⁵², Z. Xu ^{14c}, B. Yabsley ¹⁴⁷, S. Yacoob ^{33a}, Y. Yamaguchi ¹⁵⁴, E. Yamashita ¹⁵³,
H. Yamauchi ¹⁵⁷, T. Yamazaki ^{17a}, Y. Yamazaki ⁸⁵, J. Yan ^{62c}, S. Yan ¹²⁶, Z. Yan ²⁵,
H.J. Yang ^{62c,62d}, H.T. Yang ^{62a}, S. Yang ^{62a}, T. Yang ^{64c}, X. Yang ³⁶, X. Yang ^{14a}, Y. Yang ⁴⁴,
Y. Yang ^{62a}, Z. Yang ^{62a}, W-M. Yao ^{17a}, Y.C. Yap ⁴⁸, H. Ye ^{14c}, H. Ye ⁵⁵, J. Ye ^{14a}, S. Ye ²⁹,
X. Ye ^{62a}, Y. Yeh ⁹⁶, I. Yeletsikh ³⁸, B.K. Yeo ^{17b}, M.R. Yexley ⁹⁶, P. Yin ⁴¹, K. Yorita ¹⁶⁸,
S. Younas ^{27b}, C.J.S. Young ³⁶, C. Young ¹⁴³, C. Yu ^{14a,14e,ah}, Y. Yu ^{62a}, M. Yuan ¹⁰⁶,
R. Yuan ^{62b}, L. Yue ⁹⁶, M. Zaazoua ^{62a}, B. Zabinski ⁸⁷, E. Zaid ⁵², Z.K. Zak ⁸⁷,
T. Zakareishvili ^{149b}, N. Zakharchuk ³⁴, S. Zambito ⁵⁶, J.A. Zamora Saa ^{137d,137b}, J. Zang ¹⁵³,
D. Zanzi ⁵⁴, O. Zaplatilek ¹³², C. Zeitnitz ¹⁷¹, H. Zeng ^{14a}, J.C. Zeng ¹⁶², D.T. Zenger Jr ²⁶,
O. Zenin ³⁷, T. Ženiš ^{28a}, S. Zenz ⁹⁴, S. Zerradi ^{35a}, D. Zerwas ⁶⁶, M. Zhai ^{14a,14e},
B. Zhang ^{14c}, D.F. Zhang ¹³⁹, J. Zhang ^{62b}, J. Zhang ⁶, K. Zhang ^{14a,14e}, L. Zhang ^{14c},
P. Zhang ^{14a,14e}, R. Zhang ¹⁷⁰, S. Zhang ¹⁰⁶, S. Zhang ⁴⁴, T. Zhang ¹⁵³, X. Zhang ^{62c},
X. Zhang ^{62b}, Y. Zhang ^{62c,5}, Y. Zhang ⁹⁶, Y. Zhang ^{14c}, Z. Zhang ^{17a}, Z. Zhang ⁶⁶,
H. Zhao ¹³⁸, P. Zhao ⁵¹, T. Zhao ^{62b}, Y. Zhao ¹³⁶, Z. Zhao ^{62a}, A. Zhemchugov ³⁸,
J. Zheng ^{14c}, K. Zheng ¹⁶², X. Zheng ^{62a}, Z. Zheng ¹⁴³, D. Zhong ¹⁶², B. Zhou ¹⁰⁶, H. Zhou ⁷,
N. Zhou ^{62c}, Y. Zhou ⁷, C.G. Zhu ^{62b}, J. Zhu ¹⁰⁶, Y. Zhu ^{62c}, Y. Zhu ^{62a}, X. Zhuang ^{14a},
K. Zhukov ³⁷, V. Zhulanov ³⁷, N.I. Zimine ³⁸, J. Zinsser ^{63b}, M. Ziolkowski ¹⁴¹, L. Živković ¹⁵,
A. Zoccoli ^{23b,23a}, K. Zoch ⁶¹, T.G. Zorbas ¹³⁹, O. Zormpa ⁴⁶, W. Zou ⁴¹, L. Zwalinski ³⁶.

¹Department of Physics, University of Adelaide, Adelaide; Australia.

²Department of Physics, University of Alberta, Edmonton AB; Canada.

^{3(a)}Department of Physics, Ankara University, Ankara; ^(b)Division of Physics, TOBB University of Economics and Technology, Ankara; Türkiye.

⁴LAPP, Université Savoie Mont Blanc, CNRS/IN2P3, Annecy; France.

⁵APC, Université Paris Cité, CNRS/IN2P3, Paris; France.

⁶High Energy Physics Division, Argonne National Laboratory, Argonne IL; United States of America.

⁷Department of Physics, University of Arizona, Tucson AZ; United States of America.

⁸Department of Physics, University of Texas at Arlington, Arlington TX; United States of America.

⁹Physics Department, National and Kapodistrian University of Athens, Athens; Greece.

¹⁰Physics Department, National Technical University of Athens, Zografou; Greece.

¹¹Department of Physics, University of Texas at Austin, Austin TX; United States of America.

¹²Institute of Physics, Azerbaijan Academy of Sciences, Baku; Azerbaijan.

¹³Institut de Física d'Altes Energies (IFAE), Barcelona Institute of Science and Technology, Barcelona; Spain.

¹⁴(^a)Institute of High Energy Physics, Chinese Academy of Sciences, Beijing; (^b)Physics Department, Tsinghua University, Beijing; (^c)Department of Physics, Nanjing University, Nanjing; (^d)School of Science, Shenzhen Campus of Sun Yat-sen University; (^e)University of Chinese Academy of Science (UCAS), Beijing; China.

¹⁵Institute of Physics, University of Belgrade, Belgrade; Serbia.

¹⁶Department for Physics and Technology, University of Bergen, Bergen; Norway.

¹⁷(^a)Physics Division, Lawrence Berkeley National Laboratory, Berkeley CA; (^b)University of California, Berkeley CA; United States of America.

¹⁸Institut für Physik, Humboldt Universität zu Berlin, Berlin; Germany.

¹⁹Albert Einstein Center for Fundamental Physics and Laboratory for High Energy Physics, University of Bern, Bern; Switzerland.

²⁰School of Physics and Astronomy, University of Birmingham, Birmingham; United Kingdom.

²¹(^a)Department of Physics, Bogazici University, Istanbul; (^b)Department of Physics Engineering, Gaziantep University, Gaziantep; (^c)Department of Physics, Istanbul University, Istanbul; Türkiye.

²²(^a)Facultad de Ciencias y Centro de Investigaciones, Universidad Antonio Nariño,

Bogotá; (^b)Departamento de Física, Universidad Nacional de Colombia, Bogotá; Colombia.

²³(^a)Dipartimento di Fisica e Astronomia A. Righi, Università di Bologna, Bologna; (^b)INFN Sezione di Bologna; Italy.

²⁴Physikalisches Institut, Universität Bonn, Bonn; Germany.

²⁵Department of Physics, Boston University, Boston MA; United States of America.

²⁶Department of Physics, Brandeis University, Waltham MA; United States of America.

²⁷(^a)Transilvania University of Brasov, Brasov; (^b)Horia Hulubei National Institute of Physics and Nuclear Engineering, Bucharest; (^c)Department of Physics, Alexandru Ioan Cuza University of Iasi, Iasi; (^d)National Institute for Research and Development of Isotopic and Molecular Technologies, Physics Department, Cluj-Napoca; (^e)University Politehnica Bucharest, Bucharest; (^f)West University in Timisoara, Timisoara; (^g)Faculty of Physics, University of Bucharest, Bucharest; Romania.

²⁸(^a)Faculty of Mathematics, Physics and Informatics, Comenius University, Bratislava; (^b)Department of Subnuclear Physics, Institute of Experimental Physics of the Slovak Academy of Sciences, Kosice; Slovak Republic.

²⁹Physics Department, Brookhaven National Laboratory, Upton NY; United States of America.

³⁰Universidad de Buenos Aires, Facultad de Ciencias Exactas y Naturales, Departamento de Física, y CONICET, Instituto de Física de Buenos Aires (IFIBA), Buenos Aires; Argentina.

³¹California State University, CA; United States of America.

³²Cavendish Laboratory, University of Cambridge, Cambridge; United Kingdom.

³³(^a)Department of Physics, University of Cape Town, Cape Town; (^b)iThemba Labs, Western

Cape; (^c)Department of Mechanical Engineering Science, University of Johannesburg,

Johannesburg; (^d)National Institute of Physics, University of the Philippines Diliman

(Philippines); (^e)University of South Africa, Department of Physics, Pretoria; (^f)University of Zululand,

KwaDlangezwa; (^g)School of Physics, University of the Witwatersrand, Johannesburg; South Africa.

³⁴Department of Physics, Carleton University, Ottawa ON; Canada.

³⁵(^a)Faculté des Sciences Ain Chock, Réseau Universitaire de Physique des Hautes Energies - Université Hassan II, Casablanca; (^b)Faculté des Sciences, Université Ibn-Tofail, Kénitra; (^c)Faculté des Sciences Semlalia, Université Cadi Ayyad, LPHEA-Marrakech; (^d)LPMR, Faculté des Sciences, Université Mohamed Premier, Oujda; (^e)Faculté des sciences, Université Mohammed V, Rabat; (^f)Institute of Applied

- Physics, Mohammed VI Polytechnic University, Ben Guerir; Morocco.
- ³⁶CERN, Geneva; Switzerland.
- ³⁷Affiliated with an institute covered by a cooperation agreement with CERN.
- ³⁸Affiliated with an international laboratory covered by a cooperation agreement with CERN.
- ³⁹Enrico Fermi Institute, University of Chicago, Chicago IL; United States of America.
- ⁴⁰LPC, Université Clermont Auvergne, CNRS/IN2P3, Clermont-Ferrand; France.
- ⁴¹Nevis Laboratory, Columbia University, Irvington NY; United States of America.
- ⁴²Niels Bohr Institute, University of Copenhagen, Copenhagen; Denmark.
- ⁴³(^a) Dipartimento di Fisica, Università della Calabria, Rende; (^b) INFN Gruppo Collegato di Cosenza, Laboratori Nazionali di Frascati; Italy.
- ⁴⁴Physics Department, Southern Methodist University, Dallas TX; United States of America.
- ⁴⁵Physics Department, University of Texas at Dallas, Richardson TX; United States of America.
- ⁴⁶National Centre for Scientific Research "Demokritos", Agia Paraskevi; Greece.
- ⁴⁷(^a) Department of Physics, Stockholm University; (^b) Oskar Klein Centre, Stockholm; Sweden.
- ⁴⁸Deutsches Elektronen-Synchrotron DESY, Hamburg and Zeuthen; Germany.
- ⁴⁹Fakultät Physik, Technische Universität Dortmund, Dortmund; Germany.
- ⁵⁰Institut für Kern- und Teilchenphysik, Technische Universität Dresden, Dresden; Germany.
- ⁵¹Department of Physics, Duke University, Durham NC; United States of America.
- ⁵²SUPA - School of Physics and Astronomy, University of Edinburgh, Edinburgh; United Kingdom.
- ⁵³INFN e Laboratori Nazionali di Frascati, Frascati; Italy.
- ⁵⁴Physikalisches Institut, Albert-Ludwigs-Universität Freiburg, Freiburg; Germany.
- ⁵⁵II. Physikalisches Institut, Georg-August-Universität Göttingen, Göttingen; Germany.
- ⁵⁶Département de Physique Nucléaire et Corpusculaire, Université de Genève, Genève; Switzerland.
- ⁵⁷(^a) Dipartimento di Fisica, Università di Genova, Genova; (^b) INFN Sezione di Genova; Italy.
- ⁵⁸II. Physikalisches Institut, Justus-Liebig-Universität Giessen, Giessen; Germany.
- ⁵⁹SUPA - School of Physics and Astronomy, University of Glasgow, Glasgow; United Kingdom.
- ⁶⁰LPSC, Université Grenoble Alpes, CNRS/IN2P3, Grenoble INP, Grenoble; France.
- ⁶¹Laboratory for Particle Physics and Cosmology, Harvard University, Cambridge MA; United States of America.
- ⁶²(^a) Department of Modern Physics and State Key Laboratory of Particle Detection and Electronics, University of Science and Technology of China, Hefei; (^b) Institute of Frontier and Interdisciplinary Science and Key Laboratory of Particle Physics and Particle Irradiation (MOE), Shandong University, Qingdao; (^c) School of Physics and Astronomy, Shanghai Jiao Tong University, Key Laboratory for Particle Astrophysics and Cosmology (MOE), SKLPPC, Shanghai; (^d) Tsung-Dao Lee Institute, Shanghai; China.
- ⁶³(^a) Kirchhoff-Institut für Physik, Ruprecht-Karls-Universität Heidelberg, Heidelberg; (^b) Physikalisches Institut, Ruprecht-Karls-Universität Heidelberg, Heidelberg; Germany.
- ⁶⁴(^a) Department of Physics, Chinese University of Hong Kong, Shatin, N.T., Hong Kong; (^b) Department of Physics, University of Hong Kong, Hong Kong; (^c) Department of Physics and Institute for Advanced Study, Hong Kong University of Science and Technology, Clear Water Bay, Kowloon, Hong Kong; China.
- ⁶⁵Department of Physics, National Tsing Hua University, Hsinchu; Taiwan.
- ⁶⁶IJCLab, Université Paris-Saclay, CNRS/IN2P3, 91405, Orsay; France.
- ⁶⁷Centro Nacional de Microelectrónica (IMB-CNM-CSIC), Barcelona; Spain.
- ⁶⁸Department of Physics, Indiana University, Bloomington IN; United States of America.
- ⁶⁹(^a) INFN Gruppo Collegato di Udine, Sezione di Trieste, Udine; (^b) ICTP, Trieste; (^c) Dipartimento Politecnico di Ingegneria e Architettura, Università di Udine, Udine; Italy.
- ⁷⁰(^a) INFN Sezione di Lecce; (^b) Dipartimento di Matematica e Fisica, Università del Salento, Lecce; Italy.
- ⁷¹(^a) INFN Sezione di Milano; (^b) Dipartimento di Fisica, Università di Milano, Milano; Italy.

- 72^(a) INFN Sezione di Napoli; ^(b) Dipartimento di Fisica, Università di Napoli, Napoli; Italy.
- 73^(a) INFN Sezione di Pavia; ^(b) Dipartimento di Fisica, Università di Pavia, Pavia; Italy.
- 74^(a) INFN Sezione di Pisa; ^(b) Dipartimento di Fisica E. Fermi, Università di Pisa, Pisa; Italy.
- 75^(a) INFN Sezione di Roma; ^(b) Dipartimento di Fisica, Sapienza Università di Roma, Roma; Italy.
- 76^(a) INFN Sezione di Roma Tor Vergata; ^(b) Dipartimento di Fisica, Università di Roma Tor Vergata, Roma; Italy.
- 77^(a) INFN Sezione di Roma Tre; ^(b) Dipartimento di Matematica e Fisica, Università Roma Tre, Roma; Italy.
- 78^(a) INFN-TIFPA; ^(b) Università degli Studi di Trento, Trento; Italy.
- 79 Universität Innsbruck, Department of Astro and Particle Physics, Innsbruck; Austria.
- 80 University of Iowa, Iowa City IA; United States of America.
- 81 Department of Physics and Astronomy, Iowa State University, Ames IA; United States of America.
- 82 Istinye University, Sariyer, Istanbul; Türkiye.
- 83^(a) Departamento de Engenharia Elétrica, Universidade Federal de Juiz de Fora (UFJF), Juiz de Fora; ^(b) Universidade Federal do Rio De Janeiro COPPE/EE/IF, Rio de Janeiro; ^(c) Instituto de Física, Universidade de São Paulo, São Paulo; ^(d) Rio de Janeiro State University, Rio de Janeiro; Brazil.
- 84 KEK, High Energy Accelerator Research Organization, Tsukuba; Japan.
- 85 Graduate School of Science, Kobe University, Kobe; Japan.
- 86^(a) AGH University of Krakow, Faculty of Physics and Applied Computer Science, Krakow; ^(b) Marian Smoluchowski Institute of Physics, Jagiellonian University, Krakow; Poland.
- 87 Institute of Nuclear Physics Polish Academy of Sciences, Krakow; Poland.
- 88 Faculty of Science, Kyoto University, Kyoto; Japan.
- 89 Research Center for Advanced Particle Physics and Department of Physics, Kyushu University, Fukuoka ; Japan.
- 90 Instituto de Física La Plata, Universidad Nacional de La Plata and CONICET, La Plata; Argentina.
- 91 Physics Department, Lancaster University, Lancaster; United Kingdom.
- 92 Oliver Lodge Laboratory, University of Liverpool, Liverpool; United Kingdom.
- 93 Department of Experimental Particle Physics, Jožef Stefan Institute and Department of Physics, University of Ljubljana, Ljubljana; Slovenia.
- 94 School of Physics and Astronomy, Queen Mary University of London, London; United Kingdom.
- 95 Department of Physics, Royal Holloway University of London, Egham; United Kingdom.
- 96 Department of Physics and Astronomy, University College London, London; United Kingdom.
- 97 Louisiana Tech University, Ruston LA; United States of America.
- 98 Fysiska institutionen, Lunds universitet, Lund; Sweden.
- 99 Departamento de Física Teórica C-15 and CIAFF, Universidad Autónoma de Madrid, Madrid; Spain.
- 100 Institut für Physik, Universität Mainz, Mainz; Germany.
- 101 School of Physics and Astronomy, University of Manchester, Manchester; United Kingdom.
- 102 CPPM, Aix-Marseille Université, CNRS/IN2P3, Marseille; France.
- 103 Department of Physics, University of Massachusetts, Amherst MA; United States of America.
- 104 Department of Physics, McGill University, Montreal QC; Canada.
- 105 School of Physics, University of Melbourne, Victoria; Australia.
- 106 Department of Physics, University of Michigan, Ann Arbor MI; United States of America.
- 107 Department of Physics and Astronomy, Michigan State University, East Lansing MI; United States of America.
- 108 Group of Particle Physics, University of Montreal, Montreal QC; Canada.
- 109 Fakultät für Physik, Ludwig-Maximilians-Universität München, München; Germany.
- 110 Max-Planck-Institut für Physik (Werner-Heisenberg-Institut), München; Germany.

- ¹¹¹Graduate School of Science and Kobayashi-Maskawa Institute, Nagoya University, Nagoya; Japan.
- ¹¹²Department of Physics and Astronomy, University of New Mexico, Albuquerque NM; United States of America.
- ¹¹³Institute for Mathematics, Astrophysics and Particle Physics, Radboud University/Nikhef, Nijmegen; Netherlands.
- ¹¹⁴Nikhef National Institute for Subatomic Physics and University of Amsterdam, Amsterdam; Netherlands.
- ¹¹⁵Department of Physics, Northern Illinois University, DeKalb IL; United States of America.
- ¹¹⁶^(a)New York University Abu Dhabi, Abu Dhabi;^(b)University of Sharjah, Sharjah; United Arab Emirates.
- ¹¹⁷Department of Physics, New York University, New York NY; United States of America.
- ¹¹⁸Ochanomizu University, Otsuka, Bunkyo-ku, Tokyo; Japan.
- ¹¹⁹Ohio State University, Columbus OH; United States of America.
- ¹²⁰Homer L. Dodge Department of Physics and Astronomy, University of Oklahoma, Norman OK; United States of America.
- ¹²¹Department of Physics, Oklahoma State University, Stillwater OK; United States of America.
- ¹²²Palacký University, Joint Laboratory of Optics, Olomouc; Czech Republic.
- ¹²³Institute for Fundamental Science, University of Oregon, Eugene, OR; United States of America.
- ¹²⁴Graduate School of Science, Osaka University, Osaka; Japan.
- ¹²⁵Department of Physics, University of Oslo, Oslo; Norway.
- ¹²⁶Department of Physics, Oxford University, Oxford; United Kingdom.
- ¹²⁷LPNHE, Sorbonne Université, Université Paris Cité, CNRS/IN2P3, Paris; France.
- ¹²⁸Department of Physics, University of Pennsylvania, Philadelphia PA; United States of America.
- ¹²⁹Department of Physics and Astronomy, University of Pittsburgh, Pittsburgh PA; United States of America.
- ¹³⁰^(a)Laboratório de Instrumentação e Física Experimental de Partículas - LIP, Lisboa;^(b)Departamento de Física, Faculdade de Ciências, Universidade de Lisboa, Lisboa;^(c)Departamento de Física, Universidade de Coimbra, Coimbra;^(d)Centro de Física Nuclear da Universidade de Lisboa, Lisboa;^(e)Departamento de Física, Universidade do Minho, Braga;^(f)Departamento de Física Teórica y del Cosmos, Universidad de Granada, Granada (Spain);^(g)Departamento de Física, Instituto Superior Técnico, Universidade de Lisboa, Lisboa; Portugal.
- ¹³¹Institute of Physics of the Czech Academy of Sciences, Prague; Czech Republic.
- ¹³²Czech Technical University in Prague, Prague; Czech Republic.
- ¹³³Charles University, Faculty of Mathematics and Physics, Prague; Czech Republic.
- ¹³⁴Particle Physics Department, Rutherford Appleton Laboratory, Didcot; United Kingdom.
- ¹³⁵IRFU, CEA, Université Paris-Saclay, Gif-sur-Yvette; France.
- ¹³⁶Santa Cruz Institute for Particle Physics, University of California Santa Cruz, Santa Cruz CA; United States of America.
- ¹³⁷^(a)Departamento de Física, Pontificia Universidad Católica de Chile, Santiago;^(b)Millennium Institute for Subatomic physics at high energy frontier (SAPHIR), Santiago;^(c)Instituto de Investigación Multidisciplinario en Ciencia y Tecnología, y Departamento de Física, Universidad de La Serena;^(d)Universidad Andres Bello, Department of Physics, Santiago;^(e)Instituto de Alta Investigación, Universidad de Tarapacá, Arica;^(f)Departamento de Física, Universidad Técnica Federico Santa María, Valparaíso; Chile.
- ¹³⁸Department of Physics, University of Washington, Seattle WA; United States of America.
- ¹³⁹Department of Physics and Astronomy, University of Sheffield, Sheffield; United Kingdom.
- ¹⁴⁰Department of Physics, Shinshu University, Nagano; Japan.

- ¹⁴¹Department Physik, Universität Siegen, Siegen; Germany.
- ¹⁴²Department of Physics, Simon Fraser University, Burnaby BC; Canada.
- ¹⁴³SLAC National Accelerator Laboratory, Stanford CA; United States of America.
- ¹⁴⁴Department of Physics, Royal Institute of Technology, Stockholm; Sweden.
- ¹⁴⁵Departments of Physics and Astronomy, Stony Brook University, Stony Brook NY; United States of America.
- ¹⁴⁶Department of Physics and Astronomy, University of Sussex, Brighton; United Kingdom.
- ¹⁴⁷School of Physics, University of Sydney, Sydney; Australia.
- ¹⁴⁸Institute of Physics, Academia Sinica, Taipei; Taiwan.
- ¹⁴⁹^(a)E. Andronikashvili Institute of Physics, Iv. Javakhishvili Tbilisi State University, Tbilisi; ^(b)High Energy Physics Institute, Tbilisi State University, Tbilisi; ^(c)University of Georgia, Tbilisi; Georgia.
- ¹⁵⁰Department of Physics, Technion, Israel Institute of Technology, Haifa; Israel.
- ¹⁵¹Raymond and Beverly Sackler School of Physics and Astronomy, Tel Aviv University, Tel Aviv; Israel.
- ¹⁵²Department of Physics, Aristotle University of Thessaloniki, Thessaloniki; Greece.
- ¹⁵³International Center for Elementary Particle Physics and Department of Physics, University of Tokyo, Tokyo; Japan.
- ¹⁵⁴Department of Physics, Tokyo Institute of Technology, Tokyo; Japan.
- ¹⁵⁵Department of Physics, University of Toronto, Toronto ON; Canada.
- ¹⁵⁶^(a)TRIUMF, Vancouver BC; ^(b)Department of Physics and Astronomy, York University, Toronto ON; Canada.
- ¹⁵⁷Division of Physics and Tomonaga Center for the History of the Universe, Faculty of Pure and Applied Sciences, University of Tsukuba, Tsukuba; Japan.
- ¹⁵⁸Department of Physics and Astronomy, Tufts University, Medford MA; United States of America.
- ¹⁵⁹United Arab Emirates University, Al Ain; United Arab Emirates.
- ¹⁶⁰Department of Physics and Astronomy, University of California Irvine, Irvine CA; United States of America.
- ¹⁶¹Department of Physics and Astronomy, University of Uppsala, Uppsala; Sweden.
- ¹⁶²Department of Physics, University of Illinois, Urbana IL; United States of America.
- ¹⁶³Instituto de Física Corpuscular (IFIC), Centro Mixto Universidad de Valencia - CSIC, Valencia; Spain.
- ¹⁶⁴Department of Physics, University of British Columbia, Vancouver BC; Canada.
- ¹⁶⁵Department of Physics and Astronomy, University of Victoria, Victoria BC; Canada.
- ¹⁶⁶Fakultät für Physik und Astronomie, Julius-Maximilians-Universität Würzburg, Würzburg; Germany.
- ¹⁶⁷Department of Physics, University of Warwick, Coventry; United Kingdom.
- ¹⁶⁸Waseda University, Tokyo; Japan.
- ¹⁶⁹Department of Particle Physics and Astrophysics, Weizmann Institute of Science, Rehovot; Israel.
- ¹⁷⁰Department of Physics, University of Wisconsin, Madison WI; United States of America.
- ¹⁷¹Fakultät für Mathematik und Naturwissenschaften, Fachgruppe Physik, Bergische Universität Wuppertal, Wuppertal; Germany.
- ¹⁷²Department of Physics, Yale University, New Haven CT; United States of America.
- ^a Also Affiliated with an institute covered by a cooperation agreement with CERN.
- ^b Also at An-Najah National University, Nablus; Palestine.
- ^c Also at Borough of Manhattan Community College, City University of New York, New York NY; United States of America.
- ^d Also at Center for High Energy Physics, Peking University; China.
- ^e Also at Center for Interdisciplinary Research and Innovation (CIRI-AUTH), Thessaloniki; Greece.
- ^f Also at Centro Studi e Ricerche Enrico Fermi; Italy.
- ^g Also at CERN, Geneva; Switzerland.

- h* Also at Département de Physique Nucléaire et Corpusculaire, Université de Genève, Genève; Switzerland.
- i* Also at Departament de Física de la Universitat Autònoma de Barcelona, Barcelona; Spain.
- j* Also at Department of Financial and Management Engineering, University of the Aegean, Chios; Greece.
- k* Also at Department of Physics, Ben Gurion University of the Negev, Beer Sheva; Israel.
- l* Also at Department of Physics, California State University, Sacramento; United States of America.
- m* Also at Department of Physics, King's College London, London; United Kingdom.
- n* Also at Department of Physics, Stanford University, Stanford CA; United States of America.
- o* Also at Department of Physics, University of Fribourg, Fribourg; Switzerland.
- p* Also at Department of Physics, University of Thessaly; Greece.
- q* Also at Department of Physics, Westmont College, Santa Barbara; United States of America.
- r* Also at Hellenic Open University, Patras; Greece.
- s* Also at Institutio Catalana de Recerca i Estudis Avancats, ICREA, Barcelona; Spain.
- t* Also at Institut für Experimentalphysik, Universität Hamburg, Hamburg; Germany.
- u* Also at Institute for Nuclear Research and Nuclear Energy (INRNE) of the Bulgarian Academy of Sciences, Sofia; Bulgaria.
- v* Also at Institute of Applied Physics, Mohammed VI Polytechnic University, Ben Guerir; Morocco.
- w* Also at Institute of Particle Physics (IPP); Canada.
- x* Also at Institute of Physics and Technology, Ulaanbaatar; Mongolia.
- y* Also at Institute of Physics, Azerbaijan Academy of Sciences, Baku; Azerbaijan.
- z* Also at Institute of Theoretical Physics, Ilia State University, Tbilisi; Georgia.
- aa* Also at L2IT, Université de Toulouse, CNRS/IN2P3, UPS, Toulouse; France.
- ab* Also at Lawrence Livermore National Laboratory, Livermore; United States of America.
- ac* Also at National Institute of Physics, University of the Philippines Diliman (Philippines); Philippines.
- ad* Also at Technical University of Munich, Munich; Germany.
- ae* Also at The Collaborative Innovation Center of Quantum Matter (CICQM), Beijing; China.
- af* Also at TRIUMF, Vancouver BC; Canada.
- ag* Also at Università di Napoli Parthenope, Napoli; Italy.
- ah* Also at University of Chinese Academy of Sciences (UCAS), Beijing; China.
- ai* Also at University of Colorado Boulder, Department of Physics, Colorado; United States of America.
- aj* Also at Washington College, Chestertown, MD; United States of America.
- ak* Also at Yeditepe University, Physics Department, Istanbul; Türkiye.
- * Deceased